UNIVERSIDADE FEDERAL DE PERNAMBUCO
CENTRO DE TECNOLOGIA E GEOCIÊNCIAS
DEPARTAMENTO DE ENGENHARIA DE PRODUÇÃO
PROGRAMA DE PÓS-GRADUAÇÃO EM ENGENHARIA DE PRODUÇÃO

PAULO GABRIEL SANTOS CAMPOS DE SIQUEIRA

STOCHASTIC MODEL FOR QUANTITATIVE ECOLOGICAL RISK ASSESSMENT OF OIL SPILLS NEAR FERNANDO DE NORONHA ARCHIPELAGO

Recife
2022

PAULO GABRIEL SANTOS CAMPOS DE SIQUEIRA

STOCHASTIC MODEL FOR QUANTITATIVE ECOLOGICAL RISK ASSESSMENT OF OIL SPILLS NEAR FERNANDO DE NORONHA ARCHIPELAGO

Master thesis presented to UFPE for the master's degree attainment as part of the requirements of the Programa de Pós-Graduação em Engenharia de Produção.

Concentration area: Operations Research

Advisor: Prof. Dr. Márcio José das Chagas Moura

Recife

2022

Catalogação na fonte
Bibliotecária Margareth Malta, CRB-4 / 1198

S618s Siqueira, Paulo Gabriel Santos Campos de.
Stochastic model for quantitative ecological risk assessment of oil spills near Fernando de Noronha Archipelago / Paulo Gabriel Santos Campos de Siqueira. - 2022.
132 folhas, il., gráfs., tabs.

Orientador: Prof. Dr. Márcio José das Chagas Moura.
Dissertação (Mestrado) – Universidade Federal de Pernambuco. CTG. Programa de Pós-Graduação em Engenharia de Produção, 2022.
Inclui Referências e Apêndice.
Texto em inglês.

1. Engenharia de Produção. 2. Avaliação quantitativa de riscos. 3. Modelagem ecológica. 4. Acidentes marítimos. 5. Modelagem de vazamento óleo. 6. Análise de variabilidade Bayesiana. I. Moura, Márcio José das Chagas (Orientador). II. Título.

UFPE

658.5 CDD (22. ed.) BCTG/2022-136

PAULO GABRIEL SANTOS CAMPOS DE SIQUEIRA

STOCHASTIC MODEL FOR QUANTITATIVE ECOLOGICAL RISK ASSESSMENT OF OIL SPILLS NEAR FERNANDO DE NORONHA ARCHIPELAGO

Master thesis presented to UFPE for the master's degree attainment as part of the requirements of the Programa de Pós-Graduação em Engenharia de Produção.

Concentration area: Operations Research

Approved in: 16/02/2022.

EXAMINATION BOARD

_____

Prof. Dr. Márcio José das Chagas Moura (Advisor)
Universidade Federal de Pernambuco

_____

Prof[a]. Dr[a]. Isis Didier Lins (Internal Examiner)
Universidade Federal de Pernambuco

_____

Prof[a]. Dr[a]. Marília Abílio Ramos (External Examiner)
University of California Los Angeles

ACKNOWLEDGMENTS

I thank God for granting me serenity and health, especially during the pandemic that marked the completion of this work.

To my parents, Paulo and Mara, and to my sister, Bárbara, for all the love, affection and support in my decisions. In addition to being all the basis that allows me to move forward.

To my advisor, Professor Márcio, for his trust, support and valuable teachings. Also to Professor Heitor, who has been with me since graduation, for his trust, friendship, availability, teachings and tireless revisions. To Professor Paulo Estevão, for his commitment to preparing us professionally. And to Professor Isis, whose comments contributed to improving the quality of the work.

Juliana for all the love, affection and for being able to make the days lighter. To Maria Laura, Beatriz, Adel, Maria Luísa and Alexsandra, for their friendship, support, special moments and for helping to make everything more possible:

To the colleagues I made during the master's degree: Plínio, Naévio and Mariana, for their mutual help, companionship and support in difficult moments during the course.

To Professor Marcus Silva and Syumara Queiroz, for their help with the MEDSLIK-II.

To the experts who took the time to answer the questionnaire and contributed to this research.

To the *Pós-Graduação em Engenharia de Produção* (PPGEP-UFPE) for the academic opportunities.

To the *Programa de Recursos Humanos* (PRH) of the *Agência Nacional do Petróleo* (ANP) 38.1: *Análise de Riscos e Modelagem Ambiental na Exploração, Desenvolvimento e Produção de Petróleo e Gás*, and to the *Coordenação de Aperfeiçoamento de Pessoal de Nível Superior* (CAPES) for the financial support in the development of this research.

“The true way passes over a rope which is not strechted high up, but just above the ground. It seems to be intended more for stumbling than for crossing.” (KAFKA).

ABSTRACT

Industrial accidents, such as toxic spills, have caused catastrophic damage to ecological environments (animals and plants), so that an effective method to assess ecological risks has been demanded. The high number of vessels, including oil tankers that circulate the globe, along with extreme events such as storms and tropical besides cyclones due to global warming, increase the risk of potential oil spills affect oceanic islands. In Brazil, the Fernando de Noronha Archipelago (FNA) has a Conservation Unit's status, protecting endemic species and maintaining a healthy island ecosystem. Moreover, the consequences of a spill can be even aggravated since FNA lacks infrastructure and mitigation plans for such accidents. The methodology used to quantify such risks is based on stochastic population modeling and can consider extreme and rare events, such as oil spills. It considers both the event's frequency of occurrence and the magnitude of the adverse ecological effects, capable of quantifying ecological risks as a probability of extinction (or decline) of a given species representative of the ecosystem. It can also predict populations' responses to toxic exposure via population-level endpoints such as abundance. Other models are integrated into the assessment: (i) oil spill simulation to compute the oil concentration reaching FNA, and (ii) the Bayesian Population Variability Analysis, to estimate the accidents frequency occurrence from databases and expert opinions. Then, we can assess the ecological risks of such accidents and summarize these results in risk categories to be easily communicated to the general public. Finally, the results obtained would provide relevant information that can aid decision-makers in avoiding such a disastrous event and/or mitigating its impacts.

Keywords: quantitative risk assessment; ecological modeling; maritime accidents; fate and transport modeling; Bayesian variability analysis.

RESUMO

Acidentes industriais, como vazamentos de produtos tóxicos, têm causado danos catastróficos aos ambientes ecológicos (animais e plantas), de modo que se faz necessário um método eficaz de avaliação dos riscos ecológicos. O elevado número de embarcações, incluindo petroleiros que circulam pelo globo, juntamente com eventos extremos como tempestades tropicais além de ciclones devido ao aquecimento global, aumentam o risco de possíveis vazamentos de óleo afetar as ilhas oceânicas. No Brasil, o Arquipélago de Fernando de Noronha (AFN) possui status de Unidade de Conservação, protegendo espécies endêmicas e mantendo um ecossistema insular saudável. Além disso, as consequências de um derramamento podem ser agravadas, uma vez que o AFN carece de infraestrutura e planos de mitigação para tais acidentes. A metodologia utilizada para quantificar esses riscos é baseada em modelagem populacional estocástica e pode considerar eventos extremos e raros, como vazamentos de óleo. Ela considera tanto a frequência de ocorrência do evento quanto a magnitude dos efeitos ecológicos adversos, sendo capaz de quantificar os riscos ecológicos como probabilidade de extinção (ou declínio) de uma determinada espécie representativa do ecossistema. Além disso, também é possível prever as respostas das populações à exposição tóxica por meio de características como a abundância populacional. Outros modelos são integrados à avaliação: (i) simulação da trajetória do óleo no oceano para calcular a concentração de óleo atingindo o arquipélago, e (ii) análise de variabilidade populacional Bayesiana, com o objetivo de estimativar as frequências de ocorrência de acidentes a partir de bancos de dados e opiniões de especialistas. Com isso, podem-se avaliar os riscos ecológicos causados por tais acidentes e resumir esses resultados em categorias de risco para serem facilmente comunicados ao público em geral. Finalmente, os resultados obtidos forneceriam informações relevantes que podem auxilar os tomadores de decisão a evitar tais eventos desastrosos e/ou mitigar seus impactos.

Palavras-chave: avaliação quantitativa de riscos; modelagem ecológica; acidentes marítimos; modelagem de vazamento óleo; análise de variabilidade Bayesiana.

LIST OF FIGURES

ARTICLE 1

ARTICLE 2

ARTICLE 3

LIST OF TABLES

ARTICLE 1

ARTICLE 2

ARTICLE 3

CONTENTS

1 INTRODUCTION

1.1 INITIAL REMARKS

This work is within the field of the Quantitative Ecological Risk Assessment (QERA). QERA is a formal process of estimating the probability of adverse effects to an ecosystem, in the short and long-term, due to exposure to one or more stressors (e.g., crude oil) (EPA, 1998). QERA can be based on mathematical models capable of providing quantitative risk results. These models simulate a single defined species' population dynamics. The species usually is a plant or animal (e.g., corals, fishes, turtles) that humans want to protect by mitigating the impacts on the ecosystem's health.

QERA results can aid decision-making in many real applications, such as pesticide regulatory programs, water discharges, mitigation measures to treat contaminated areas, installation of new facilities (AKÇAKAYA et al., 2004; BARTELL et al., 1999; CHEN, 2005; NAITO et al., 2002; PAUWELS, 2002). In the Brazilian context, the ERA could be required when there is an ecological asset to be protected from stressors (e.g., chemical, physical or biological), mainly in environmental licensing, introduction of exotic species, and the assessment of contaminated areas or existing sources of pollution (CETESB, 2020). These applications show QERA is an essential field of study within Production Engineering. It is beneficial for industries and governments to provide information necessary to licensing, risk management, and environmental management.

When applying QERA in the context of oil spills, risks are estimated considering an exposure assessment and the effects (CETESB, 2020). In the exposure assessment, spatio-temporal models of dispersion should be used to model the stressor dispersion (i.e., oil). When assessing the effects, it is recommended to use laboratory (or field) tests and experiments, simulating exposure scenarios. However, this approach is not enough to providing useful information when determining risks in QERA. This information only indicates if individual effects are expected, i.e., probability of death of a single individual, and it lacks the long-term impacts at a population level.

Thus, to overcome such limitations, the risk assessment focuses on long-term adverse effects in the species population. We apply a QERA methodology that integrates different models: 1) a frequency assessment method that accounts for the accidents rates that lead to oil spills; 2) a computational routine to simulate the oil transport and transformation in the ocean; 3) ecotoxicological information that addresses for individual-level effects due to the oil

exposure; and finally, 4) a probabilistic ecological model that can consider uncertainties and variability in parameters and can describe the impacts of the pollution at a population level. Figure 1 depicts this integration.

Figure 1 - Model integration that constitutes the QERA methodology

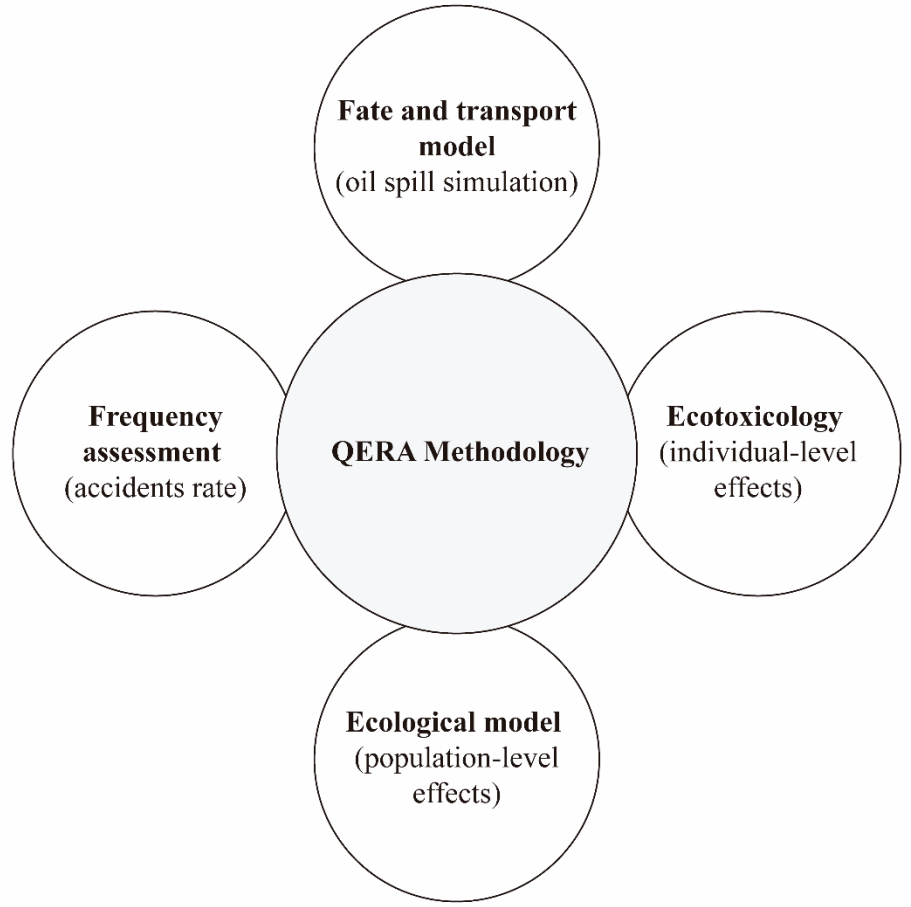

Source: Adapted from (DUARTE, 2011) (p. 7)

1.2 RATIONALE AND CONTRIBUTION

Oceanic islands are considered hotspots of biodiversity and host of a large number of endemic species. Additionally, their isolation makes them a repository of threatened species as priority regions for legal conservation acts (GILLESPIE, 2001; GOVE et al., 2016; WHITTAKER; FERNÁNDEZ-PALACIOS, 2007). Among Brazilian oceanic islands, Fernando de Noronha Archipelago (FNA) is the best-studied. FNA is located between latitudes $03°45'S$ and $03°\,57'S$ and longitudes $32°\,19'W$ and $32°\,41'W$, in the Western Equatorial South Atlantic. It is situated approximately 345 km away from the northeast coast

of Brazil, and it is composed of 21 islands and islets with a total area of $26\ km^2$ (Figure 2) (IBAMA, 2005).

FNA has the Conservation Unit status, protecting endemic species and maintaining a healthy island ecosystem (SERAFINI; FRANÇA, 2010). It has the largest number of marine and terrestrial species, attributed to its extension and habitat heterogeneity. Two-thirds of FNA consist of the Marine National Park of FN (PARNAMAR-FN), a marine protected area (MPA) that reaches the 50-meter isobathic line (ICMBIO, 2013). The fundamental objective of creating PARNAMAR-FN is to preserve natural ecosystems with great ecological significance and scenic beauty, enabling scientific research, activities of environmental education, recreation, and ecotourism (BRASIL, 2000).

Figure 2 - Location of the Fernando de Noronha Archipelago (latitude x longitude) in the South Atlantic Ocean.

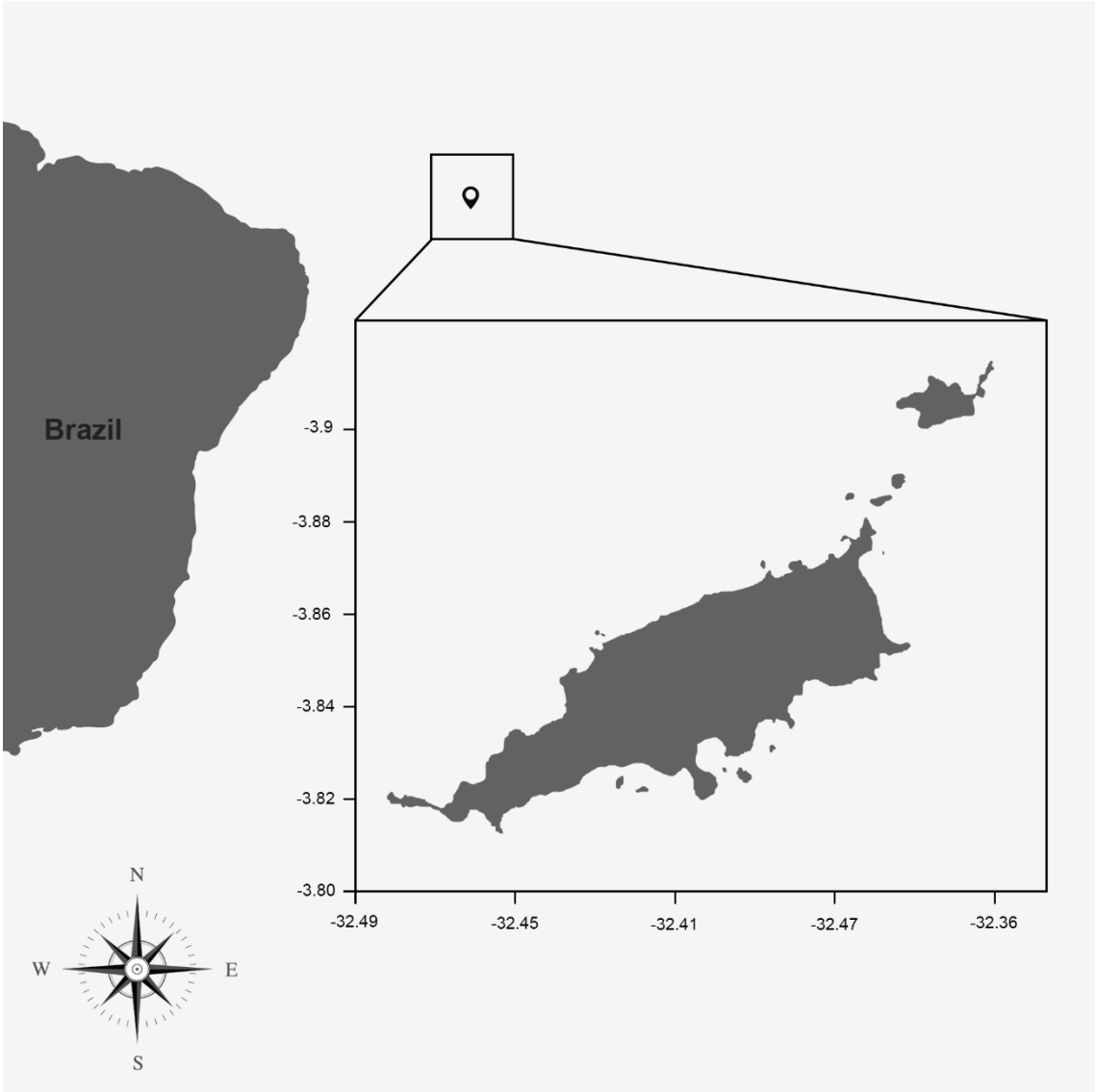

Source: The Author (2021)

The high number of vessels, including oil tankers that circulate the globe, along with extreme events such as storms and tropical cyclones due to global warming, increase the risk of oil spills affecting oceanic islands. However, FNA lacks infrastructure and mitigation plans when facing an oil spill, which could intensify the accident's consequences (QUEIROZ et al., 2019). Managers need to assess and manage ecological risks (hereafter ecorisks) caused by routine (i.e., high frequency/low consequence) human activities within PARNAMAR-FN. Then, these assessments should also contemplate improbable, significant events (i.e., low frequency/high impact). Although there is little evidence of large spills in recent years, it remains a latent threat (IUCN, 2020). In 2019, an oil spill reached more than $4{,}000km$ of the Brazilian northeastern coast and a total of $5{,}000$ ton of oil residures were collected (DANIEL, 2019). More recently, oil fragments have been reported to reach the FNA coast (ICMBIO, 2021). Still, recent industrial accidents such as toxic spills have caused catastrophic damage to the environment and significant economic losses to the responsible company. Table 1 presents a summary of recent accidents globally.

Table 1 - Recent most severe oil spills worldwide.

Industrial accident	Event Year	Location	Impact
The Wakashio, a Japanese bulk carrier, struck a coral reef	2020	Mauritius' coast in the Indian Ocean	Thousands of tonnes of crude oil spilled into the sea, choking marine life in a pristine lagoon.
Oil spill on the northeastern coast of Brazil	2019	Brazil	4,000 km of the coast reported oil's presence, and 5,000 tons of residues from the spill were collected. Damages to corals, mangroves, and marine ecosystems
A collision of the Suezmax Sanchi tanker with a cargo ship.	2018	Shanghai	The ship caught fire and burned for a week. 32 crew members on board were killed; An oil stain of 11 kilometers was formed on the sea surface.
FPSO production ship spill SeaRose	2018	Canada	Approximately 250,000 liters of crude oil from the SeaRose FPSO off the southeastern coast of Newfoundland.
Agia Zoni II	2017	Greece	Approximately 500 tonnes of heavy fuel oil were released at sea, contaminating the Salamina and Athens coastlines.
Leakage of a Chevron owned oil well in the Campos Basin	2011	Brazil	32,000 to 52,000 liters of crude oil enter the ocean every day. There was a minor environmental impact, and no oil reached

Industrial accident	Event Year	Location	Impact
			the Rio de Janeiro shores.
Marine oil spill by a stricken container ship	2011	Coast of New Zealand	About 350 tonnes of oil into the sea. Nearly 1,300 birds have died in the spill.
Explosion in the Deep-Water Horizon platform	2010	Gulf of Mexico	Death of 11 people, more than 600 endangered species

Source: The Author (2021)

As we can see, oil spills originated from transport and handling activities in the ocean caused most incidents. According to the International Tanker Owners Pollution Federation Limited (ITOPF) database, it is estimated that from 1970 to 2020, about 5.86 million tons of oil were discharged into the sea (ITOPF, 2021). The estimate also tells that about 15,000 tonnes/year of crude oil were dumped into aquatic environments in the last ten years (ITOPF, 2021). The oil trade plays a vital role in economic development, and then there is a rise in the maritime transportation of oil volume. Indeed, the oil tankers are responsible for around 90% of the oil transported worldwide (CHEN et al., 2019). Regarding environmental impacts, the oil can contaminate beaches and damage coastal tourism areas, resulting in widespread oceanic pollution and a fatal effect on marine life (SIMECEK-BEATTY; LEHR, 2017). For instance, birds, fish, and other marine life can suffer mass mortality that severely damages marine resources (CHEN et al., 2019).

On average, 75 ships navigate daily on routes near FN (MEDEIROS, 2009), using landmarks to determine the ship's position at sea more precisely and consistently. Many of these ships are oil tankers. The first round of a QERA for oil spills near FNA was conducted by (DUARTE; DROGUETT, 2016), focusing on whether the risks of catastrophic oil spills are tolerable or need management (i.e., recovery or control measures that may reduce risks). However, this study was conservative because it did not assess the fate and transport of the oil in the ocean. The ecosystem's exposure to the pollutants and the frequency estimates were roughly estimated. Thus, this work aims at performing an improved QERA in FNA, including the oil's fate and transport model and a more reliable frequency assessment. Moreover, we constructed a novel stochastic population model to describe the bioindicator dynamics, i.e., the coral reef fish *Sparisoma axillare*. This species was chosen due to its importance to the reef health, responsible for its construction and deconstruction (MALLELA; FOX, 2018).

Thus, this work has two main contributions: a) the FNA application to generate results that can contribute to the ecosystem conservation; and b) a new application of the

methodology proposed by (DUARTE, 2016; DUARTE et al., 2019), allowing to identify limitations and suggest improvements integrating four different models (Figure 1), contributing to the QERA state-of-the-art. These contributions are detailed below:

- The FNA has two Federal Unities of Conservation (UFC): the PARNAMAR-FN (BRASIL, 1988) and the Fernando de Noronha MPA – MPA/FN (BRASIL, 1986), which shows its ecological relevance and the need for adopting conservation measures. Despite the high number of ships that travel near FNA, it does not have infrastructure or contingency plans if a spill occurs (QUEIROZ et al., 2019), which would amplify its impact. One of the effects is the adverse consequence on coral reefs and their marine life. Its loss could have socio-ecological consequences because it protects the coast, is essential for eco-tourism in the area, and contributes to the fisheries. The impacts would affect the environment and the FNA inhabitants that depend on the island's natural resources for survival. Thus, this work results would help decide on measures to avoid such a catastrophic event and mitigate its impacts.
- We integrate different models to perform QERA. At first, we opted for an unprecedented method in the context of maritime accidents, i.e., the Bayesian Population Variability Analysis (BPVA), that can aggregate information from databases and expert's judgments to estimate better the frequency of accidents that can cause oil spills (DROGUETT; GROEN; MOSLEH, 2004; MOURA et al., 2016). Regarding the simulation of oil spills trajectories and transformations in the ocean near FNA, we use the Lagrangian fate and transport model MEDSLIK-II (DE DOMINICIS et al., 2013a, 2013b). Moreover, a stochastic ecological reference model (the benchmark) for a bioindicator species is built to quantify the impacts on the FNA ecosystem due to oil exposure. This impact is quantified as the risk of decline of the bioindicator. In this way, the methodology compares several scenarios to the benchmark to quantitatively assess, rank, categorize, and communicate risks in the long term due to oil spills. This approach allows us to describe the ecosystem dynamics under future scenarios' influence. Thus, the work will contribute to science advancement by integrating new models into the risk assessment resulting in interdisciplinary work.

1.3 OBJECTIVES

1.3.1 General objective

The primary objective is to improve the QERA methodology proposed by (DUARTE et al., 2019) using oil spill simulation, frequency estimates from data and experts' opinions, and a stochastic model to more accurately quantify ecorisks (i.e., adverse effects to plants and animals) to FNA. Furthermore, it can also provide beneficial results to aid decision-making regarding the best strategies to cope with an oil spill in FNA.

1.3.2 Specific objectives

- To provide a theoretical basis regarding QERA and the models that compose the assessment;
- To use computational routines to simulate the oil trajectory and physicochemical transformations in the ocean;
- To estimate the frequency of accidents using information from maritime accidents database and expert opinions;
- To build a stochastic population model for a coral reef fish that is representative of the FNA ecosystem;
- To quantify the risks that a potential oil spill in the archipelago surroundings can cause to the ecosystem;
- To compare the results of this dissertation with the results of the first-round QERA performed by (DUARTE; DROGUETT, 2016).

It is not the purpose of this work to conduct risk management. However, we will discuss the risk assessment results and suggest some management measures.

1.4 DISSERTATION STRUCTURE

The remainder of this work is structured as follows. The specific objectives are presented in dedicated chapters mainly because Chapters 4 and 5 require sophisticated mathematical models with potential for scientific publication. Thus, they were written separately to facilitate further publication. Finally, Chapter 6 integrates the four models and also has potential for publication. The summary of the chapters that structure the dissertation is presented as follows:

- Chapter 2 provides a theoretical background to understand this work thoroughly and reviews the literature regarding risk assessment for oil spills. It examines the basic concepts of ecology, the role of ecological modeling in risk assessments, the modeling of oil spills on the ocean surface, and finally, the combined use of databases and experts' judgments to improve frequency assessments;
- Chapter 3 details the Quantitative Ecological Risk Assessment (QERA) methodology used in this research;
- Chapter 4 presents the frequency assessment for the occurrence of maritime accidents that can lead to oil spills. This chapter content was approved for presentation at the 5th conference of the Brazilian Association of Risk Analysis, Process Safety, and Reliability (ABRISCO). It is also being prepared for submission in a high impact journal;
- Chapter 5 presents the results of the oil spills simulation near FNA. This chapter content was also approved for presentation in the 5th conference of the ABRISCO, and it is also being prepared for submission in a high impact journal;
- Chapter 6 consists of applying the QERA methodology for oil spills near FNA. Results from Chapter 4 and Chapter 5 will be incorporated into this chapter;
- Chapter 7 provides concluding remarks, acknowledges limitations, and proposes future work directions.

2 THEORETICAL BASIS AND PRELIMINARY LITERATURE REVIEW

2.1 BASIC CONCEPTS OF ECOLOGY

Ecology is the science that studies relations among living beings and the environment in which they live and their reciprocal influences, including the human aspects that affect and interact with the planet's natural systems (ODUM; BARRET, 2005). The environment is the sum of all external conditions affecting an organism's life, development, and survival (EPA, 2011). The environment encompasses humans, materials, physical and ecological environments (i.e., plants, animals, and microbes).

The biological world is very complex, divided into biological hierarchy levels, as shown in Figure 3. The ecology studies only from individual organism level to higher levels, and EPA provides definitions to these (EPA, 2011):

- Organism refers to any form of animal or plant life.
- Population refers to a group of interbreeding organisms occupying a particular space. Each population has its characteristics: abundance, birth rate (fecundity), deaths rate (mortality), age distribution, dispersion, and growth rate.
- Ecosystem refers to the interacting system of a biological community and its nonliving environmental surroundings.
- Landscapes are the traits, patterns, and structure of a specific geographic area, including its biological composition, physical environment, and anthropogenic or social patterns. A space where interacting ecosystems are grouped and repeated in a similar form.

Figure 3 - Hierarchy of biological endpoints.

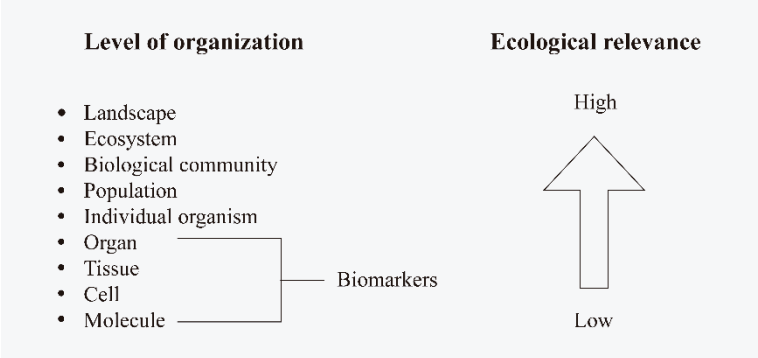

Source: Adapted from Pastorok et al. (2002, p. 4).

Habitats used by most species around industrial sites are becoming fragmented by human activities. Consequently, several distinct populations of the same species live separated, despite interacting at some level (e.g., exchange of individuals). There are relatively few cases where the entire population resides within the same area. Hence, most species are distributed across space as a large population of connected minor populations. This way of living characterizes a metapopulation, a set of populations of the same species in the same general geographic area with a potential for migration among them (PASTOROK et al., 2002). This way, some ecological models are designed to link the Geographic Information System (GIS) with a metapopulation model, combining geographic and demographic data for risk assessment.

The methodology used in this work focuses on population and metapopulation-level risks, i.e., the potential for adverse effects on (meta)populations.

2.1.1 Ecotoxicology

Ecotoxicology is defined as the branch of toxicology concerned with studying toxic effects caused by natural or synthetic pollutants, the constituents of ecosystems, animals (including humans), vegetables, and microbial, in an integral context (TRUHAUT, 1977).

Ecotoxicology plays an essential role in ERA because it provides knowledge about toxic effects on individual organisms caused by chemical exposure and the representative species in an ecosystem. Knowledge of individual-level effects is essential to predict higher-level effects such as population abundance (or density), community species richness, productivity, or organisms' distributions. Likewise, because the assessment of all species of an ecosystem would require huge costs and a long time, knowledge of the representative species is necessary to make the evaluation tractable.

2.1.2 Population dynamics

Population dynamics is an ecology discipline that studies changes in population abundance. These studies are essential to analyze and understand what happens to the population in natural conditions (without chemical exposure). Incidentally, population models are used to predict and simulate the dynamics of a population. This section will introduce the main components in population dynamics, whereas Section 3.5 will present a comprehensive overview of population modeling.

The populations that constitute an ecosystem are open systems, i.e., they exchange energy and matter with the external environment. Hence, any attempt to describe and predict a

population dynamic requires knowledge about the interactions between system components, i.e., organisms that compound the population, the system itself, and the external environment (AKÇAKAYA; BURGMAN; GINZBURG, 1999). We need to define the survival, mortality and fecundity, migration, foraging behavior, and density-dependence when appropriate, to characterize a population's dynamics,

Firstly, survival means the number of individuals in a population alive after a given time, and the survival rate indicates the proportion. Age-specific survival rates can be estimated by the equation below:

$$S_x(t) = N_{x+1}(t+1)/N_x(t) \quad (2.1)$$

Where:

- $S_x(t)$: the proportion of individuals present in a given year (t) within a given age class (x) that survives into the next age class $(x+1)$ in the following year $(t+1)$;
- $N_{x+1}(t+1)$: number of individuals in age class $x+1$ at time $t+1$;
- $N_x(t)$: number of individuals in age class x at time t;

Given that, mortality is the number of individuals of a population that died in a given period. The death rate can be expressed as $1 - S_x(t)$.

Concerning fecundity (F), by definition, it means "the number of live offspring per individual in a given age class that will survive to be counted in the first age class"(PAUWELS, 2002). However, calculating fecundity depends on the available data. If sufficient information is available, fecundity can be estimated by the equation:

$$F_x(t) = \frac{p_0(t)N_0(t+1)}{N_x(t)} \quad (2.2)$$

Where:

- $p_0(t)$: proportion of juveniles (age 0) that were produced by individuals in age class x at time t;
- $N_0(t+1)$: number of juveniles at time $t+1$;

Field data need to be collected to estimate survival and fecundity. Still, if the target species' data are insufficient, one could extrapolate the related species' information to the target species (PAUWELS, 2002).

There are also features concerning the movement of a population, i.e., migration and foraging behavior. The term migration denotes all or part of a population moving from one habitat to another (AIDLEY, 1981). Incidentally, it is the primary way of interaction within a metapopulation. Foraging behavior consists of an organism's methods to acquire and utilize

sources of energy and nutrients. These methods encompass location, storage, consumption, and retrieval of resources.

Moreover, the foraging theory tries to predict how an animal would choose to forage within its habitat, considering the knowledge of competition, predation risk, and resource availability (KAREN-KOY, 2007). The larger the foraging area, the more food will be available. In contrast, the organism will spend more energy and take more risks since the exposure to predators in areas beyond its natural habitat will be greater. It is important to emphasize that the population foraging area should be considered in a QERA when the environment's spatial structure has crucial effects on the population dynamics.

Another fundamental process within the population dynamics is its regulation via density dependence on survival, mortality, fecundity, and population movement. The population growth rate phenomenon depends on the current population density (or abundance) (AKÇAKAYA; ROOT, 2013). As is observed in wildlife populations, they are often changing in size, but fluctuating around an equilibrium abundance for long periods, unless a disturbance occurs (e.g., pollution, harvest, culling, poaching, catastrophe, etc.). Consequently, it is essential to incorporate density dependence to describe a population dynamic because it causes the population to reach a stationary state (which may fluctuate due to stochasticity). This equilibrium population, known as carrying capacity, is the abundance level above which the population tends to decline (PAUWELS, 2002).

Many possible mechanisms yield density dependence: fecundity may decrease, mortality may increase with competition for limited resources, the crowded conditions may lead to social strife or cannibalism. Population growth may also be affected negatively as population size reaches shallow levels. This phenomenon, arising from Allee effects, draws a small population away from the carrying capacity and toward extinction. A brief example can clarify the concept of density-dependence: on the one hand, when there are too many organisms living in the same space and being part of the same population, food may become less available, and competition among the individuals starts. Consequently, negative density dependence manifests itself (e.g., more individuals dying and emigrating) so that the abundance will decrease to a quantity in which food is sufficient for all individuals again.

To conclude, another fundamental component of population dynamic is the natural variability in all its features. In other words, changes in survival, fecundity, migration, and carrying capacity may occur unpredictably. For this reason, any attempt to describe a population dynamic should account for stochasticity in those parameters to better represent reality.

2.2 RISK, HAZARD, THREAT, CONTROL MEASURE, RECOVERY MEASURE, CONSEQUENCES AND ACCIDENTAL SCENARIO

The American Institute of Chemical Engineers (AIChE) defines risk as a measure of human injury, ecological damage, or economic loss regarding the accident likelihood and the magnitude of the consequences (AICHE, 2000). This definition is sufficient for the representation of risk in this work.

This work focuses on ecological risks, the magnitude of the consequences regards environmental damage and is quantified as a measure of time and population probability of extinction (or decline). This measure is widely accepted and used by the scientific community in ERA and the quantitative measure used by the International Union for Conservation of Nature (IUCN) to classify plants and animals at risk (IUCN, 2012).

It is also essential to differentiate between the terms hazard and risk. The former is a potential source of damage, whereas the latter combines the likelihood of damage and its severity (in defined circumstances). For example, on the one hand, a significant volume of oil under pressure has the potential to cause damage, so it is a hazard. On the other hand, overpressure may cause an oil spill with defined circumstances (such as total mass released, time of the spill, hydraulic flow) and cause specific damage that can be measured. Combining the oil spill's likelihood of occurrence with the magnitude of the damage characterizes the risk.

As already mentioned, the hazard is a potential source of damage (usually in energy). Threats are the initiator events, which could cause the hazard to be released, although hazard and threats are sometimes taken to mean the same. Control measures (e.g., safety management systems, alarms, automatic stops) are barriers and preventive actions that can control the threats and avoid the accident (top event) occurrence to reduce the risk of the top event's frequency of occurrence. The top event is the accident. Recovery measures are mitigation actions to reduce the magnitude of the consequences and so reduce the risk. They can be, for example, re-routing of spills, burning the oil before it reaches an ecosystem, pollution remediation, habitat protection, translocation, or reintroducing individuals in the population. Consequences are the damage, impacts, or effects. Notably, preventive measures include both control and recovery measures. Finally, an accidental scenario, or just scenario (SCN), is consolidated by defined circumstances to all these factors.

Lastly, there are two types of toxic risks: risk to human health and ecological risk. The former refers to the potential that adverse effects on human health may occur or occur due to

exposure to a toxic substance. The latter refers to the possibility that adverse ecological effects may arise or occur due to exposure to a poisonous substance.

2.3 Quantitative Ecological Risk Assessment

A Quantitative Risk Assessment (QRA) quantifies frequent incidents with minor impacts to even rare events with significant consequences. The principal motivation of carrying out a QRA is that its results demonstrate the risks caused by the establishment or industrial activity, prioritize which risks require some action, and decide between different measures to reduce those risks. Thus, the QRA is necessary for objective decision-making related to the establishment's safety, surrounding communities, and ecological environment.

Specifically, the Ecological Risk Assessments (ERA) transform scientific data into meaningful information about human activities' environmental risk (EPA, 1998). When the information is provided by assigning values (i.e., quantifying) the risks, the ERA can be addressed as a Quantitative Ecological Risk Assessment (QERA). So, QERA can be defined as the formal process of estimating the probability of adverse ecological effects due to exposure to one or more stressors in the short and long term.

Adverse ecological effects are changes that are considered undesirable because they alter valued structural or functional characteristics of ecosystems or their components. They are evaluated through assessment endpoints and measurement endpoints. An evaluation of adversity may consider the type, intensity, and scale of the effect and recovery potential (EPA, 1998). According to Pastorok *et al.* (2002), we have that:

- Assessment endpoints: they are environmental characteristics or values that are to be protected, e.g., wildlife population abundance, species diversity.
- Measurement endpoints: quantitative expressions of an observed or measured biological response, such as the effects of a toxic chemical on survivorship or fecundity, related to the valued environmental characteristic chosen as the assessment endpoint.

Endpoints could be expressed as effects on individual organisms, populations, communities, ecosystems, and landscapes. Thus, the definition of QERA allows for risk assessment to be conducted at various levels within the biological hierarchy (Figure 3). However, many QERAs consider only individual endpoints and fail to view population, ecosystem, or landscape endpoints.

Hence, a QERA that ignores population-level effects and focuses only on individual-level endpoints may lead to inaccurate risk estimates. This approach will cause errors in

environmental and risk management decisions and lead to inefficiency. Overestimation of risk can lead to a waste of resources to mitigate apparent problems that are not important. In contrast, underestimating risk can lead to inadequate risk management to control and prevent adverse effects on the ecological environment.

Population-level effects or higher-level effects can be obtained with the use of ecological models in the QERA. Such ecological models are essentially used to translate individual-level endpoints' responses into impact on population, ecosystem, or landscapes endpoints. Particularly, when they focus on population-level effects, they are called population models.

In a straightforward case, a population model can predict the expected numbers of individuals in a population in the future from estimates of survivorship and fecundity for individual organisms. Thus, chemical effects can be modeled by perturbing the survivorship and fecundity values based on knowledge about changes in these parameters obtained from toxicity test results (PASTOROK et al., 2002).

Risk assessment can evaluate the probability of future population extinction (or decline) under several environmental conditions, SCNs, and management actions. QERA approach based on ecological models (particularly population models) to obtain population-level measures has excellent advantages. The following section introduces a theoretical basis for the use of ecological modeling in risk assessment.

2.4 ECOLOGICAL MODELING IN RISK ASSESSMENT

An ecological model is a mathematical expression that describes or predicts ecological processes or endpoints such as population abundance (or density), community species richness, productivity, or distributions of organisms (PASTOROK et al., 2002). Thus, population and metapopulation models are a classification of ecological models.

The mathematical expression is essentially used to translate individual-level effects (e.g., increased mortality, reduced fecundity) using measurement endpoints into population-level impacts (e.g., decreased abundance, increased risk of extinction) using assessment endpoints. So that one can estimate the risk of adverse effects on a population via toxicity data expressed as negative effects on the individual organism. That is the primary rationale for ecological modeling in risk assessment. Moreover, once formulated, the ecological model may help assess natural recovery, develop monitoring programs, plan restoration strategies, or derive remedial action goals (PASTOROK et al., 2002).

It is important to note that there are several other components in population dynamics rather than survival and fecundity, as described in Section 2.1.2. They can also be incorporated into a population model. Some extensions to a population model are shown below. For more details, see the references (AKÇAKAYA; BURGMAN; GINZBURG, 1999; PASTOROK et al., 2002):

- Age or stage structure;
- Sex structure;
- Parameters vary with time due to stochasticity
- Parameters vary with time due to deterministic trends;
- Parameters vary in space: population-specific models for metapopulations;
- Parameters vary with abundance: density dependence;
- Additive effects: introduction, harvest, migration between subpopulations in a metapopulation, and catastrophes (e.g., industrial accidents).

Figure 4 illustrates the idea of a straightforward ecological model at the population level (i.e., population model). The left side of the image (green boxes) describes the natural dynamics of the population in the future, i.e., without chemical exposure. In contrast, the right site (red boxes) considers chemical exposure. In this straightforward illustration, the future population abundance (assessment endpoint) is predicted through the survival and fecundity rates (measurement endpoints) and the initial population abundance. Once again, several other variables can influence future population abundance. On the one hand, including different variables makes the model more realistic; on the other, it becomes more complicated and requires more data. It depends mainly on the modeler’s knowledge about the population, the available data and resources, and the modeling’s objectives.

Figure 4 - The basic idea of a population model without (left side) and with (right side) chemical exposure.

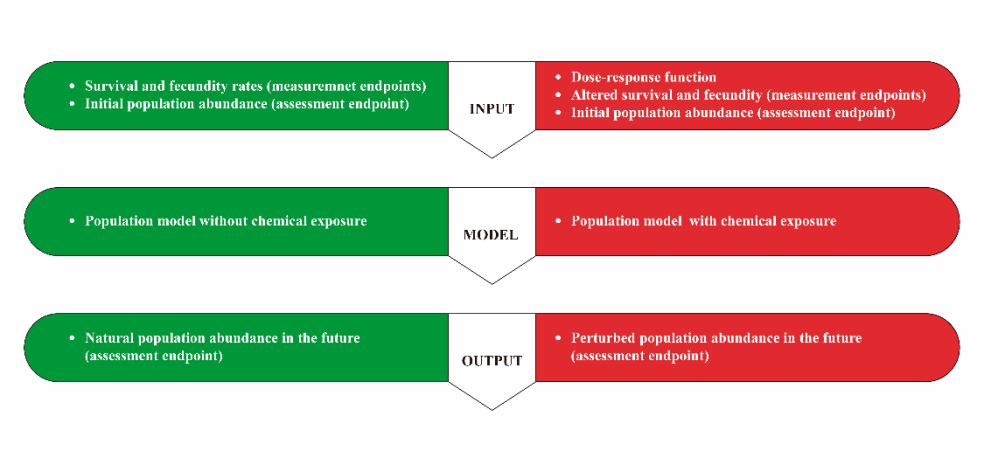

Source: Adapted from Duarte (2016, p. 38 and 39).

Generally, field sampling is used to estimate values to the measurement endpoints and the assessment endpoints' initial conditions. In contrast, an exposure-response assessment is conducted to describe the relationship between the concentration of the chemical and the magnitude of the individual-level responses of native species (represented by changes in measurement endpoints). This relationship is usually specified by a dose-response function so that it is necessary data on the long-term effects of the chemical on the species being analyzed.

The purpose of the methodology used is to conduct a QERA at the population level. The reason for choosing (meta)population modeling is that apart from providing ecologically relevant endpoints, (meta)population models are much more tractable than higher-level models. Figure 5 illustrates this point of view. Despite that, it is possible to strategically choose populations of native species that can effectively represent the ecosystem integrity. Besides, any genuine attempt to model population dynamics should account for stochasticity, mainly because a fluctuation is a prominent and often predominant feature of ecological environments. How to model stochasticity will be discussed in Section 2.4.2.

Figure 5 - Relevance and tractability of ecological models concerning endpoints.

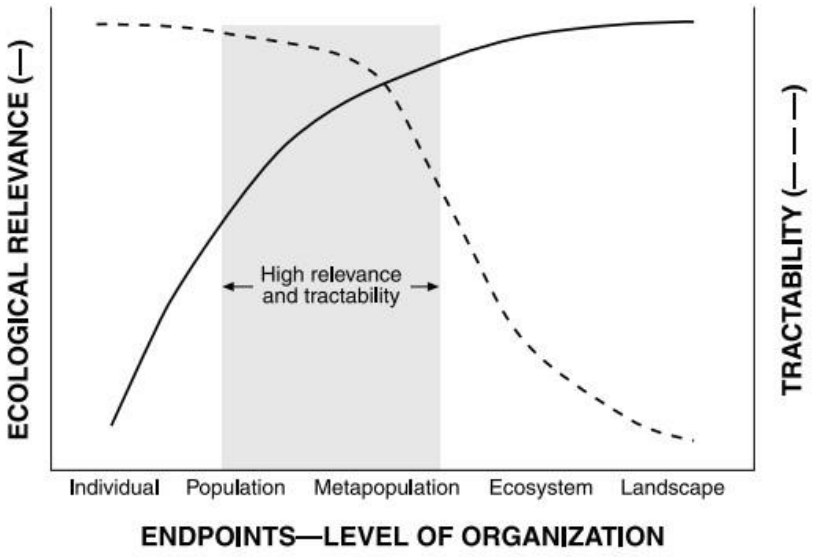

Source: Pastorok et al. (2002, p. 213).

2.4.1 Age and stage structure

The age or stage structure of a population refers to age/stage classes within the population. They attempt to consider that individuals of different ages have different characteristics reflected in their vital rates (e.g., survival and fecundities rates). In contrast,

individuals of the same age have similar characteristics. For instance, juveniles may have lower survival rates than adults, or juveniles may not reproduce until they become adults. Conversely, in an unstructured (scalar) population model, the population is represented by a single age/stage, which denotes the population's totality. Thus, unstructured models are considered a particular case of structured models, with only one class of organisms (PAUWELS, 2002).

Structured models are helpful if individuals' vital rates in different classes are different enough to justify their life span's discretization. Individual classes mean their ages or stages. For example, a fish population model with a life span of nearly 4 years could be structured by their ages, e.g., zero-year-old, one year, two years, and three years, or by their stages: juveniles (zero-year-old) and adults (one-year-old or more). The criteria to structure a model by stages instead of ages are: individuals' ages are unknown; vital rates depend on stage or size rather than age; growth is plastic; some individuals are developmentally disabled or have accelerated vital rates.

Those individuals of the same age/stage are assumed to have the same survival and fecundity rates. However, those rates may differ between classes. This way, a structured population model has a survival rate, S_x, a fecundity rate, F_x, and an abundance at time t, $N_x(t)$ for each age/stage class x. Each class's abundances form a vector of numbers (one for each class), whereas the vital rates are combined to form a transition matrix used in most population models to account for age or stage structure. It is a transition matrix with a unique structure called a Leslie matrix for age-structured models (LESLIE, 1945) and a Lefkovitch matrix for stage-structured models (LEFKOVITCH, 1965). Below is an example of a Leslie matrix:

$$L = \begin{bmatrix} F_0 & F_1 & F_2 \\ S_0 & 0 & 0 \\ 0 & S_1 & 0 \end{bmatrix} \tag{2.1}$$

The reason for arranging the survival rates and fecundities in the form of a matrix is to provide a convenient way to make projections of the population's structure from one generation to the next (PAUWELS, 2002). For example, for an age-structured model, the distribution of abundances in the next step is given by the matrix multiplication:

$$\begin{bmatrix} N_0(t+1) \\ N_1(t+1) \\ N_2(t+1) \end{bmatrix} = \begin{bmatrix} F_0 & F_1 & F_2 \\ S_0 & 0 & 0 \\ 0 & S_1 & 0 \end{bmatrix} \begin{bmatrix} N_0(t) \\ N_1(t) \\ N_2(t) \end{bmatrix} \tag{2.2}$$

Where $N_x(t)$ denotes the number of individuals of age class x at time t.

Assessors may then choose which age/stage classes they are interested in assessing. In most cases, they will be interested in the total population abundance, the sum of the age abundances. In some cases, however, they may be interested in the abundance of a specific class only.

2.4.2 Stochasticity

The variability and uncertainty in populations and their environment is a fundamental component of population dynamics. Population models that assume all parameters to be constant (i.e., deterministic models) fail to account for unpredictable natural population dynamics fluctuations. Conversely, stochastic models allow us to consider these fluctuations. They involve replacing constant parameters, such as survival and fecundity rates and carrying capacity, with random variables responding to a probability distribution function (PDF), usually a normal or lognormal with a certain mean and variance.

There are many different kinds of stochasticity to be incorporated into a stochastic population model, such as:

- Environmental temporal fluctuations (i.e., temporal variation in parameters);
- Spatial variation (e.g., population-specific parameters for metapopulations);
- Measurement and sampling errors that introduce additional uncertainty in parameter estimates of a population;
- Demographic stochasticity because individuals only occur in whole numbers and most parameters may be fractional numbers, there will be additional uncertainty in the number of survivors and births in the next time-step;
- Model uncertainty, i.e., uncertainty concerning the structure of the equations used to describe the population;
- Catastrophes, i.e., extreme environmental events that adversely affect significant proportions of a population (e.g., fire, drought, flood).

Nevertheless, catastrophes will be a particular type of stochasticity in the methodology used. It allows SCN to be considered as significant and rare environmental events included in a population model with a certain probability of occurrence per step that may be constant or vary with time. In other words, at each time step, a catastrophe (or an AS) may happen with a certain probability. If it happens, its effects of pollution can be modeled by changes in parameters since the present time step; if not, all parameters remain the same.

The risk can be estimated through multiple simulations of the ecological model via Monte Carlo. Since a stochastic model has probabilistic components characterized by random

variables responding to a PDF, there will be a different result for every single run. Thus, the results will also form a PDF that will characterize the risk estimates (e.g., risk of extinction and population decline). Following such a procedure will allow variability to be evaluated as a degree of confidence and estimate upper and lower bounds on risk measures to assess uncertainty.

Thus, a population model with random variables, representing reality better, is a stochastic model since the input variables and initial conditions respond to a PDF. Hence, the model does not provide a single result but a distribution of consequences associated with probabilities. The following section presents the ways of expressing the results of a stochastic population model.

2.4.3 How to express risk estimates

The most traditional measure to summarize the results of a population model is the expected population trajectory (i.e., the expected number of individuals in a population in the future), which is usually expressed by a mean, a ±1 standard deviation, a minimum, and maximum values. However, several ecological-related problems and questions that population models address are phrased in terms of probabilities. For instance, a specific population of a particular species may have a 50% chance of extinction in the next 10 years (i.e., a "critically endangered" population according to IUCN, the International Union for Conservation of Nature (IUCN, 2012)).

The probability is usually derived from multiple runs (Monte Carlo) of a population model and may be expressed in many ways as bellow (PASTOROK et al., 2002). The selection of a specific expression for the probability depends partly on the assessment's objectives and partly on available information for the species being modeled (PASTOROK et al., 2002).

- **Interval decline probability** is the probability of a population declining by as much as a given percentage of its initial value at any time during the period of prediction.
- **Interval extinction probability:** the probability of a population falling as low as a given abundance at any time during the period of prediction.
- **Terminal decline probability:** the probability of a population being as much as a given percentage lower than its initial value at the end of a simulation.
- **Terminal extinction probability:** the probability of a population being as low as a given abundance at the end of a simulation.

- **Interval explosion probability:** the probability of a population equaling or exceeding a given abundance at any time during the period of simulation.
- **Terminal explosion probability:** the probability of a population being as great as or greater than a given abundance at the end of a simulation.
- **Time to extinction:** the time required by a population to decrease to less than a given threshold abundance.
- **Time to explosion:** the time required by a population to exceed a given threshold abundance.

There are other practical single measures to summarize the predictions of the risk curves (AKÇAKAYA; ROOT, 2013):

- **Expected minimum abundance:** the average (overall replications) of the minimum population abundance of the trajectory. It estimates the smallest population size that is likely to occur within the simulated time.
- **The median time to extinction:** is the median value in the PDF of the time to extinction, i.e., the probability that the population will go below a given threshold before that time is 50%.

2.5 LITERATURE REVIEW

Due to the significant impacts of oil pollution, the development of risk assessment models for oil spills is an ongoing research area. Various new methodologies for quantifying such risks have been applied in the marine environment (AMIR-HEIDARI et al., 2019; AMIR-HEIDARI; RAIE, 2018, 2019; ARZAGHI et al., 2018; GUO, 2017).

Guo (2017) has developed a statistical model for probabilistic oil spill risk assessment. The statistical risk assessment model integrates a wave-current coupled model (coupling SELFE (ZHANG; BAPTISTA, 2008) and SWAN (BOOIJ; RIS; HOLTHUIJSEN, 1999)), a deterministic oil spill model (GUO et al., 2014), and a probabilistic methodology. In that model, multiple hypothetical spill scenarios are modeled. The risk index for each receptor cell is calculated as the product of five variables: spill probability, cell area, average oil slick thickness, mean exposure duration, and sensitivity index.

Arzaghi et al. (2018) proposed an ecological risk assessment methodology using Bayesian Networks (BN). BN are directed acyclic graphs used for reasoning under uncertainty by considering casual relationships (represented by directed arcs) among many random variables (defined by chance nodes). The overall risk is estimated considering the risk

quotient, i.e., the Predicted Exposure Concentration (PEC) ratio over the Predicted No Effect Concentration (PNEC).

Amir-Heidari and Raie (2018) have developed a structured framework for probabilistic risk assessment of oil spills from offshore oil wells. The authors used GNOME (ZELENKE et al., 2012) and ADIOS (LEHR et al., 2002) to simulate the spills and obtain oil concentrations. The scenarios with different release sources (i.e., production wells), release amounts, and frequencies were assessed. The risks were calculated as the product of the frequency of occurrence of the spill (estimated by empirical formulations, the concentration that reaches each receptor (i.e., a part of the shoreline), and the sensitivity (vulnerability) index. The risks for each receptor were calculated, aggregating the risks posed by different sources.

Amir-Heidari and Raie (2019), in another work, presented a stochastic model for oil spill risk assessment as an attempt to cover the limitations of the NOAA's Trajectory Analysis Planner (TAP II). In this new model, the input variables (e.g., release volume, duration, rate) were defined as probability distributions to propagate the uncertainties through the model.

GNOME and ADIOS were once again used. In research by Amir-Heidari et al. (2019), they developed a model for spatial and stochastic oil spill risk assessment, utilizing a shipwreck case study. They estimated the probability of an oil spill from the wreck using expert elicitation and Bayesian updating in a Fault Tree Analysis (FTA) framework. Similarly, the risks were measured by the spill mean probability and the mean impact (exposure times the sensitivity index) of the spill for the receptors.

All those works were instrumental for ecological risk assessment for oil spills in the marine environment. However, in the risk quantification, the consequence assessment was made based on the concentrations that reach a specific region and are helpful only to estimate individual effects, not the actual impact on the environment. Our approach quantifies risks as the extinction probability of a representative species due to the exposure to the pollutant through a stochastic ecological model. Such a model is a mathematical expression used to translate individual-level effects (e.g., increased mortality due to oil exposure) using measurement endpoints into population-level impacts (e.g., decreased abundance, increased risk of extinction). Thus, we can estimate how the spill will impact the environment surrounding the spill. Besides, our work simulates the oil trajectory and transformations in the ocean from transportation accidents, using a Bayesian approach to estimate the probability of such accidents.

3 QUANTITATIVE ECOLOGICAL RISK ASSESSMENT METHODOLOGY

The QRA methodology used is based on population modeling and can consider extreme and infrequent events, and it is flexible for microbial and ecological risks (DUARTE et al., 2019). When assessing microbial risks, the methodology can quantify risks to humans due to exposure to one or more pathogens, such as the risks to the public health system due to the COVID-19 pandemic (SIQUEIRA et al., 2021). For ecological risks, the methodology considers both the event's frequency of occurrence and the magnitude of the adverse ecological effects, capable of quantifying ecological risks caused by events with a low frequency of occurrence and catastrophic consequences. It can also predict populations' responses to toxic exposure (via population-level endpoints), considering the relationships between individuals, the species' life history, and ecology. The methodology can assess the risk of population extinction (or decline) in the future under the influence of a catastrophic accident and human impacts (DUARTE et al., 2013; DUARTE; DROGUETT, 2016; DUARTE; DROGUETT; MOURA, 2018). More details on the methodology can be found in Duarte et al. (2019) and Duarte (2016).

The steps of the methodology are as follows:

1. Characterization of the problem;
2. Identification of hazards and consolidation of scenarios;
3. Assess exposure to risks;
4. Frequency estimates
5. Population modeling
6. Risk quantification and categorization

The methodology is iterative so that revaluation may occur during any part of the risk assessment. We illustrate the methodology as a flowchart, with each step's main inputs and outputs in Figure 6. The general steps are described in the following sections. Specific methods used in each step, as presented in the specific objectives, will be presented as subsections of the respective step.

Figure 6 - Flowchart for the Quantitative Ecological Risk Assessment methodology.

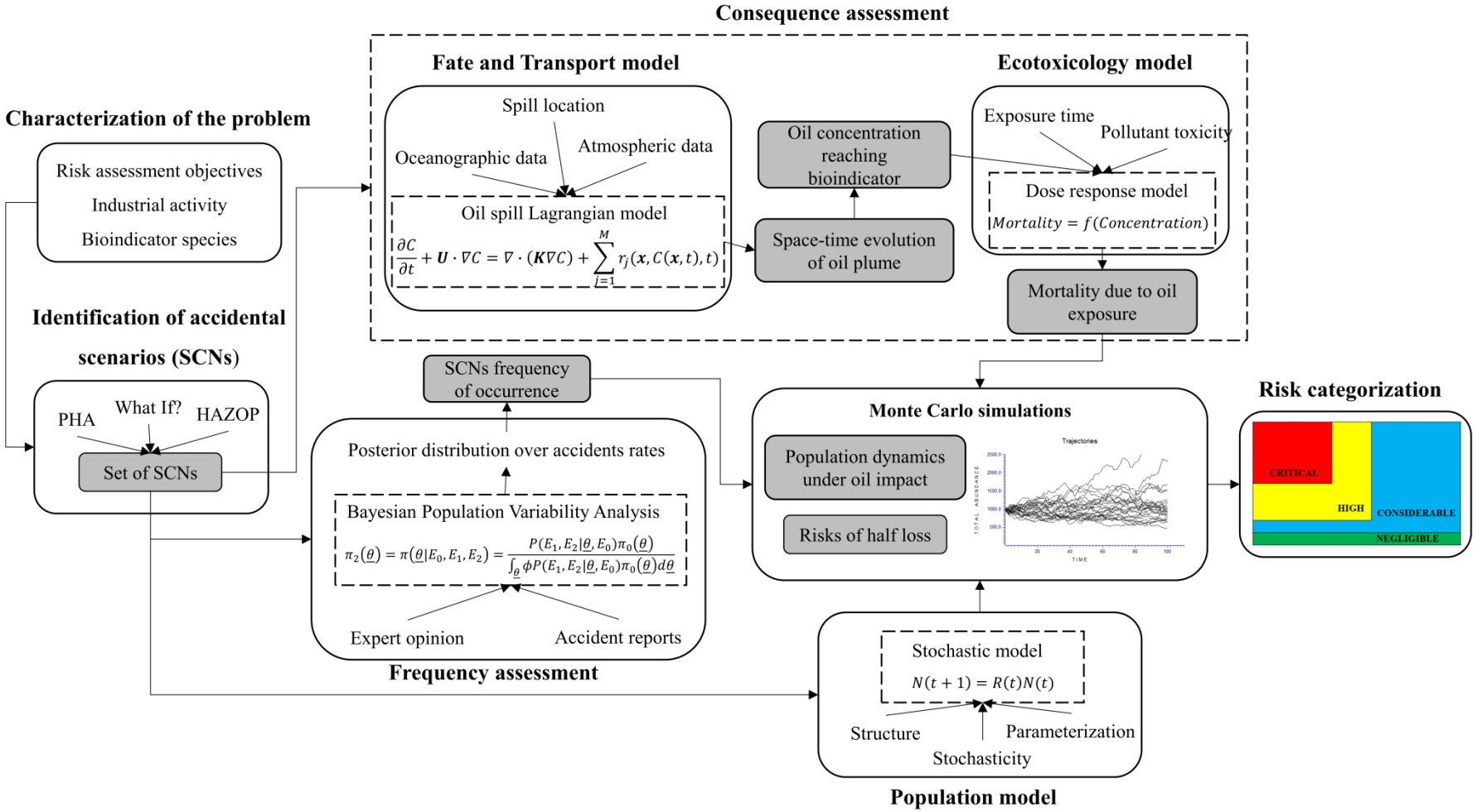

Source: The Author (2021)

3.1 CHARACTERIZATION OF THE PROBLEM

The first step is a planning phase on which the entire risk assessment depends. When appropriate, it requires engagement between the risk assessor and other experts such as risk managers, environmental managers, ecologists, technical managers, operators, and other interested parties (e.g., industrial leaders, government, environmental groups, any segment of society about ecological risks). They should be able to:

1. Define the risk assessment issues and objectives: The risk assessor should ensure that risk management is aided. This way, they should reach a general agreement on characteristics such as the objectives for the QERA (including criteria for success), expected outputs of the QERA, data, and information already available.
2. Characterize the establishment and installations to be included in the QERA: Here, the risk assessor should collect technical information that characterizes the establishment concerning its physical structure, process conditions, chemicals of potential concern, and installations (e.g., storage tanks, transport units, pipelines, loading equipment) that deals with those chemicals.
3. Characteristics of the ecological components: The purpose is to gather information about environmental features affected by accidents in the establishment. The representative species, or bioindicator, is defined alongside information such as habitat and life stages. The bioindicator is more sensitive and serves as an early warning indicator of ecological effects.

3.2 IDENTIFICATION OF HAZARDS AND CONSOLIDATION OF SCENARIOS (SCNs)

It is a qualitative risk assessment step that aims to identify all the initiator events of accidents and their possible consequences. We can apply structured techniques to 1) systematically consolidate all SCNs; 2) to qualitatively rank the risks related to each SCN according to their frequency and severity; 3) to select those AS that should be included for the risk assessment.

The methodology uses the Preliminary Hazard Analysis (PHA) to perform this step (ERICSON, 2005). A worksheet is generally used to report the qualitative information that consolidates each SCN, such as hazard, initiator event, causes, control measures, possible consequences to the ecological environment, frequency, and severity classes.

After the identification of all SCNs, one should select the most relevant to a more detailed assessment. Therefore, one should establish the criterion considered in the selection of the appropriate SCNs. For a conservative approach, one can use a standard based only on the severity class. Therefore, in this work, the severity III or IV (Table 2) criterion is adopted to trigger SCNs for further analysis in the next step.

Table 2 - Severity classes.

Class	Description
I (Minor)	No damage or minor system damage, and does not cause ecological damage
II (Major)	Irrelevant ecological damage
III (Critical)	Considerable ecological damage caused by the release of chemicals, reaching areas beyond the boundaries of the establishment. An accidental scenario results in ecological damage with a short recovery time.
IV (Catastrophic)	Catastrophic ecological damage caused by the release of chemicals, reaching areas beyond the boundaries of the establishment. Accidental scenario results in ecological damage with prolonged recovery time.

Source: Adapted from Petrobras (2008).

Because PHA is often used as an initial risk study in an early stage of a project, this step's results may already be available. In fact, in a human QRA, accidents with the potential to damage humans are identified, which can usually cause ecological damage. In this case, most accidents have already been identified, and the risk assessor should review the environmental effects (i.e., possible consequences) caused by these accidents. This step also systematically identifies the existing accidents and potential ecological damage, leading to improved emergency preparation.

3.3 ASSESS EXPOSURE TO RISKS

This step should be conducted for all SCNs selected in the previous step to a further and more detailed assessment. One must estimate the bioindicator species' exposure to impacts (e.g., harvest, chemical exposure). For SCNs that deal with exposure to chemicals, we may need to apply mathematical models that simulate the occurrence and movement of toxic releases in the water, atmosphere, and soil.

This application includes describing the chemical dispersion and predicting the concentration that reaches bioindicator species over time, i.e., concentrations $C_i(x, y, z, t)$ in location (x, y, z) and at time t, within a defined area (spatial boundaries) for each SCN i. Chemical fate and transport models have often been used to describe and predict the distribution and concentration of chemicals in the environment. Preliminary guidance on fate and transport models is given in Section 3.3.1. We also suggest the references (DE DOMINICIS et al., 2013a, 2013b; QUEIROZ et al., 2019; SEBASTIÃO; GUEDES SOARES, 1995).

For some SCNs, meteorological conditions may influence the chemical dispersion and, consequently, the estimated exposure concentration. A meteorological scenario is defined by parameters that depend on environmental media (e.g., air, soil, water) the chemical moves through. Such meteorological parameters could be, e.g., weather stability class; wind direction and speed; air, soil/bund, water temperature; ambient pressure; humidity; tides of the sea; ocean currents; the season of the year. In such cases, a set of meteorological conditions for each SCN i must be generated. Thus, if one has m SCNs selected from the second step and n meteorological scenarios defined here, one has now mn new SCNs, each with a specific function of exposure concentrations $C_i(x, y, z, t)$. It is helpful to group the data in a limited number of representative meteorological parameters, not to yield an excessive number of new SCNs for the QERA.

To avoid wasting resources, for the following steps, one should select only the exposure SCNs in which population-level effects are likely to occur so that population-level ecorisks should be quantified. The methodology suggests using the hazard quotient (i.e., the estimated exposure concentration divided by a no-effect concentration), a commonly applied criterion (EURECO, 1997). The hazard quotient is calculated as the Predicted Environmental Concentration (PEC) divided by the Predicted No-Effect Concentration (PNEC) to indicate acceptable risk when it is lower than 1 (i.e., PEC < PNEC). The former is provided by the results of chemical fate and transport models. The latter is by ecotoxicological data on the assessed species, usually as a concentration-based endpoint known as No Observed Effect Level.

However, because PEC/PNEC is quite an uncertain measure, we deal with its uncertainty in a very conservative way, in the sense that we do not want to discard SCNs due to uncertainty in this measure. EurEco (1997) suggested using a 100 times lower criterion, i.e., the acceptable risk is only when PEC/PNEC < 0.01. Thus, when PEC/PNEC > 0.01, we select a set of SCNs likely to contribute to causing population-level effects for the next step.

3.3.1 Modeling the Fate and Transport of Oil in the Ocean

For this work, we chose the Lagrangian model MEDSLIK-II to perform the oil spill simulations (DE DOMINICIS et al., 2013a, 2013b). The simulation of the transport, diffusion, and transformation of spilled oil in the ocean can be done using a Lagrangian formalism coupled with Eulerian circulation models. The Lagrangian formalism can track mass elements, such as the droplets of oil in the water; while in the Eulerian approach, the focus is on the flow properties in a specified point in space as a function of time so that one can model the ocean currents (FOX et al., 2014).

Some of the Lagrangian operational models are COZOIL (REED; GUNDLACH; KANA, 1989), SINTEF OSCAR (REED; AAMO; DALING, 1995), OILMAP (SPAULDING et al., 1994), GULFSPILL (AL-RABEH; LARDNER; GUNAY, 2000), ADIOS (LEHR et al., 2002), MOTHY (DANIEL et al., 2003), MOHID (CARRACEDO et al., 2006), POSEIDON OSM (ANNIKA et al., 2001; NITTIS et al., 2006), OD3D (HACKETT; BREIVIK; WETTRE, 2006), the Seatrack Web SMHI model (AMBJORN, 2006), MEDSLIK (LARDNER et al., 2006; ZODIATIS et al., 2008), GNOME (ZELENKE et al., 2012), OILTRANS (BERRY; DABROWSKI; LYONS, 2012), and MEDSLIK-II (DE DOMINICIS et al., 2013a, 2013b).

The wind – shear and stokes drift as a function of the wind speed – and surface currents are the primary forces for oil transport in the aquatic environment (SPAULDING, 2017). Beyond transportation, oil spills impact depends mainly on the environmental conditions that control the weathering processes at the site of the spill (e.g., currents, climate, waves) and the time required to engage mitigation operations (LEE et al., 2015; MARTA-ALMEIDA et al., 2013; NRC, 2003). Weathering is a general definition for changes in oil properties due to physical, chemical, and biological processes when the spill is exposed to environmental conditions (e.g., in aquatic systems). The main weathering processes which govern the fate of an oil slick at sea are spreading (S), evaporation (E), dispersion (D) and emulsification (M). They are illustrated in Figure 7. The general equation for a tracer concentration $C(x, y, z, t)$ in units of mass over volume, mixed in the marine environment is (DE DOMINICIS et al., 2013a):

$$\frac{\partial C}{\partial t} + \boldsymbol{U} \cdot \nabla C = \nabla \cdot (\boldsymbol{K} \nabla C) + \sum_{j=1}^{M} r_j(\boldsymbol{x}, C(\boldsymbol{x}, t), t) \quad (2.1)$$

Where $\frac{\partial C}{\partial t}$ is the local time rate of change of the concentration; $\boldsymbol{U}$ is the sea current mean-field with components (U, V, W); $\boldsymbol{K}$ is the diffusivity tensor with parameterizes the

turbulent effects; $r_j(\boldsymbol{x}, C(\boldsymbol{x}, t), t)$ are the M transformation rates that modify the tracer concentration through the weathering processes, detailed in the following sections (DE DOMINICIS et al., 2013a).

The surface volume is subdivided into a thin part, V^{TN}, and a thick part, V_{TK}. This assumption is made to use the Mackay transformation processes algorithms. In this approach, the weathering processes are considered separately for the thin and thick slick (DE DOMINICIS et al., 2013a). The surface oil volume (V_S) is written as:

$$V_s = V^{TN} + V^{TK} \tag{2.2}$$

Where:

$$V^{TN}(x, y, t) = A^{TN}(t)T^{TN}(x, y, t) \tag{2.3}$$

$$V^{TK}(x, y, t) = A^{TK}(t)T^{TK}(x, y, t) \tag{2.4}$$

A^{TK} and A^{TN} are the areas occupied by the thick and thin surface slick volume, and T^{TK} and T^{TN} are the thicknesses of the thick and thin surface slicks.

Figure 7 - Main weathering processes acting on an oil spill.

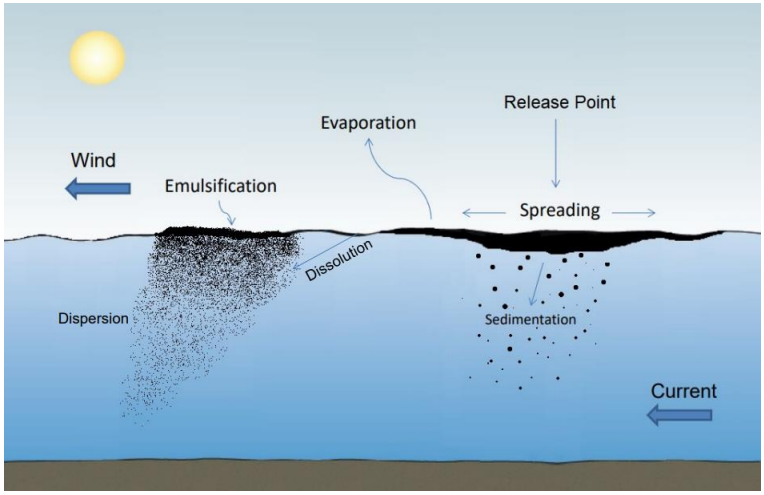

Adapted from TRB and NRC (2014)

3.3.1.1 Spreading

The most dominant process in the first stage of a spill is spreading low pour point (i.e., the temperature below which the oil loses its liquid properties) oil on water. The spreading strongly influences late processes, such as evaporation and dispersion (SEBASTIÃO; GUEDES SOARES, 1995). Spreading consists of two processes: the first is the area lost due

to oil converted from the thick to the thin slick, and the second is due to Fay's gravity-viscous phase of spreading. (AL-RABEH; LARDNER; GUNAY, 2000).

When the oil comes into contact with water, they rapidly reach water temperature, which may be below the waxy oils' pour point. Thus, a pre-requisite for spreading a particular type of oil or refined product after spillage is that its pour point must be lower than the ambient seawater temperature. A high pour point characterizes crude oils with high wax content or refined products, and these materials will quickly solidify either immediately or shortly after spillage at sea. The formation of wax crystal matrices in oil also reduces the oil's ability to disperse naturally as tiny droplets into the ocean, hence the shape often of sizable floating tarballs (SEBASTIÃO; GUEDES SOARES, 1995).

Many oils spilled on the surface of calm water will spread in a continuous layer within a circular pattern due to gravity and net surface tension (or spreading coefficient). The spreading coefficient is the difference between tension and the sum of air/oil surface tension and the oil/water interfacial tension. Although viscosity does affect the spread rate, particularly shortly after spillage, many oils tend to spread on a water surface at about the same rate even though they may possess different viscosities. The dominant physicochemical parameters of the crude oil that determine spreading are thus in addition to its pour point, density, and spreading coefficient (SEBASTIAO; SOARES, 1995).

The thin and thick slick volume rates due to spreading are written as (DE DOMINICIS et al., 2013a):

$$\left.\frac{dV^{TK}}{dt}\right|_{(S)} = -\left.\frac{dV^{TN}}{dt}\right|_{(S)} + T^{TK}FG \tag{2.5}$$

$$\left.\frac{dV^{TN}}{dt}\right|_{(S)} = T^{TN}\left.\frac{dA^{TN}}{dt}\right|_{(S)} \tag{2.6}$$

FG is Fay's gravity spreading, which is defined later. Mackay's model (MACKAY et al., 1979; MACKAY; PATERSON; TRUDEL, 1980) approximates the thin slick area increment by:

$$\left.\frac{dA^{TN}}{dt}\right|_{(S)} = C_1^{(S)}(A^{TN})^{1/3}(T_0^{TK})^{4/3}\exp\left(\frac{-C_3^{(S)}}{T^{TK}+\epsilon}\right) \tag{2.7}$$

Where $C_1^{(S)}$ (s^{-1}) is the constant rate of spreading of the thin slick; $C_3^{(S)}$ (m) controls the dependence on the thickness of the spreading of the thin slick; T_0^{TK} is $1\,m$ and ϵ is a constant parameter for the thickness offset. For the thick slick, Fay's spreading is assumed to be:

$$FG = C_2^{(S)}(A^{TK})^{1/3}(T^{TK})^{4/3} \quad (2.8)$$

$C_2^{(S)}$ is a constant rate of spreading of the thick slick.

The time rate of change of the area of the thick slick due to spreading is:

$$\left.\frac{dA^{TK}}{dt}\right|_{(S)} = \frac{1}{T^{TK}}\left.\frac{dV^{TK}}{dt}\right|_{(S)} \quad (2.9)$$

3.3.1.2 Evaporation

Evaporation is the primary initial process involved in the removal of oil from the sea. The evaporation rate is determined by the oil's physicochemical properties and is increased by spreading, high water temperatures, strong winds, and rough seas. By evaporation, low boiling components will rapidly be removed, thus reducing the remaining slick volume. For many oils, evaporation from the surface slick is the most important mass loss process during the first hours of an oil spill (SEBASTIÃO; GUEDES SOARES, 1995).

The evaporation rate decreases for larger spill volumes since the slick's surface area/volume ratio for these larger spills decreases, i.e., the slick thickness increases. As expected, the rate of evaporation increases with increasing temperature and wind speed. However, this effect is relatively small. Consequently, removing lighter hydrocarbons through evaporation, since the volume reduces, the density and viscosity increase. These parameters' change is essential concerning natural dispersion, emulsification, dissolution, and oil sinking (SEBASTIÃO; GUEDES SOARES, 1995).

The volume of oil lost by evaporation is computed using Mackay's algorithm for evaporation (MACKAY; PATERSON; TRUDEL, 1980). The evaporation changes the volume of the thick and thin parts of the slick. The temporal rate of change of the volume lost by evaporation from the thick slick, V^{TK}, can be expressed as:

$$\left.\frac{dV^{TK}}{dt}\right|_{(E)} = \left.\frac{df_{TK}}{dt}\right|_{(E)} [V^{TK}(t_0) + V^{TN}(t_0)] \quad (2.10)$$

Where $V^{TK}(t_0)$ and $V^{TN}(t_0)$ are the initial thick and thin slick volumes, respectively, and $\left.\frac{df_{TK}}{dt}\right|_{(E)}$ is the time rate of change of the fraction of oil evaporated. For the thick oil slick, the time rate of change of the fraction of oil evaporated is

$$\left.\frac{df_{TK}}{dt}\right|_{(E)} = \frac{P_0 \exp(-cf_{TK}t)}{P_{oil}} K_M \frac{A^{TK}}{V^{TK}}(1 - f_{TK}) \quad (2.11)$$

$$P_{oil} = \frac{RT}{V_{MOL}} \quad (2.12)$$

Where P_{oil}(bar) is the oil vapor pressure; P_0 is the initial vapor pressure (depends on the oil type used); c (s^{-1}) is a constant that measures the rate of decrease of vapor pressure with the fraction already evaporated; $A^{TK}(t)$ is the area of the thick part of the slick; K_M (ms^{-1}) is the evaporative exposure to the wind; T (K) is the temperature; R $(bar\ m^3 mol^{-1} K)$ is the gas constant and V_{MOL} $(mol\ m^{-3})$ is the molar volume of the oil. For K_M we assume:

$$K_M = C_1^{(E)} \left(3.6 \frac{W}{W_0}\right)^{\gamma} \tag{2.13}$$

Where $\frac{W}{W_0}$ is the non-dimensional 10m wind modulus (W_0 is $11 ms^{-1}$); γ is a constant, and $C_1^{(E)}$ (ms^{-1}) is the evaporation rate.

For the thin slick oil, the time rate of change of the volume is equal to:

$$\left.\frac{dV^{TN}}{dt}\right|_{(E)} = \left.\frac{df_{TN}}{dt}\right|_{(E)} [V^{TK}(t_0) + V^{TN}(t_0)] \tag{2.14}$$

Where $\left.\frac{df_{TN}}{dt}\right|_{(E)}$ is the time rate of change of oil fraction evaporated from the thin slick.

The evaporative component in the thin slick is assumed to disappear immediately. Still, through the spreading process, the thin slick is fed by oil from the thick slick that, in general, has not yet fully evaporated. Equating the oil content of the thin slick before and after the flow, we obtain

$$\left.\frac{df_{TN}}{dt}\right|_{(E)} = \left.\frac{dV^{TN}}{dt}\right|_{(S)} \frac{(f_{MAX} - f_{TK})}{V^{TN}} \tag{2.15}$$

Where f_{MAX} is the initial fraction of the evaporative component, representing the maximum value that the oil fraction evaporated from the thin slick can attain. Besides, evaporation leads to an increase in the viscosity of the oil, which is calculated by:

$$\eta = \eta_0 \exp(K^{(E)} f_{TK}) \tag{2.16}$$

Where η_0 $(m^2 s^{-1})$ is the initial viscosity, which depends on the oil type used, and $K^{(E)}$ is a constant that determines the increase of viscosity of evaporation.

3.3.1.3 Emulsification

Emulsification refers to the process by which water becomes mixed with the oil in the slick. The emulsification result is a significant increase in volume (3 or 4 times the volume of the original stabilized oil), a substantial increase in density, and a substantial increase in viscosity (SEBASTIÃO; GUEDES SOARES, 1995).

The mousse formation causes an increase in viscosity that the Mooney equation can compute (SEBASTIÃO; GUEDES SOARES, 1995):

$$\eta_{EM} = \eta \exp\left[\frac{2.5 f^W}{1 - C_1^{(M)} f^W}\right] \tag{2.17}$$

Where η is defined by Eq. 3.18, f^W is the fraction of water in the oil-water mousse, $C_1^{(M)}$ is a constant controlling the effect of water fraction on mousse viscosity. Emulsification is assumed to continue until μ_{EM} reaches a maximum value η_{max}, which corresponds to a mousse composed of floating tarballs. Mackay's models (MACKAY et al., 1979) for the rate of change in f^W is given by

$$\frac{df^W}{dt} = C_2^{(M)} \left(\frac{W}{W_0} + 1\right)^2 \left(1 - C_3^{(M)} f^W\right) \tag{2.18}$$

Where W/W_0 is the non-dimensional wind speed calculated at the slick center; $C_2^{(M)}$ is a constant which controls the rate of water absorption in the mousse; $C_3^{(M)}$ is a constant that controls the maximum water fraction in the mousse.

3.3.1.4 Dispersion

The wave action on the oil drives it into the water, forming a cloud of droplets beneath the spill. The droplets can be classified as large droplets that quickly rise and coalesce again with the surface spill or tiny droplets that rise more slowly and can be immersed long enough to diffuse into the lower water columns layers. In the latter case, the droplets are lost from the surface spill and considered to be permanently dispersed. What characterizes the tiny droplets is that their rising velocity under buoyancy forces is comparable to their diffusive velocity. For large droplets, it is much higher (DE DOMINICIS et al., 2013a).

The time rate of change of the thick slick volume due to water column dispersal of tiny droplets is given by Mackay's formula (MACKAY et al., 1979):

$$\left.\frac{dV^{TK}}{dt}\right|_{(D)} = \frac{1}{2}\left(C_1^{(D)} - \upsilon_s\right) C_S A^{TK} + \frac{dX_S}{dt} \tag{2.19}$$

Where $C_1^{(D)}$ and υ_s are, respectively, the downward diffusive velocity and rising velocity of tiny droplets. C_S is the fraction of tiny droplets, while X_S is the volume of tiny droplets beneath the thick slick, and it is equal to:

$$X_S = C_S u_m A^{TK} \tag{2.20}$$

Where u_m (m) is the vertical thickness of the droplet cloud. The large droplets are not regarded as dispersed since they eventually re-coalesce with the slick. The fraction of tiny droplets is calculated using the following expression:

$$C_S = \frac{2C_3^{(D)}\left(\frac{W}{W_0}+1\right)^2 T^{TK} S_{TK}}{\upsilon_s + C_1^{(D)}} \tag{2.21}$$

Where $C_3^{(D)}$ is a constant which controls the rate of dispersion of all droplets by waves, and S_{Tk} is the fraction of tiny droplets in the dispersed oil beneath the thick slick, and it is given by:

$$S_{TK} = \left[1 + C_4^{(D)}\left(\frac{\eta_{EM}}{\eta_{EM0}}\right)^{\frac{1}{2}}\left(\frac{T^{TK}}{1e-3T_0^{TK}}\right)\left(\frac{\tau}{\tau_0}\right)\right]^{-1} \tag{2.22}$$

Where $C_4^{(D)}$ controls the fraction of droplets below a critical size; τ $(kg\ s^{-2})$ is the interfacial surface tension between oil, and η_{EM} is the emulsified oil viscosity. The emulsification influences the mousse viscosity that, in turn, affects the dispersion. τ_0 and η_{EM0} are the interfacial surface tension scale and emulsified oil viscosity scale, respectively.

For the thin slick dispersion, only tiny droplets are considered. It is assumed that these droplets are all lost from the surface spill at the following rate:

$$\left.\frac{dV^{TN}}{dt}\right|_{(D)} = C_3^{(D)}\left(\frac{W}{W_0}+1\right)^2 T^{TN} A^{TN} S_{TN} \tag{2.23}$$

$$S_{TN} = \left(1 + C_5^{(D)}\frac{\tau}{\tau_0}\right)^{-1} \tag{2.24}$$

Where $C_5^{(D)}$ is control dispersion from the thin slick and S_{TN} is the fraction of tiny droplets in the dispersed oil beneath the thin slick.

3.4 FREQUENCY ESTIMATES

For the selected SCNs in the previous step, the frequency of occurrence should be estimated. The output of the QERA is very dependent on this estimate. An under-or sub-estimate of this value can lead to rough errors in calculating the ecological risk. In some risk assessments, an accident's occurrence frequency can be estimated from historical records in databases or references since they represent the case.

Due to some facilities' complexity, it might be necessary to use expert opinion and Reliability Engineering techniques (e.g., event tree, Event Sequence Diagrams, Bayesian Belief Networks). By doing so, we can correct the generic frequencies considering the

influence of control measures (e.g., safety management systems, alarms, automatic stops) and human errors that might contribute to the occurrence of the SCN. For a general view on reliability theory, models, methods, and applications, see (O'CONNOR; PATRICK, 2002; RAUSAND; HOYLAND, 2004). For specific information about techniques such as Event Sequence Diagrams (ESD), Bayesian Belief Networks (BBN), and Human Reliability Analysis (HRA) see (FIRMINO; DROGUETT, 2004; HOLLNAGEL, 1998; KORB; NICHOLSON, 2003; STAMATELATOS et al., 2002; SWAIN; GUTTMANN, 1983).

Besides, historical records and statistical inference are usually sufficient for the objectives of most QERAs. If greater confidence in the results is required, the methodology suggests using BBNs to integrate historical records with expert opinion or Bayesian Population Variability Analysis (DROGUETT; GROEN; MOSLEH, 2004; ZHANG et al., 2016). For example, for the maritime accidents that cause an oil spill, we will incorporate ship pilots' statements with previous statistics to reduce uncertainty in estimates of the frequency of oil spills.

The frequencies concerning meteorological parameters that consolidate each SCN (defined in the previous step) should also be considered. Consequently, meteorological statistics (deduced, for example, from a nearby and representative meteorological station) should be used to define fractional frequencies or the number of observations to each meteorological scenario.

Finally, only SCNs that contribute significantly to the ecological risk should be included in the QERA under the conditions that (1) the frequency of occurrence is equal to or greater than 10^{-8} per year and (2) PEC/PNEC is greater than 0.01. The first criterion is taken from the 'Purple Book' method (CPR18E, 2005), which also uses this criterion to decide whether the identified SCN must undergo a quantitative risk assessment. Therefore, this criterion is used to filter SCNs for population modeling in the next step. The fourth step's output is then a set of SCNs likely to contribute to the ecological/microbial risk, with their respective frequency estimates of occurrence and exposure if such an SCN should occur.

3.4.1 Bayesian Population Variability Analysis

To estimate the oil tankers accidents frequency, one must consider the inherent uncertainty of the assessment. This assumption agrees with Singpurwalla's statements when considering a Bayesian approach for reliability analysis (SINGPURWALLA, 2006). Thus, given the uncertainty about the accident rate of the ships, one can obtain the uncertainty variability of the whole population of vessels. This uncertainty can be represented as a

probability distribution, denoted by the Population Variability Distribution (PVD). The assessment of the PVD is performed through the Population Variability Analysis (PVA). Hence, we chose this approach to be used in the frequency estimate step of our assessment.

The basics that back up the Bayesian Population Variability Analysis (BPVA) are provided in this section. As a typical PVA procedure, we assume that a family of parametric distributions describes the PVD (DROGUETT; GROEN; MOSLEH, 2004; KAPLAN, 1983; MOSLEH; APOSTOLAKIS, 1985; PÖRN, 1996). If there are enough data for each ship, we can directly define the accident rate's PVD parameters from the dataset.

Let λ denote a random variable that defines the accident rate and $\phi(\lambda) = \phi(\lambda|\theta_1, .., \theta_p)$ be a parametric PVD with p parameters. A probability distribution $\pi(\underline{\theta}) = \pi(\theta_1, \dots, \theta_p)$ over the model parameters can be used to describe the uncertainty over the PVD. Then, the estimated population variability density $\hat{p}(\lambda)$ can be taken as:

$$\hat{p}(\lambda) = \int \dots \int_{\theta_1,\dots,\theta_p} \phi(\theta_1, .., \theta_p)\pi(\theta_1, \dots, \theta_p)d\theta_1 \dots d\theta_p \quad (2.25)$$

Thus, $\hat{p}(\lambda)$ consists of a weighted mix of distributions of the chosen model, instead of being formed by a single "best" distribution preferably obtained from the set of possible distributions, for instance, by using Maximum Likelihood Estimation (MODARRES; KAMINSKIY; KRIVTSOV, 1999). In the BPVA, the assessment of λ may be based on three different types of information:

- E_0: prior state knowledge on λ, such as the analyst experience with the system or component;
- E_1: exposure data (run-time) from operating experience with similar systems in similar applications (e.g., maritime accidents database);
- E_2: estimates about the accident measure λ from sources such as expert opinions.

E_0 is the prior evidence and provides information about $\pi(\underline{\theta})$. In other words, $\pi_0(\underline{\theta}) = \pi(\underline{\theta}|E_0)$ is the prior probability distribution over the parameters $\underline{\theta}$ and $\hat{p}_0(\lambda) = \hat{p}(\lambda|E_0) = \int_{\underline{\theta}} \phi(\lambda|\underline{\theta})\pi_0(\underline{\theta})d\underline{\theta}$ is the prior PVD of λ. The evidence E_1 includes available data obtained from accident datasets. The data consists of the number of occurrences of each accident (i.e., collision, fire, and explosion) annually or within a given time window. Additionally, E_2 includes estimates from expert opinions about the system's design, manufacturing, and operation in similar applications. This type of information is usually a point estimate, the best estimate, or a range of values centered around it. Alternatively, a probability distribution can express this range using the best estimate of the distribution's mean or median. In the

following sections, we also consider assessing the analyst's confidence in estimating a given expert.

Therefore, we can develop the distribution of the population variability parameters based on types E_0, E_1 and E_2 information by applying Bayes' theorem:

$$\pi_2(\underline{\theta}) = \pi(\underline{\theta}|E_0, E_1, E_2) = \frac{P(E_1,E_2|\underline{\theta},E_0)\pi_0(\underline{\theta})}{\int_{\underline{\theta}} \phi P(E_1,E_2|\underline{\theta},E_0)\pi_0(\underline{\theta})d\underline{\theta}} \tag{2.26}$$

where $P(E_1, E_2|\underline{\theta}, E_0)$ is the likelihood of evidence E_1 and E_2. Then, the PVD over λ, conditional on both E_0, E_1, and E_2 i.e., the posterior PVD is given by $\hat{p}_2(\lambda) = \hat{p}(\lambda|E_0, E_1, E_2) = \int_{\underline{\theta}} \phi(\lambda|\underline{\theta})\pi_2(\underline{\theta})d\underline{\theta}$.

Assuming exposure evidence E_1 and source estimates E_2 are independent, the likelihood function becomes $P(E_1, E_2|\theta, E_0) = P(E_1|\theta, E_0)P(E_2|\theta, E_0)$, where the first and second factors of the right side are the likelihood of exposure data and estimates evidence, respectively. By writing this expression considering the likelihood of the information for each system, we have:

$$P(E_1, E_2|\underline{\theta}, E_0) = \prod_{i=1}^{m} P(E_{1i}|\underline{\theta}, E_0)P(E_{2i}|\underline{\theta}, E_0) \tag{2.27}$$

where $P(E_{1i}|\theta, E_0)$ and $P(E_{2i}|\theta, E_0)$, respectively, are the probability of observing evidence E_{1i} and E_{2i} for the *i*th system out of m systems. Note that an accident measure can generate the likelihood for the *i*th system λ_i, which is one of the possible values of the random variable λ that is distributed according to $\phi(\lambda|\underline{\theta})$. Thus, we calculate the probability of observing evidence E_{1i} and E_{2i} by allowing the accident measure to assume all possible values, i.e., we average $P(\underline{\theta}, E_0)$ over the distribution of λ:

$$P(E_{1i}|\underline{\theta}, E_0)P(E_{2i}|\underline{\theta}, E_0) = \int_{\lambda} P(E_{1i}|\lambda, E_0)P(E_{2i}|\lambda, E_0)\phi(\lambda|\underline{\theta})d\lambda \tag{2.28}$$

which can be replaced into (2.29) to obtain the likelihood function using all the information available.

When writing the likelihood as (2.30), the estimated and exposure data are coupled, i.e., the source's estimate of the accident rate is for the system the exposure data have been observed. We can deal with exceptional cases when only one type of information is available for the *i*th system. For instance, when there are only exposure data, the likelihood is $\int_{\lambda} P(E_{1i}|\lambda, E_0)\phi(\lambda|\underline{\theta})d\lambda$; while that if there is just source information, the likelihood is $\int_{\lambda} P(E_{2i}|\lambda, E_0)\phi(\lambda|\underline{\theta})d\lambda$.

For risk assessment purposes, the frequency estimates of undesirable events, such as industrial accidents, are usually done via historical records from fault or accidents and expert

opinion. However, the fault data may not exist, such as the case of new facilities with specific operational conditions, new equipment, or rare events (e.g., industrial accidents as oil spills) (RAMOS, 2012). The Bayesian approach allows integrating the fault or accident data with expert opinion. With this integration, subjective information can be quantified and used on objective problems. This approach is beneficial for the risk assessment because most information is subjective (RAMOS, 2012).

Other techniques can also be used to assess the frequency of accidents involving vessels on course. For instance, the Fault Tree Analysis can be used to determine the causes of an accident (UĞURLU et al., 2020). Moreover, the Bayesian Networks are a Direct Acyclic Graph (DAG) whose nodes and edges are created to understand probabilistic influences (MARTINS; MATURANA, 2013). The relationship between connected nodes is given through the Bayes' theorem. With this approach, we can model complex systems and improve the representations of the relation between the events (MARTINS; MATURANA, 2013; SINGPURWALLA, 2006; TRUCCO et al., 2008).

3.5 POPULATION MODELING

This step is an iterative process (see Figure 8). Firstly, a population or metapopulation model is formulated to describe the natural population dynamics of key species in the area in a no-impact SCN (i.e., without exposure to the chemicals). This SCN is called the benchmark scenario (SCN-0). If more than one is analyzed, it is necessary to formulate a population model for each representative species (bioindicators). The population dynamics must be described via assessment endpoints defined in the first step. Then, the frequency estimates and predicted exposure magnitude and timing for each risk SCN are integrated with SCN-0 to create a set of sub-models representing each scenario SCN-i ($i = 1,2,3 \ldots$).

Figure 8 - The iterative process of population modeling.

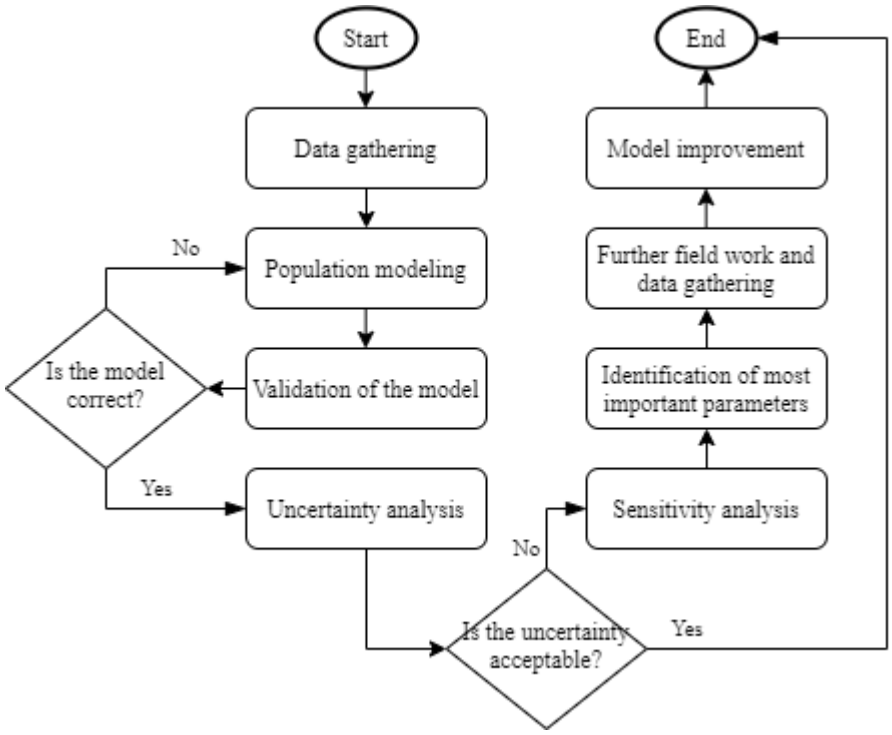

Source: Adapted from Duarte (2016, p. 69).

Input data will be necessary to parameterize the population model. The quality and predictiveness of the model depend mainly on the quality and quantity of these data. If data for the key species are insufficient, one could extrapolate the information from related ones or use expert opinion.

Typically, a population model requires information on the following input variables (PASTOROK et al., 2002; PAUWELS, 2002): age/size structure; specific survival and fecundity rates for each age/size; rates of immigration or emigration; initial abundance for each age/size; estimates of variability for the vital rates and initial abundances; density-dependence effects; geographic and habitat distribution of critical species; and foraging behavior. The required level of detail for a particular variable depends on the assessment objectives.

Once the population model is formulated, it should be validated to ensure a good approximation of reality and reliable predictions. The validation of a model is typically done by measuring the conformance of predictions with empirical data. This measure may be used to characterize the reliability of other predictions.

After the model's validation, we should conduct an uncertainty analysis of risk estimates to determine if the level of uncertainty is acceptable. A simple way to deal with

uncertainties is to derive worst and best-case estimates of extinction risks based on parameter changes. Such a procedure will let the risk assessor estimate a range (upper and lower bounds) to risk measures, such as time to extinction or decline risk. The more remarkable are the uncertainties in parameter values, the wider these bounds will be. If these bounds are too broad, uncertainty may be unacceptable and not meet risk managers' needs. At best, these bounds should be narrow enough to make decisions taken by risk managers based on the lower bound the same as those found on the upper bound (i.e., the difference between the lower and upper bound should be regardless for risk managers).

If uncertainty is acceptable, then it is the end of this step. Otherwise, if the present model provides risk estimates with an unacceptable level of uncertainty, then a sensitivity analysis can point out the most important parameters which need better estimates. Then, further fieldwork and data gathering on these parameters can improve the model. Finally, one has an improved model (with a validated structure and more precise parameters), which must be further analyzed until validated and achieve acceptable uncertainties.

3.6 RISK QUANTIFICATION AND CATEGORIZATION

The final step simulates SCNs separately (for isolated risks) or together (for evaluating cumulated risks). The risk results may be represented as probability-consequence curves derived from multiple runs (Monte Carlo) and expressed in many ways (Section 3.5.3).

Many software programs are available for population model construction and probabilistic simulation via Monte Carlo methods (KALOS; WHITLOCK, 2008). The methodology suggests the software RAMAS Metapop v. 6.0 (AKÇAKAYA; ROOT, 2013), allowing fast stochastic simulation of an SCN. One can simulate hundreds of SCNs by varying the most uncertain parameters in one's model within a range of coherence, comparing them, and picking the most relevant ones (e.g., those that maximize/minimize the risk) to present the results. The range of plausibility can be assumed based on a literature review and expert opinion.).

For QERA, the main result is a cumulative density function (CDF) for the time to half loss (HL) (i.e., the time required by a population to decrease to less than half of its initial size). Although RAMAS software automatically builds the CDF, it is essential to understand that the resulting CDF is created using a Monte Carlo simulation. For every Monte Carlo run, a single-point estimate for the discretized time to extinction or HL (T) is calculated. After many Monte Carlo runs (e.g., 10,000), one will have a set of single-point estimates for the time to HL and their number of occurrences. Thus, one can calculate the probability of

occurrence of each "single-point estimate" (e.g., $P(T) = number\ of\ events\ of\ T/10{,}0000$). Then, for each time t, it is possible to cumulate the probabilities of all T lower than t, which results in the CDF for the time to HL, i.e.:$F_T(t) = P(T \leq t)$. So, $F_T(t)$ means the probability that HL will occur at or before a time t. This function can be plotted in a graph. A Monte Carlo simulation's great advantage over deterministic analysis is that results show not only what could happen but how likely each outcome is.

The risk results obtained (e.g., CDF for the time to extinction) can be categorized into threat classes according to the International Union for Conservation of Nature (IUCN) (IUCN, 2012). The only quantitative IUCN criteria are expressed in terms of time and probability of total extinction (zero individuals) as follows:

- CRITICALLY ENDANGERED (CE): the probability extinction within 10 years or 3 generations, whichever is longer (up to a maximum of 100 years), is $\geq 50\%$;
- ENDANGERED (EN): the probability extinction within 10 years or 3 generations, whichever is longer (up to a maximum of 100 years), is $\geq 20\%$;
- VULNERABLE (VU): the probability extinction within 100 years is $\geq 10\%$;
- NEGLIGIBLE (NE): the probability extinction within 100 years is $< 10\%$;

Hence, IUCN categories are appropriate for classifying species affected by a range of local, regional, and global environmental changes and human disturbance. However, the IUCN categories are too optimistic (in the sense of underestimating risk categories) for local applications, where the aim is to describe the interaction of local environmental conditions and human impacts with a local population, which is the purpose of the QERA methodology. Thus, the methodology proposes and uses different and more conservative categories for QERA. Communicating risks caused by a single industrial activity is more conservative in expressing risk criteria as "half loss" (i.e., 50% population size decline) instead of total extinction. Therefore, the methodology categorizes risks as follows:

- CRITICAL RISK (CR): the probability of HL within 10 years or 3 generations, whichever is longer (up to a maximum of 100 years), is $> 50\%$;
- HIGH RISK (HI): the probability of HL within 20 years or 5 generations, whichever is longer (up to a maximum of 100 years), is $> 20\%$;
- CONSIDERABLE RISK (CO): the probability of HL within 100 years is $> 10\%$;
- NEGLIGIBLE RISK (NE): the probability of HL within 100 years is $< 10\%$.

4 FATE AND TRANSPORT SIMULATION OF POTENTIAL OIL SPILLS NEAR FERNANDO DE NORONHA ARCHIPELAGO

The content of this chapter was accepted for presentation at the 5th conference of the Brazilian Association of Risk Analysis, Process Safety, and Reliability (ABRISCO). It is also being prepared for further scientific publication.

Oil spills in the ocean are a significant threat that has caused catastrophic impacts on coastal countries' marine environment and ecosystems. Therefore, it is essential to assess the risk of potential oil spills and then provide information to decision-makers regarding the best strategies to mitigate impacts. One of the fundamental steps in a risk assessment is to measure the exposure of a given location to hazardous substances. This paper focuses on this assessment: we simulate potential oil spills from oil tankers that navigate near Fernando de Noronha Archipelago (FNA). The simulation considers the oil's fate (i.e., the physical and chemical transformations) and transport in the ocean. We use the Lagrangian model MEDSLIK-II to simulate various scenarios that are characterized by: the amount of oil spilled, based on recent spills and the tank capacity of typical oil tankers; the location of the hypothetical spillage, placed in ship routes that are near FNA; and the metoceanographic conditions that vary throughout the year (e.g., currents and wind velocities). The simulation results are the oil concentrations that can reach FNA. This information is to be integrated with a risk assessment for oil spills in this region. Thus, we can better estimate the exposure to the risks and provide more accurate results.

4.1 INTRODUCTION

Oil spills in the ocean are a significant threat that has caused catastrophic impacts on coastal countries' marine environment and ecosystems (CHEN et al., 2019). The high number of vessels, including oil tankers that circulate the globe and extreme events such as storms and tropical cyclones due to global warming, increase the risk of potential oil spills affecting oceanic islands (QUEIROZ et al., 2019). Despite the immense efforts of international and national maritime authorities over the years to enhance ship safety, many shipping accidents still occur (ITOPF, 2021; UNG, 2019). For instance, in the 2010s, a total of 63 spills occurred, releasing 164,000 tons of oil, which was the least amount spilled in the last decades (ITOPF, 2021). Furthermore, the oil trade plays a vital role in economic development. There

is a rising in the maritime transportation of the volume of oil. The oil tankers are responsible for around 90% of the oil transported worldwide (CHEN et al., 2019).

The evaluation of oil spill behavior in risk assessment of oil tanker spills is fundamental to assess the spatial and temporal extent of the impact and which vulnerable ecosystems will suffer the consequences. Oil spill simulation models have been developed for simulating oil slick trajectories and fates (fate and transport models) under actual environmental conditions from spills created from marine traffic, oil production, or other sources (KERAMEA et al., 2021; SPAULDING, 2017). Therefore, oil spill risks are determined by the potential hazard of oil pollution and the environmental characteristics, e.g., ocean currents, winds, waves, and sea surface temperature (SST).

The simulation of the transport, diffusion, and transformation of spilled oil in the ocean can be done using a Lagrangian formalism coupled with Eulerian circulation models. The Lagrangian formalism can track mass elements, such as the droplets of oil in the water; while in the Eulerian approach, the focus is on the flow properties in a specified point in space as a function of time so that one can model the currents and wind fields (FOX et al., 2014). Thus, with the Lagrangian approach, the model can compute the oil concentration on the water (DE DOMINICIS et al., 2013a).

In this research, we used a Lagrangian fate and transport model, the MEDSLIK-II (DE DOMINICIS et al., 2013a, 2013b), to simulate oil spills trajectories and transformations in the ocean environment near the Fernando de Noronha Archipelago (FNA). Input data from oceanographic (i.e., currents and sea surface temperature) and atmospheric Eulerian models used in the MEDSLIK-II model solve the advection-diffusion and weathering process, as illustrated in Figure 1. These results are fundamental to quantify the impacts of potential oil spills that may occur due to oil tankers accidents that navigate nearby the FNA when integrated into a Quantitative Ecological Risk Assessment (DUARTE et al., 2013, 2019; DUARTE; DROGUETT, 2016).

Figure 1 - Simplified scheme of the MEDSLIK-II with the inputs (oceanographic and atmospheric Eulerian models) and the output (fate and transport of oil spill).

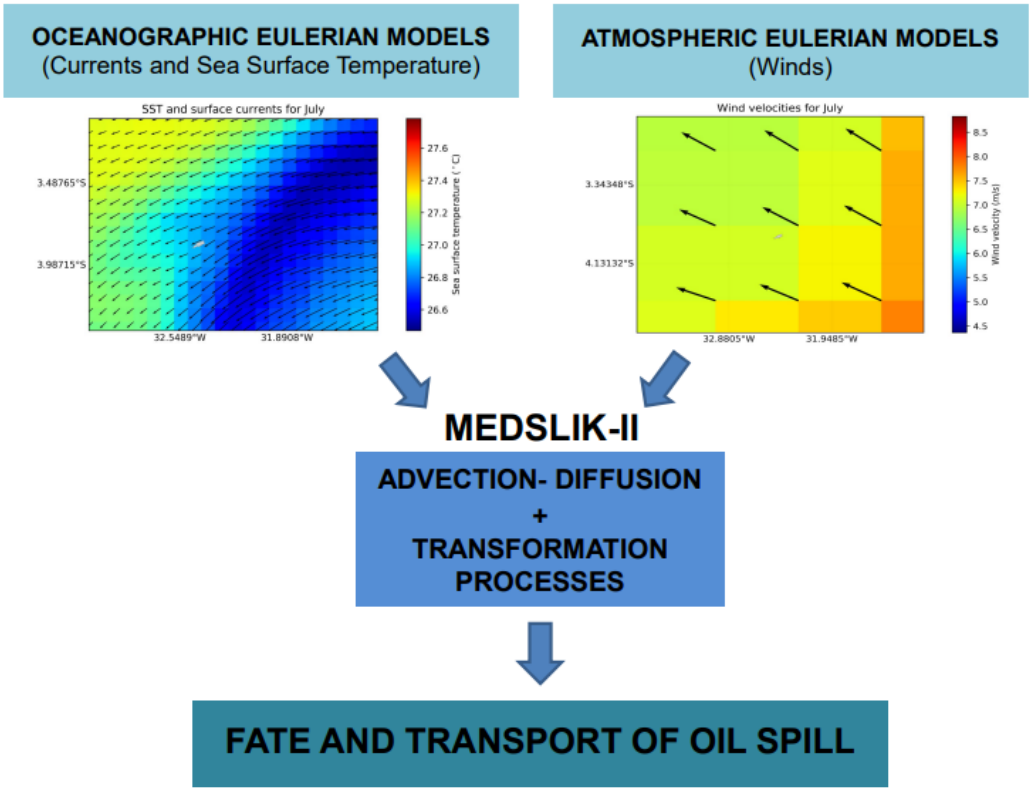

Source: The Author (2021)

The remainder of this work is structured as follows. First, Section 4.2 describes the metoceanographic conditions around the archipelago (i.e., ocean currents, sea surface temperature, and wind speed) and the main ship routes. Section 4.3 details the dataset used, defines the spillage points on the most critical route and describes the fate and transport model used, i.e., the MEDSLIK-II. In section 4.4, we present and discuss the results regarding the oil spill simulations. Lastly, we offer closing remarks about the simulations performed.

4.2 DESCRIPTION OF THE PROBLEM

The FNA is in a warm tropical region. The air temperature on average is $25°C$ and a well-defined dry season between August and February, and a rainy season between March and July, averaging $1400mm$ rainfall (SERAFINI; FRANÇA, 2010). The prevailing winds are the southeast trade winds. The greater intensity occurs between July and August (TCHAMABI et al., 2017). The highest sea surface temperatures (SST) occur between March and June, typically exceeding $28°C$ due to the occurrence of the southwestern tropical Atlantic warm pool (CINTRA et al., 2015) and the lowest between August and November

($SST \sim 26.6°C$) (HOUNSOU-GBO et al., 2015; SILVA et al., 2009; TCHAMABI et al., 2017). On the ocean surface, the central branch of the South Equatorial Current (cSEC) flows westward until it reaches the North Brazil Current (NBC) near the coast (LUMPKIN; GARZOLI, 2005; STRAMMA; SCHOTT, 1999). The cSEC is stronger between March and July and weaker between August and February (LUMPKIN; JOHNSON, 2013; TCHAMABI et al., 2017).

The main ship routes nearby FNA are presented in Figure 2. The routes were identified by (DUARTE; DROGUETT, 2016) on Pilot Charts, which show the most recommended routes for navigation (i.e., those taking best advantage of currents, winds, and possible nearby landmarks to help determine the ship's position) for each month of the year based on metoceanographic data collected by the Brazilian Navy from 1951 to 1972 (BRASIL, 1993) The three main routes are:

1. Ponce and Cólon – Cape of Good Hope (PC-CGH – November – going), minimum distance to FNA: 4.96 nautical miles (nm)
2. Recife – Madeira Island (REC – MI – Augusto – going and return), minimum distance to FNA: 16.38 nm;
3. Recife – Cape Noaudhibou (REC – CN – March – going and return), minimum distance to FNA: 12.58 nm;

4.3 METHODOLOGY

4.3.1 Data source

The global bathymetry data is provided from GEBCO, a terrain model for ocean and land, giving elevation data (in meters) on a 15 arc-second interval grid (GEBCO, 2021). The coastline data is based on the Global Self-consistent Hierarchical High-resolution Geography (GSHHG) from the National Oceanic Atmospheric Administration (NOAA) (NOAA, 2018).

The global oceanographic inputs are from the Global Ocean $1/12°$ Physics Analysis and Forecast provided by CMEMS, which includes temperature (SST), salinity, currents, sea level, mixed layer depth, and ice parameters top to bottom over the global ocean (CMEMS, 2021). For this study, only the SST and current data were retrieved. The atmospheric data (i.e., wind velocities) were collected from the ERA-Interim atmospheric fields, provided by the ECMWF (BERRISFORD et al., 2011; ECMWF, 2019).

Figure 2 - Main routes near FNA: Ponce and Colón – Cape of Good Hope (PC – CGH, going); Recife – Madeira Island (Rec – MI, going and return); Recife – Cape Noaudhibou (REC – CN, going and return). Six landmarks are represented in the figure: (A) Pico's Hill; (B) FN Lighthouse; (C) São Pedro's Church; (D) Antenna; (E) Ovo's Island; (F) Pontinha. Scale 1: 4222.

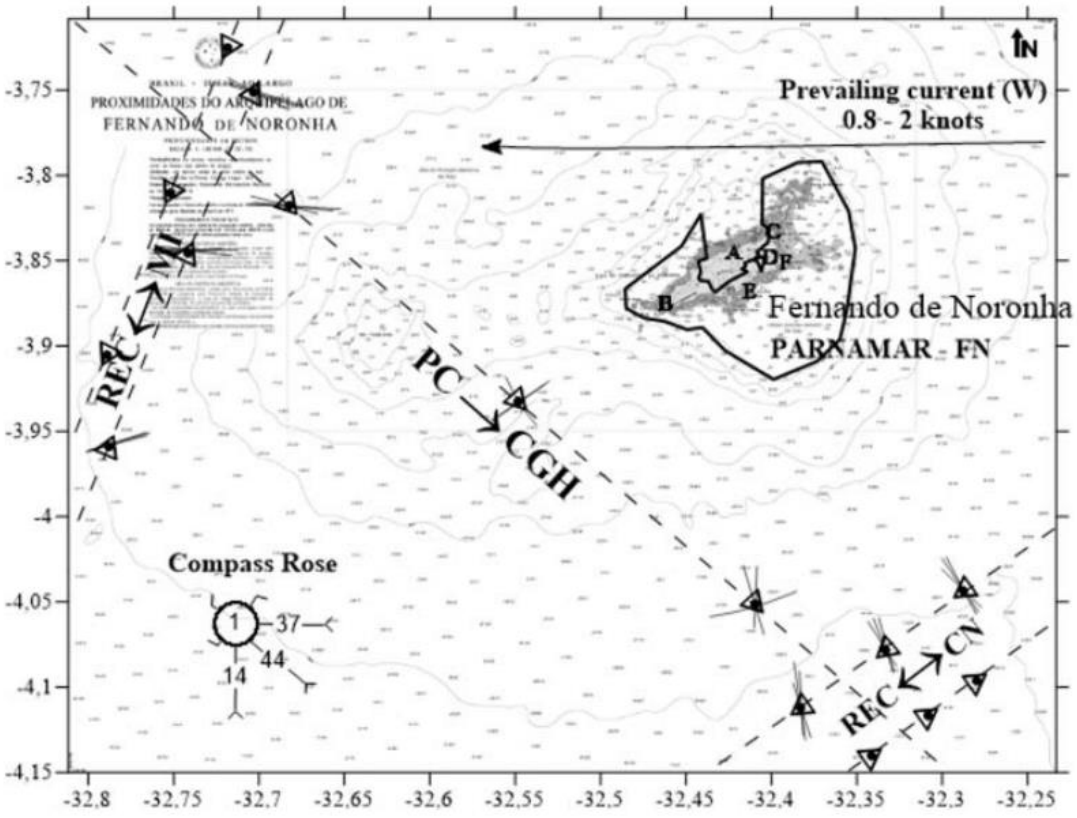

Source: Duarte and Droguett (2016)

4.3.2 Definition of Spillage Scenarios

The primary forces that act on the oil spill are the currents and winds. We chose the monthly averaged currents and winds for March and July. The rationale is that the cSEC starts to intensify in March, but with a lower wind speed, reaching its highest intensity in July, strengthening the southeast trade winds (LUMPKIN; GARZOLI, 2005; MOLINARI, 1982).

The route that possesses a significant hazard is the REC – CN, which passes from south to east of FNA (DUARTE; DROGUETT, 2016). It is conceptually possible that an oil spill on this route would be transported to the archipelago coast due to prevailing winds and currents. We defined three initial spill releasing points on this route. These points were determined on the eastern side of the FNA, also known as the Windward Side (WS), that faces the open ocean and where the sea is more exposed to the action of winds and ocean currents (ASSUNÇÃO et al., 2016; IVAR DO SUL; SPENGLER; COSTA, 2009). Moreover, these release points were selected based on traffic density on the route from the archipelago of the

main vessel tracks registered in the Marine Traffic website (MARINETRAFFIC, 2021; QUEIROZ et al., 2019). The points are: $P1$ $(3°31.3'S;\ 31°33'W)$, $P2$ $(3°44.3'S;\ 31°51'W)$ and $P3$ $(3°50.87'S;\ 31°58.8'W)$ (Figure 3).

Figure 3 - Location of FNA and coordinates of the release points P1, P2, and P3 for the oil spill simulations

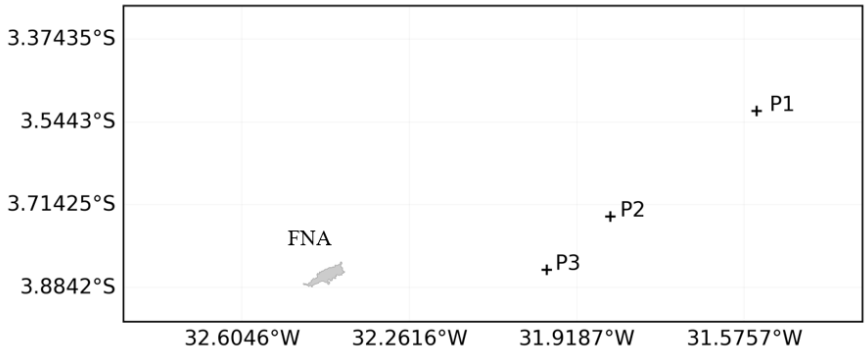

Source: The Author (2021)

We also assumed an instantaneous volume of oil spilled values $9{,}100$ tonnes, based on a single typical Suezmax cargo tank (IMO, 2008). The oil used in the simulations is the 28° API (intermediate oil type, density approximately $886.6\ kg/m^3$) which is the most used in the Brazilian oil and gas exploratory activities (ANP, 2021). Once the spill starts, we simulate the fate and transport of the oil during $48h$ and store the main results every half hour. Therefore, we simulated the oil spill cases considering the weathering conditions for each month at each point of release, resulting in six scenarios. The names of the scenarios result from the combination of the releasing point and the month of the spill, summarized in Table 1.

Table 1 - Summary of the oil spill simulation scenarios.

	Release Points		
	$P1$	$P2$	$P3$
March	$P1M$	$P2M$	$P3M$
July	$P1J$	$P2J$	$P3J$

Source: The Author (2021)

4.3.3 MEDSLIK-II

The MEDSLIK-II is a Lagrangian oil model designed to simulate oil slick transport and transformation processes for spills on the maritime surface (Figure 1) (DE DOMINICIS et al., 2013a, 2013b). When an oil spill occurs, the wind and surface currents are the primary forces for oil transport in the aquatic environment (SPAULDING, 2017). Therefore, the oil transport in the ocean is primarily attributed to advection by the large-scale flow field, and turbulent flow components cause the dispersion. Beyond transportation, oil spills impact depends mainly on the environmental conditions that control the weathering processes at the site of the spill (e.g., currents, climate, waves) and the time required to engage mitigation operations (LEE et al., 2015; MARTA-ALMEIDA et al., 2013; NRC, 2003). Weathering is a general definition for changes in oil properties due to physical, chemical, and biological processes when the spill is exposed to environmental conditions (e.g., in aquatic systems). The main weathering processes are illustrated in Figure 7 and detailed in Section 3.3.1

The general equation for a tracer concentration ($C(x, y, z, t)$) with units of mass per volume, mixed in the marine environment is given by:

$$\frac{\partial C}{\partial t} + \boldsymbol{U} \cdot \nabla C = \nabla \cdot (\boldsymbol{K} \nabla C) + \sum_{j=1}^{M} r_j(\boldsymbol{x}, C(\boldsymbol{x}, t), t) \tag{4.1}$$

where $\frac{\partial}{\partial t}$ is the local time-rate-of-change operator, $\boldsymbol{U}$ is the three-dimensional distribution of the horizontal ocean current components $\boldsymbol{u}$ and $\boldsymbol{v}$, $\boldsymbol{K}$ is the turbulent diffusivity tensor, which parameterizes the sub-grid scale processes; the position vector (x, y, z) is denoted by $\boldsymbol{x}$; and $r_j(\boldsymbol{x}, C(\boldsymbol{x}, t), t)$ are the M transformation rates that modify the tracer concentration through the weathering processes (i.e., physical and chemical transformations).

Following the Lagrangian approach, the oil slick is constituted of oil particles that move like water parcels. However, the weathering processes acting on the entire slick instead of on the single-particle properties. Thus, the active tracer equation can be effectively split into two component equations:

$$\frac{\partial C_1}{\partial t} = \sum_{j=1}^{M} r_j(\boldsymbol{x}, C_1(\boldsymbol{x}, t), t) \tag{4.2}$$

$$\frac{\partial C}{\partial t} = -\boldsymbol{U} \cdot \nabla C_1 + \nabla \cdot (\boldsymbol{K} \nabla C_1)\ , \tag{4.3}$$

where C_1 is the oil concentration due to the weathering processes, while the final time rate of change of C is given by the advection-diffusion acting on C_1. The model first solves (4.2) by considering the weathering processes acting on the total oil slick volume: thus, oil slick state

variables must be defined. The structural state variables correspond to the oil concentrations: on the sea surface, dispersed, sedimented on the bottom, and beached on the coast parcels.

The slick state variables are used for the transformation processes, and the particle state variables are used to solve the advection-diffusion processes. Then, the Lagrangian formalism is applied to solve 4.3, the advection-diffusion part of the equation, discretizing the surface oil slick in particles with position increments given by:

$$d\boldsymbol{x}(t) = \boldsymbol{U}(\boldsymbol{x}, t)dt + \boldsymbol{Z}\sqrt{2\boldsymbol{K}dt} \quad (4.4)$$

where dt is the model time step; $\boldsymbol{Z}$ are independent random vectors normally distributed, i.e., $\boldsymbol{Z} \in N(0,1)$; and $\boldsymbol{K}$ is the turbulent diffusion diagonal tensor. The first part of the right side of the equation is the deterministic part of the flow field, while the second is the stochastic term, which characterizes random motion. Finally, the oil concentration is computed by assembling the particles with their associated properties.

4.4 RESULTS

4.4.1 Oceanographic and Atmospheric Results

The metoceanographic results are fundamental to describing the fate and transport of oil on the ocean. The influence of the wind affects the direction of oil transport. In March, the winds have a southwest direction with 2.86 m/s average speed, while in July, the wind are in a northeast direction with 7.52 m/s average speed (Figure 4). The mean SST was higher in July, averaging 29.3 $°C$, while for March the temperature averaged 27.01 $°C$ (Figure 5). Regarding the surface current, the most intense occurred in July, averaging 0.54 m/s southwestward. In March, the current presents a little deviation to the northeast, with a mean intensity equal to 0.17 m/s (Figure 5). The oil transport was mainly westward due to the surface current direction. Therefore, the northeast direction in July and the greater wind intensity contributed to carrying the oil plume to FNA.

Figure 4 - Average wind speed distribution (colors, m/s) and direction (arrows) for March (a) and July (b).

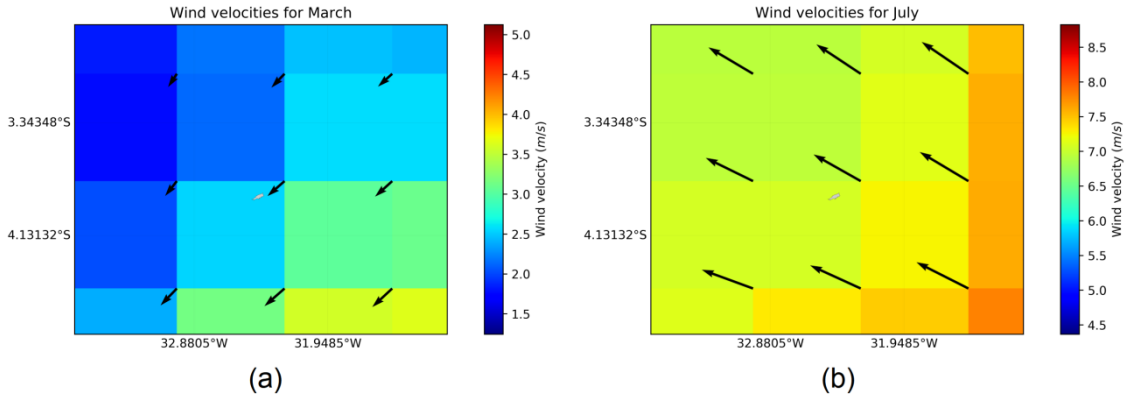

Source: The Author (2021)

Figure 5 - Average sea surface temperature distribution (colors, °C) and surface current direction (arrows) for March (a) and July (b).

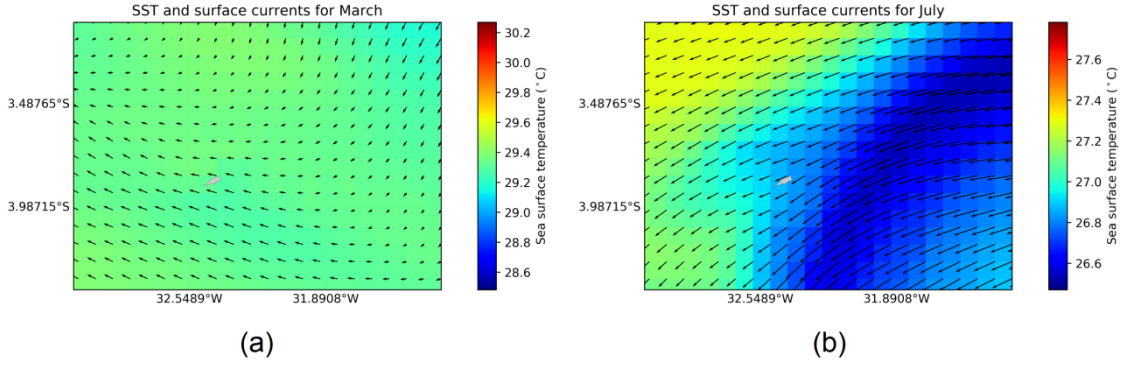

Source: The Author (2021)

4.4.2 Oil Spill Simulations

The primary simulation for each scenario results is the percentages of the original oil volume that: evaporated, remained on the surface, dispersed in the water columns, and sedimented on the sea bottom and the coast. These results for the final time-step of the simulation are summarized in Table 2. In March, it was observed that the maximum percentage of evaporation was reached after 5.5 hours, while in July, the maximum was achieved within 3 hours. Also, the top rate of evaporated oil was similar in each month: approximately 35.84% in March and 35.83% in July (Table 2).

Table 2 - Summary for each scenario of the percentage of oil that evaporated, remained on the sea surface, dispersed on the water column, and fixed on the coast and the sea bottom.

Scenario	Evaporated (%)	On the sea surface (%)	Dispersed on the water column (%)	Fixed on the coast and the sea bottom (%)
$P1M$	35.84	63.89	0.27	0
$P2M$	35.84	63.90	0.26	0
$P3M$	35.84	63.90	0.26	0
$P1J$	35.83	63.18	0.93	0.06
$P2J$	35.83	0.02	0.21	63.94
$P3J$	35.83	63.29	0.88	0

From: The Author (2021)

The density and viscosity increase is due to the emulsification of the water in the oil. For the spills simulated March, the density and the viscosity of the water-oil emulsion did not stabilize until the end of the simulation. The viscosities started at $220.02\ Pa.s$ and increased to $2306.57\ Pa.s$ for P_1, $2301.39\ Pa.s$ for P_2 and $2296.82\ Pa.s$ for P_3. Similarly, for the emulsion density, that increased from $885\ kg/m^3$ to $996.65\ kg/m^3$ for the releases that originated from points P_1 and P_2 and $996.68\ kg/m^3$ for P_3. None of the spills simulated in March reached FNA.

For the simulations in July, the density stabilized around 22 hours after the start of the simulation, with the final value being $996.75\ kg/m^3$ and remained equal until the end of the simulation for the releases from all three points. Similar to what happened in March, the variation in viscosity reached a stable value simultaneously with the density. The maximum emulsion viscosities are $2727.4\ Pa.s$ for P_1, $2721.91\ Pa.s$, for P_2, and $2714\ Pa.s$ for P_3. After the evaporation process ends, around 64.17% of the oil remains on the surface. The final dispersed percentages can be seen in Table 2.

The oil reached the shore in two of the spillage scenarios in July: $P1J$ and $P2J$. In scenario $P1J$, a small amount of oil that spread from the slick reached FNA. The final amount of oil on the shore and the sea bottom after 48 hours was equivalent to 0.06% of the initial volume of the spill ($\sim 5.46\ ton$). For scenario $P2J$, the oil reached the shore after 20 hours, initially with 0.5% ($\sim 45.5\ ton$) of the total volume spilled. By the end of the $48h$ simulation time, the entire oil fixed on the coast and at the bottom of the sea is approximately 63.94% ($\sim 5{,}819\ ton$). This oil portion is a substantial amount that can cause severe ecological damage and require cleanup efforts on a large scale.

The oil spill trajectory and concentrations on the sea surface for the release point P_2 for 10, 20, and 30 hours are presented in Figure 6. The illustration is helpful to show how the metoceanografic conditions influence the oil slick trajectory.

4.5 DISCUSSION

The oil evaporation rate in the MEDSLIK-II depends on the physicochemical properties of the oil, spreading rate, SST, and winds intensity (DE DOMINICIS et al., 2013a; SEBASTIÃO; GUEDES SOARES, 1995). Our simulation results showed that more than one-third of the volume spilled evaporates in the first few hours after the spill, i.e., $5.5h$ for the spills occurring in March, and $3h$ for the ones in July. The emulsification formation varied with the month and happened after the portion evaporated reached its maximum. Since the winds are more potent in July, the emulsification occurs faster (within $\sim 22h$), as they provide energy for emulsification, but not enough to disperse it again (Lee 2015). In March, the wind intensity was lower, and the emulsion viscosity was still increasing within the simulation time. Still, the oil formed a stable and high viscosity emulsion that prevented the oil from spreading.

For lighter oils ($API > 30°$), the evaporation is more significant, and thus the impacts of a spill reaching an ecosystem would be reduced. On the other hand, heavier oils ($API < 22°$), rich in asphaltenes and wax, would form more stable mousses with a low evaporative rate, thus preventing the spreading. Regarding intermediate oil types as the one simulated, the evaporative loss was not significant since a considerable volume of oil reached FNA in $P2J$ ($\sim 5{,}819\ ton$). Moreover, the low percentage of oil dispersed and sedimented indicates that advective processes are more considerable than buoyancy effects.

Figure 6 - Scenario P2M: Oil concentration on the water (ton/km²) after (a) 10 hours, (c) 20 hours, and (3) 30 hours. Scenario P2J: Oil concentration on the water (ton/km²) after (b) 10 hours, (d) 20 hours, and (f) 30 hours. The crosses represent the oil spill releasing points.

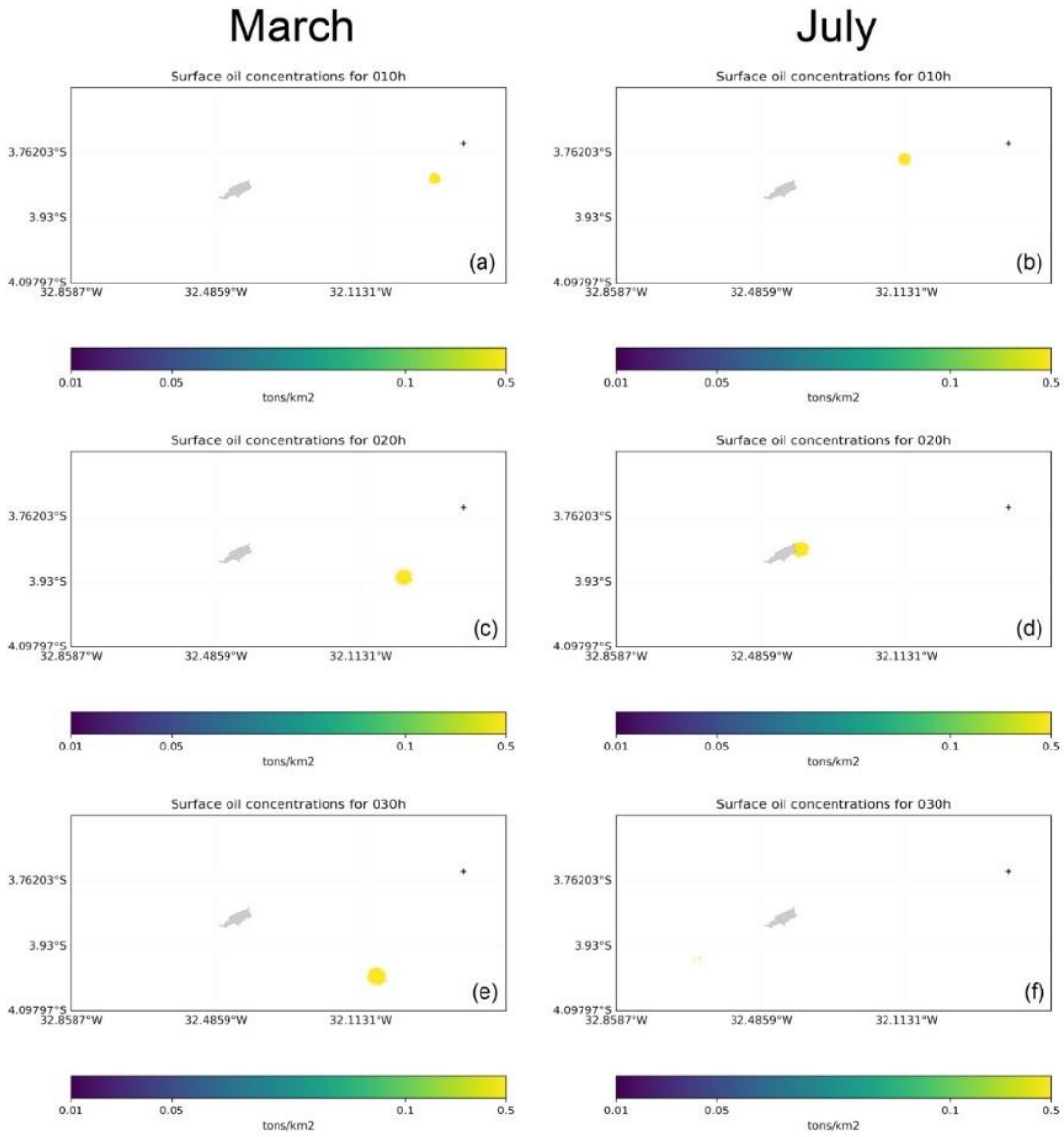

Source: The Author (2021)

The natural dispersion reduces the volume of the slick at the surface and reduces the evaporative loss; however, it does not alter the physicochemical properties of the oil (SEBASTIÃO; GUEDES SOARES, 1995). The wind speed and viscosity directly impact the percentage dispersed in the water columns, i.e., the higher the wind speed and the oil density, the more oil will be incorporated into the water column. The oil density did not vary significantly for both months, and the average wind speed in July ($7.52\ m/s$) is higher than in March ($2.86\ m/s$); thus, the oil dispersed in July is also higher, 0.93% ($\sim 8.43\ ton$) in July against 0.27% ($\sim 2.46\ ton$). The amount of oil dispersed into the water have serious

consequences to the environment, since toxic components to marine life from the oil are mixed on the water, i.e., the polycyclic aromatic hydrocarbon (PAH) (e.g., naphthalene, acenaphthene, fluorine, pyrene) (HONDA; SUZUKI, 2020).

The combination of current and wind direction being westwards is problematic if an oil spill occurs on the east side of FNA. The westward current and the predominant northeast wind in July intensify the oil transport towards FNA. It is important to note that the wind dictated the direction of the plume trajectory while the current dominated the flow. The southeast direction of the winds in March prevented the oil from reaching the archipelago. Still, the advective process predominates over the degradation effects (e.g., evaporation) in all scenarios. Thus, oil spills in July are of concern regarding catastrophic pollution in the archipelago.

The metoceanographic and physicochemical processes brought a high parcel of the oil that first reaches FNA within 20h. A total amount of around 63.95% of oil ($\sim$5,819 ton) is on the archipelago shore or sediment on the shallow water depths by the end of the simulation. This beaching is illustrated in Figure 6F when little oil is still being transported. The advective transport makes the time window for an effective response very narrow, potentially intensifying the impacts. Furthermore, mitigation actions such as the use of dispersants are very toxic to the environment (SHAFIR; VAN-RIJN; RINKEVICH, 2007). Thus, preventive actions should be prioritized instead of mitigating measures.

A highly uniform oil slick reaches FNA, with little spreading and 0.5 ton/km^2 of oil concentration. The regions affected encompass the Rata islet to the Sueste bay. They are susceptible areas with rich ecological hotspots. For instance, the coral reefs of FNA are of fundamental importance to the archipelago. They are sessile and sensitive to pollutants; the corals serve as food and shelter to many types of animals such as worms, crustaceans, sponges, sea urchins, and many fishes (YENDER et al., 2010). The loss of coral will affect humans and marine and terrestrial organisms since they protect the shoreline, support tourism, and contribute to fisheries.

Some species are essential to ecological tourism, such as sharks, sea turtles, and the spinner dolphin (*Stenella longirostris*) (QUEIROZ et al., 2019). Moreover, FNA presents several threatened fish species. The presence of such endangered species implies more conservation efforts. A recent assessment revealed that 17% of all fish species registered are threatened or near-threatened according to the International Union for the Conservation of Nature (IUNC) and the Chico Mendes Institute for Biodiversity Conservation (ICMBio) conservation status (SCHMID et al., 2020).

Even though oil tankers accidents are infrequent, these ships typically navigate nearby FNA. The damages suffered from the oil spills by the marine and terrestrial life may impact the ecosystem and also socioeconomic aspects of FNA. The ecological tourism and the domestic fishery will be reasonably affected, thus placing the FNA inhabitants in a critical situation.

4.6 CONCLUSION

Simulations of fate and transport of oil spills are critical in a risk assessment for oil spills. This work simulated hypothetical oil spills with oil tankers that navigate near the Fernando de Noronha Archipelago. The model simulated the oil trajectory and the weathering processes (evaporation, spreading, dispersion, emulsification, and coastal adhesion) that act on the spill, giving as results the percentages of oil affected by each of the processes mentioned above and the portions that remain on the coast and the sea. The simulations showed a potential for a high volume of oil reaching FNA, causing considerable damage to the environment and affecting the FNA community (e.g., fishing and tourism activities) for spills occurring in July, where the winds and currents are more potent. The advective forces dominate the weathering process; thus, the oil slick reaches FNA in a short time window. Hence, there would be little time to prepare for mitigation actions, and some measures like oil dispersants are very lethal to marine life. Thus, the simulation reinforces the need for preventive measures when facing potential oil spills.

5 FREQUENCY ASSESSMENT OF MARITIME ACCIDENTS USING BAYESIAN POPULATION VARIABILITY ANALYSIS

The content of this chapter was accepted for presentation at the 5th conference of the Brazilian Association of Risk Analysis, Process Safety, and Reliability (ABRISCO). It is also being prepared for further scientific publication.

Industrial accidents, such as toxic spills, have caused catastrophic environmental damage to animals and plants. The high number of vessels, including oil tankers that circulate the globe and extreme events such as storms and tropical cyclones due to global warming, increases the risk of potential oil spills affecting oceanic islands. The frequency estimate is a fundamental step in any risk assessment. However, some types of accidents correspond to rare, extreme events, i.e., low frequency-high consequences. In this context, classical statistical approaches are ineffective since available data are generally sparse and contain censored recordings. Thus, we here propose a Bayesian population variability-based method to estimate the distributions of accident rates. We can merge sparse data from accident databases and the judgment of experts such as pilots, captains, and chief officers. Finally, this assessment is used in the case of oil tankers that navigate nearby Fernando de Noronha Archipelago in Brazil. The frequency results will be incorporated into a further quantitative ecological risk assessment.

5.1 INTRODUCTION

Industrial accidents, such as oil spills, have caused catastrophic environmental damage to animals and plants. The high number of vessels, including oil tankers that circulate the globe and extreme events such as storms and tropical cyclones due to global warming, increases the risk of potential oil spills affecting oceanic islands. Despite the immense efforts of international and national maritime authorities to enhance ship safety over the years, many shipping accidents may still occur (ITOPF, 2021; UNG, 2019).

For instance, in the 2010s, a total of 63 spills happened, releasing 164,000 tons of oil, which was the minimum amount leaked in the last decades (ITOPF, 2021). In the Brazilian context, an oil spill with origin still unknown reached the northeastern coast in 2019 (IBAMA, 2020). Furthermore, the oil trade plays a vital role in economic development, and then there is a rise in the maritime transportation of oil volume. Indeed, the oil tankers are responsible for around 90% of the oil transported worldwide (CHEN et al., 2019).

Apart from threatening the crew's life and resulting in significant economic losses, oil spills are among the most hazardous pollutants for marine contamination, with catastrophic impacts on coastal countries' environments and ecosystems (CHEN et al., 2019). The oil spills are mainly caused by collision, contact, grounding, fire, explosion, and non-accidental structural failures and are defined as follows (IMO, 2008):

- Collision: striking or being struck by another ship, whether underway, anchored, or moored. This category does not include striking underwater wrecks.
- Contact: striking any fixed or floating objects other than those included under collision or grounding.
- Grounding: being around or hitting/touching shore or sea bottom or underwater objects (e.g., wrecks).
- Fire: incidents where the fire is the initial event.
- Explosion: incidents where the explosion is the initial event.
- Non-accidental structural failure: when the hull presents cracks and fractures, affecting the ship's seaworthiness.

However, when considering oil tankers that travel in the open sea near oceanic islands, we assume there is no grounding possibility due to water depths. Yet, there are no objects around that could characterize a contact. There was a significant drop in spills caused by the non-accidental structural failure after the 1990s (ITOPF, 2021). Thus, we did not consider this cause in our assessment. Collisions are responsible for about 40% of oil spills, while fire and explosion together correspond for more than 10%. The total amount of oil spilled by these three types of accidents since 1970 is very similar (ITOPF, 2021). Therefore, we focus our assessment on the rate of collision, fire, and explosion.

In the risk assessment of oil tanker spills, many different models and methods have been used to evaluate the frequency of the accidents. For instance, the International Maritime Organization (IMO) developed a tool for risk evaluation, the Formal Safety Assessment (FSA) for crude oil tankers, and used historical data in the frequency assessment step (IMO, 2008). (ELIOPOULOU; PAPANIKOLAOU, 2007) and (PAPANIKOLAOU et al., 2007) have used classical, statistical methods to evaluate the frequencies of accidents from 1978 to 2003 quantitatively. Fault Tree Analysis (FTA) is a traditional method to determine the causes of a maritime accident. (UĞURLU et al., 2015) analyzed maritime collision and grounding of oil tankers with FTA, while (UĞURLU et al., 2020) assessed variable conditions that would lead to an accident in a fishing vessel, such as environmental and operational conditions.

Regarding Bayesian Networks (BN), (UNG, 2019) evaluates the probability of collision integrating FTA with a modified Fuzzy BN based on Cognitive Reliability Error Analysis Method (CREAM), developed to assess the human error. (ANTÃO; SOARES, 2019) also evaluated human error contribution in different weather conditions, and (JIANG et al., 2020) and (ZHANG et al., 2016) proposed a BN-based risk analysis approach to investigate and predict marine accidents' probabilities. (MARTINS; MATURANA, 2013) applied BN for human reliability analysis in oil tanker operations. The contribution of organizational factors in accidents was also investigated by (TRUCCO et al., 2008).

(MARTINS; MATURANA, 2010) have developed a Human Reliability Analysis in maritime transportation following IMO's FSA guidelines, and (MARTINS; PESTANA; DROGUETT, 2020) integrated expert opinion with fuzzy analysis to assess the probability of accidents. Furthermore, (JIN et al., 2019) enriched the current literature by using machine learning-based methods (e.g., support vector machines) to assess the probability of maritime accidents.

Despite the advances aforementioned, to the best of the authors' knowledge, no statistics-based approaches have considered the heterogeneity in accidents, i.e., different characteristics of the ships (e.g., size, age) and the accident region (e.g., areas with severe meteo-oceanographic conditions). Some methods consider various factors (e.g., vessel's age and size, ship flag, and environmental factors) as variables that influence the likelihood of accidents (JIANG et al., 2020; JIN et al., 2019), but the uncertainties of each effect are not adequately assessed, since the impact may vary from location to location and from ship to ship.

Thus, we usually deal with a heterogeneous population of vessels subject to different environmental and operational conditions and other characteristics that can alter its accident rate (e.g., waves, tides, maritime traffic in the route). Hence, it is essential to analyze the variability of these rates over the entire population of ships. However, when considering accidents in a specific location, we may lack particular information or data. Other sources such as data from similar areas (e.g., same weather conditions) and expert judgments could be used to estimate these rates better.

Therefore, this paper proposes a Bayesian method to estimate accident rates in maritime transportation that can lead to oil spills. The remainder of this paper is structured as follows. Section 5.2 offers an overview of the Bayesian Population Variability Analysis (BPVA). Section 5.3 details the elicitation of experts' opinions, the maritime databases that we adopted, and the mathematical formulations for assessing the prior distribution, the likelihood

function, and the posterior variability distribution. Then, Section 5.4 presents and discusses the results, including a sensitivity analysis in the experts' judgments. Finally, in Section 5.5, we conclude remarks.

5.2 DESCRIPTION OF THE PROBLEM

We consider each ship has a unique accident rate. The Bayesian Population Variability Analysis (BPVA), also known as the first stage in a two-stage Bayesian, or hierarchical Bayes (DROGUETT; GROEN; MOSLEH, 2004), will estimate the variability distribution within a group of non-homogeneous ships. The proposed method is also an attempt to cover the drawbacks of the FSA, such as the inability to quantify risks and the lack of reliability and effectiveness when subjective knowledge is used in the absence of historical data (JIANG et al., 2020).

The distribution of the accident rates is not analytically obtainable, and thus we rely on a Markov Chain Monte Carlo (MCMC) approach to draw the non-parametric posterior distributions. Then, we use these distributions to create different scenarios, i.e., pessimistic, optimistic, and most probable, to assess the oil spills risks to oceanic islands. To the best of the authors' knowledge, no article has performed BPVA to model maritime accidents. The procedures implemented for BPVA are based on the mathematical methods developed for risk and reliability analyses, such as those in (MOURA et al., 2016) and (GRECO; PODOFILLINI; DANG, 2021). In this work, we tailored these methods to analyze maritime accidents properly.

As a case study, we consider oil tankers that travel near the Fernando de Noronha Archipelago (FNA), which has the most significant number of marine and terrestrial species, attributed to its extension and habitats' heterogeneity. FNA has the Conservation Unit status, protecting endemic species and maintaining a healthy island ecosystem (SERAFINI; FRANÇA, 2010). Two-thirds of FNA consist of the Marine National Park (PARNAMAR-FN), a Marine Protected Area that reaches the 50-meter isobathic line (ICMBIO, 2013). However, FNA lacks infrastructure and mitigation plans if it needs to deal with an oil spill, which could intensify the accident's impacts (QUEIROZ et al., 2019). Despite there is no evidence of large spills in recent years, it remains a latent threat (IUCN, 2020), and recently pieces of oil have been reported to reach the FNA coast (ICMBIO, 2021)

5.3 METHODOLOGY FOR THE FREQUENCY ASSESSMENT

5.3.1 Accident Databases

We use the exposure data (type E_1) to formulate the likelihood function of the Bayesian model. As we present in Section 5.3.3.1, the likelihood function uses the run-time data as the number of events during the exposure time (here measured as ship-year). We consider the number of accidents that happened during the exposure time of all operational ships.

Historical data can be extracted from IHS Fairplay (former Lloyds Register Fairplay) and Lloyds Maritime Intelligent UNIT (LMIU), which are the most prominent and complete' by current standards (ELIOPOULOU et al., 2012; IMO, 2008). However, these accident databases were not designed to be used in risk assessments, and thus their usage is problematic. For instance, the information is textual; therefore, they do not offer the accidents data on a quantitative basis, making it challenging to be used in FSA procedures.

The National Technical University of Athens, Ship Design Laboratory (NTUA-SDL) purposely designed a new database for risk assessment to overcome such drawbacks, including the data from both IHS and LMIU (SAFEDOR, 2009). It enabled further processing towards quantifying event categories and direct extraction of conditional probabilities of accidental scenarios (ELIOPOULOU et al., 2012; IMO, 2008). Thus, we used two versions of the NTUA-SDL available, the first records tanker ships greater than $60{,}000\ DWT$ (i.e., the cargo capacity in tonnes) from 1980 to 2007, while the second, from 1990 to 2008, include ships greater than $20{,}000\ DWT$ and even ships greater than $320{,}000\ DWT$ (ELIOPOULOU et al., 2012; IMO, 2008).

In the context of both NTUA-SDL databases, the exposure time is given as the operational fleet at risk (OPR), which is defined as the number of ships that operate in the corresponding period of interest, and it is measured as ship-year. Thus, OPR is the number of ships exposed to an accident during the time frame of the data collection.

Moreover, we used the Annual Overview of Marine Casualties and Incidents 2020 provided by the European Maritime Safety Agency (EMSA) and the Statistics of Marine Accidents of the Japan Transport Safety Board (JTSB) (EMSA, 2020; JTSB, 2021). The EMSA's purpose is to ensure a high, uniform, and adequate level of maritime safety and security, prevention of, and response to marine pollution caused by ships and oil and gas installations (EMSA, 2020). JTSB contributes to preventing accidents, mitigating their consequences, improving transport safety and raising public awareness, and protecting the people's lives by performing appropriate incident investigations and implementing policies

and measures through the issuance of safety recommendations, opinions, and information (JTSB, 2021).

EMSA database contains data from 2014 to 2019, while the JTSB, from 2007 to 2019, only provides the number of accidents during the years—however, they lack the OPR. Therefore, we researched to find the fleet of each region, i.e., Europe and Japan, and we used an educated guess to consider that a ship operates around 80% of the year. With this, we expect a reasonable approximation of the OPR.

5.3.2 Expert opinions

As a fundamental risk analysis step, the frequency assessment can usually be done using classical statistical methods, i.e., a frequentist approach. However, as mentioned above, it may not be possible to use such a method because of the lack of historical data. Even though there are accident databases available, there are no specific data regarding accidents near FNA. More specifically, there are cases for which general information is available, but they are not representative of the analyzed system, as in FNA.

Hence, we cannot use a frequentist approach to estimate the accident rates due to different operational conditions (i.e., traffic density, environmental conditions). Therefore, in cases like this, a subjective assessment of the frequency of occurrence is a viable option. The main advantage of such an approach is to aggregate all information available, apart from the historical data, thus delivering more reliable results (MARTINS; PESTANA; DROGUETT, 2020).

We have adopted a methodology proposed by Martins et al. (2020) that assesses expert judgments in the context of maritime accidents. The experts answer a questionnaire (see Appendix), and weights are given based on their category (i.e., profession) and experience with navigation. Such a questionnaire is suggested by the Delphi method (LINSTONE; TURROF, 2002), where experts give opinions on the problem individually and anonymously. Then, the methodology performs expert elicitation and maps the linguistic responses into probabilities using Fuzzy Logic (MARTINS; PESTANA; DROGUETT, 2020). Specifically to our case, we applied a similar questionnaire to weigh each expert's opinions and assign an error factor (EF) to each of them.

Amongst the experts that answered the questionnaire, we have a captain (CA) and a chief officer (CO). CA is the first authority in the ship, responsible for ensuring that the crew complies with the law, regulations, and duties, while CO is the second authority on board the vessel. Should CA be absent or impeded, CO assumes the function to guarantee the continuity

of their duties. CO also conducts the ship mainly in the shift changeover that occurs every 6 hours. In most critical circumstances, CA makes the decisions, communicates accordingly, and performs maneuvers. Both are responsible for the navigation. For more information about these categories, the definitions are found in NORMAM 13 (BRASIL, 2003), a maritime authority standard that defines, among other things, the duties and responsibilities of a ship's CA and the crew.

Moreover, the pilots (PL) also answered the questionnaire. PL are unmanned waterway professionals who provide pilotage services, which involve advisory to the commander due to local peculiarities that make it difficult for the vessel to freely and safely move when approaching the port (BRASIL, 2011). Other experts who gave their opinions were academics (AC), mainly Ph.D. in Naval and Ocean Engineering, and other waterway professionals (WP).

We simplified the questionnaire, providing alternatives as degrees of the magnitude of the accident rate. We offered options from $1\ yr^{-1}$ to $10^{-6}\ yr^{-1}$ and lower the frequency of accidents per year. We have considered the experience in their category and the navigation experiences in both open and restricted waters because, to reach FNA, we have navigation in open waters and, since the ships locate themselves by notable points on the archipelago, they approach the land (DUARTE; DROGUETT, 2016). We also included the experience of navigating the November oceanic area of Brazil. The maritime areas are under the responsibility of a given country, divided into coastal and oceanic, with similar metoceanographic conditions (e.g., waves, currents). Thus, if an expert had experience navigating in the November oceanic area, they were subjected to the same metoceanographic conditions as if they were navigating closer to FNA. The experts were grouped into ranges of values, as shown in Table 1.

Table 1 - Qualification and experience of the experts.

Expert	Category	Category experience (in years)	Experience navigating in open or restricted waters (in years)	Experience navigating in the November oceanic area
E1	AC	> 10	> 10	Yes
E2	WP	> 10	> 10	Yes
E3	AC	> 10	$0 - 2$	No
E4	PL	> 10	$0 - 2$	No
E5	AC	> 10	> 10	No
E6	CO	$5 - 6$	$3 - 4$	No

Expert	Category	Category experience (in years)	Experience navigating in open or restricted waters (in years)	Experience navigating in the November oceanic area
E7	CO	$7-8$	$0-2$	No
E8	WP	$9-10$	$0-2$	No
E9	CM	>10	>10	Yes

Source: The Author (2021)

The expert's score relates to each one's characteristics and considers the expert's expected knowledge to answer the question; they are used to distinguish the most experienced experts and provide a level of confidence to them. The opinions will be used as information type E_2 and it will be used to construct the likelihood function (3). A traditional method was applied to determine the experts' scores with proper changes to adjust to our context (MARTINS; PESTANA; DROGUETT, 2020; SENOL et al., 2015; YUHUA; DATAO, 2005). We attributed scores as a function of their abilities. For each item evaluated, successive points are obtained and accumulated to get the expert's total score. Table 2 presents the evaluation criteria and scores obtained for each item. We then normalize the scores, considering the least possible score (1) and the maximum possible score (25).

Table 2 - The scores attributed to the experts based on their experience and knowledge.

Criteria		Score (Points)
Category		
Commander		5
First official		4
Pilot		3
Academic		2
Waterway professional		1
Additional score depending on the experience in the category (in years)	$0-2$	0
	$3-4$	1
	$5-6$	2
	$7-8$	3
	$9-10$	4
	>10	5
Experience navigating in open or restricted waters (in years)		
Additional score depending on the	$0-2$	0

Criteria		Score (Points)
experience in the navigation (in years)	$3-4$	1
	$5-6$	2
	$7-8$	3
	$9-10$	4
	>10	5
Experience working in the November oceanic area of Brazil	No	0
	Yes	5

Source: The Author (2021)

5.3.3 Bayesian Population Variability Analysis

5.3.3.1 The likelihood function

To perform PVA for λ we need to specify an appropriate probability distribution $\phi(\lambda|\underline{\theta})$ related to the underlying variability of λ, and this decision is guided by the nature of the measure. As in (DROGUETT; GROEN; MOSLEH, 2004), we assume that the population variability of λ is given by a Lognormal distribution:

$$\phi(\lambda|\underline{\theta}) = \phi(\lambda|\nu,\tau) = \frac{1}{\sqrt{2\pi}\lambda\tau}\, exp\left(-\frac{1}{2}\left(\frac{ln\,\lambda-\nu}{\tau}\right)^2\right) \tag{5.1}$$

where ν and τ are the mean and the standard deviation of the natural logarithm of λ.

The likelihood is a data-driven function that depends on the type of available evidence. We can formalize the form of E_1 and E_2 as follows:

- Type E_1 (exposure evidence): the number of failures and exposure time in service. Then, E_1 is in the form $\{(k_i, t_i), i = 1, \dots, n\}$, where k_i is the number of failures and t_i is the time to observe k_i failures for the *i*th system.
- Type E_2 (sources' estimates): estimates of possible values of λ. We assume that the analyst consults n independent sources, and the extent of their confidence in each source is represented by the multiplicative error model (MOSLEH, 1992) Thus, E_2 is in the form $\{(\rho_i, \sigma_i), i = 1, \dots, n\}$, where ρ_i is the estimated provided by the *i*th source, and σ_i is the logarithmic standard deviation representing a subjective measure of the analyst's confidence in the source *i*.

If we know the accident rate of each system λ_i we can use the Poisson distribution to estimate the likelihood of observing k_i events over time t_i:

$$P(t_i, \lambda_i, E_0) = \frac{(\lambda_i t_i)^{k_i} e^{-\lambda_i t_i}}{\Gamma(k_i+1)} \tag{5.2}$$

Following the multiplicative error model proposed by (MOSLEH, 1992), the likelihood function for the *i*th source estimate (type E_2) can be written as a Lognormal distribution with a median $ln\ \lambda_i$:

$$P(\sigma_i, \lambda_i, E_0) = \frac{1}{\sqrt{2\pi}\mu_i\rho_i}\, exp\ \left(-\frac{1}{2}\left(\frac{ln\ \rho_i - ln\ \lambda_i}{\sigma_i}\right)^2\right) \tag{5.3}$$

We consider an unbiased expert (for more information on the biased expert, see (MOSLEH; APOSTOLAKIS, 1985)). Note that if we apply the transformation $\mu_i = ln\ \rho_i$ we can write (5.3) as:

$$P(\sigma_i, \lambda_i, E_0) = P(\sigma_i, \lambda_i, E_0)\left|\frac{d\rho_i}{d\mu_i}\right|$$

And knowing that $\left|\frac{d\rho_i}{d\mu_i}\right| = e^{\mu_i}$:

$$P(\sigma_i, \lambda_i, E_0) = \frac{1}{\sqrt{2\pi}\mu_i e^{\mu_i}}\, exp\ \left(-\frac{1}{2}\left(\frac{\mu_i - ln\ \lambda_i}{\sigma_i}\right)^2\right) e^{\mu_i}$$

Thus,

$$P(\sigma_i, \lambda_i, E_0) = \frac{1}{\sqrt{2\pi}\sigma_i}\, exp\ \left(-\frac{1}{2}\left(\frac{\mu_i - ln\ \lambda_i}{\sigma_i}\right)^2\right) \tag{5.4}$$

which is a Normal distribution with mean equals to $ln\ \lambda_i$.

Since λ_i is one of the possible values of λ given by the population variability distribution $\phi(\underline{\theta})$, we average the likelihood given by Equation 2.30 over all possible values of λ to calculate the likelihood of the data unconditional to λ:

$$P(k_i, t_i, \mu_i, \sigma_i | \nu, \tau, E_0) = P_i = \int_\lambda P(k_i|t_i, \lambda_i, E_0) P(\mu_i|\sigma_i, \lambda_i, E_0) \phi(\lambda|\nu, \tau) d\lambda \tag{5.5}$$

where we have considered run-time data and estimates evidence to be independent. We also assume that the *i*th expert estimate ρ_i is for the same *i*th system for which run-time data (k_i, t_i) have been acquired. Next, replacing Equations 5.1 and 5.4 into Equation 5.5:

$$P_i = \int_\lambda P(k_i|t_i, \lambda_i, E_0) \frac{1}{2\pi\sigma_i\tau\lambda_i} \exp\left\{-\frac{1}{2}\left[\left(\frac{\mu_i - \ln\lambda_i}{\sigma_i}\right)^2 + \left(\frac{\ln\lambda_i - \nu}{\tau}\right)^2\right]\right\} d\lambda \tag{5.6}$$

We can write $\exp\left\{-\frac{1}{2}\left[\left(\frac{\mu_i - ln\ \lambda_i}{\sigma_i}\right)^2 + \left(\frac{ln\ \lambda_i - \nu}{\tau}\right)^2\right]\right\}$ as $\exp\left[-\frac{1}{2}\left(\frac{\mu'_i - ln\ \lambda_i}{\sigma'_i}\right)^2\right]$, where:

$$\sigma'_i = \sqrt{\frac{1}{\frac{1}{\tau^2}+\frac{1}{\sigma_i^2}}} \quad and \quad \mu'_i = \frac{\frac{\nu}{\tau^2}+\frac{\mu_i}{\sigma_i^2}}{\frac{1}{\tau^2}+\frac{1}{\sigma_i^2}} \tag{5.7}$$

Thus, the likelihood function (Equation 5.6) can be expressed as:

$$P_i = \int_\lambda \frac{(\lambda_i t_i)^{k_i} e^{-\lambda_i t_i}}{\Gamma(k_i+1)} \frac{1}{2\pi\sigma_i\tau\lambda} \exp\left\{-\frac{1}{2}\left[\left(\frac{\mu'_i - \ln\lambda_i}{\sigma'_i}\right)^2 + \frac{(\mu_i-\nu)^2}{\sigma_i^2+\tau^2}\right]\right\} d\lambda$$

and, after some algebraic manipulation, we have that:

$$P_i = \frac{\exp\left\{-\frac{1}{2}\left[\frac{(\mu_i-\nu)^2}{\sigma_i^2+\tau^2}\right]\right\}}{2\pi\sigma_i\tau} \int_\lambda \frac{t_i^{k_i}\lambda_i^{k_i-1}e^{-\lambda_i t_i}}{\Gamma(k_i+1)} \exp\left\{-\frac{1}{2}\left[\left(\frac{\mu'_i-\ln\lambda_i}{\sigma'_i}\right)^2\right]\right\} d\lambda \tag{5.8}$$

Note that the previous equation can also be written as a product of a Gamma and a Lognormal distribution, as follows:

$$P_i = \frac{\sigma'_i \exp\left\{-\frac{1}{2}\left[\frac{(\mu_i-\nu)^2}{\sigma_i^2+\tau^2}\right]\right\}}{\sqrt{2\pi}\sigma_i\tau t_i} \int_\lambda \frac{t_i^{k_i+1}\lambda_i^{(k_i+1)-1}e^{-\lambda_i t_i}}{\Gamma(k_i+1)} \frac{1}{\sqrt{2\pi\sigma'_i\lambda_i}} \exp\left\{-\frac{1}{2}\left[\left(\frac{\mu'_i-\ln\lambda_i}{\sigma'_i}\right)^2\right]\right\} d\lambda$$

Substituting the expressions for μ'_i and σ'_i given by (5.7) we have that:

$$P_i = \frac{\exp\left\{-\frac{1}{2}\left[\frac{(\mu_i-\nu)^2}{\sigma_i^2+\tau^2}\right]\right\}}{\sqrt{2\pi}\sigma_i\tau t_i \sqrt{\frac{1}{\frac{1}{\tau^2}+\frac{1}{\sigma_i^2}}}} \int_\lambda Ga(\lambda|k_i+1,t_i) LN\left(\lambda \middle| \frac{\frac{\nu}{\tau^2}+\frac{\mu_i}{\sigma_i^2}}{\frac{1}{\tau^2}+\frac{1}{\sigma_i^2}}, \sqrt{\frac{1}{\frac{1}{\tau^2}+\frac{1}{\sigma_i^2}}}\right) d\lambda \tag{5.9}$$

The final likelihood is obtained by replacing Equation 5.9 with Equation 2.29.

5.3.3.2 The prior distribution

The proposed procedure involves the specification of an informed continuous prior distribution over the parameter space $\underline{\theta}$. This prior state of knowledge is the type E_0 evidence and the analyst may provide central value estimates and the extent of variability for the population variability parameters ($\underline{\theta}$).

Following the multiplicative error model proposed by (DROGUETT; MOSLEH, 2013, 2014), if we specify these estimates in terms of a median (central value estimate) and the error factor (extent of variability), they follow a Lognormal distribution. If θ_{50}^j and EF_{θ^j} are the median and the error factor of the *j*th parameter $\theta^j (j = 1, \dots, p)$, then the probability density over θ^j can be given by:

$$f_{LN}\left(\theta_{50}^{j}, EF_{\theta^j}\right) = \frac{1}{\sqrt{2\pi}\theta_{50}^{j}\frac{ln\,EF_{\theta^j}}{1.645}} exp\left[-\frac{1}{2}\left(\frac{ln\,\theta^j - ln\,\theta_{50}^{j}}{\frac{ln\,EF_{\theta^j}}{1.645}}\right)^2\right] \quad (5.10)$$

where $f_{LN}(.)$ is the lognormal density.

As ν and τ are in a natural scale, (DROGUETT; GROEN; MOSLEH, 2004) suggested that the prior distributions were specified over the median ($\lambda_{50} = e^{\nu}$) and the error factor ($EF_{\lambda} = e^{1.645\tau}$) of λ, instead of over the mean ν and the standard deviation τ. Therefore, if we consider that the population variability parameters are independent, the prior density over the model's parameter space (ν, τ) is found by applying the standard density transformation as follows (DROGUETT; GROEN; MOSLEH, 2004):

$$\pi_0(\nu,\tau) = f_{LN}(\lambda_{50}) f_{LN}(EF_{\lambda}) \left|\frac{\partial(\lambda_{50}, EF_{\lambda})}{\partial(\nu,\tau)}\right| = f_{LN}(\alpha,\delta) f_{LN}(\beta,\varepsilon) 1.645 e^{(\nu + 1.645\tau)} \quad (5.11)$$

where α and β are the median estimates of λ_{50} and EF_{λ} respectively; while δ and ε are the error factor estimates of λ_{50} and EF_{λ} respectively. A discussion about other prior specifications can be found in Kaplan (KAPLAN, 1983) and Pörn (PÖRN, 1996).

5.3.3.3 The posterior distribution

The likelihood function 2;29 and the prior distribution 5.11 have been incorporated in a Bayesian inference procedure to compute the posterior distribution of the population variability parameters $\pi_2(\underline{\theta}) = \pi(\underline{\theta}|E_0, E_1, E_2)$. This expression is not analytically obtainable; it is estimated using a Markov Chain Monte Carlo-based method (GILKS; RICHARDSON; SPIEGELHALTER, 1995). Therefore, an *N*-sample set $\{(\nu_1,\tau_1), \ldots, (\nu_n,\tau_n)\}$ representing the posterior density over the parameters of the variability distribution model $\phi(\lambda|\nu,\tau)$ is generated from (2). The estimated population variability density is computed as an averaged value of the distribution model applied on the sample points, i.e., $\hat{p}(\lambda) = \frac{1}{N}\sum_{k=1}^{N}\phi(\lambda|\nu_k,\tau_k)$. The mean and variance are computed as the mean and variance of $\phi(\lambda|\nu,\tau)$ respectively, i.e., $\hat{\eta}_{\lambda} = \int_{\lambda}\lambda\hat{p}(\lambda)d\lambda = \frac{1}{N}\sum_{k=1}^{N}\eta(\nu_k,\tau_k)$ and $\sigma_{\lambda}^2 = \int_{\lambda}(\lambda - \hat{\eta}_{\lambda})\hat{p}(\lambda)d\lambda = \frac{1}{N}\sum_{k=1}^{N}\sigma^2(\nu_k,\tau_k)$.

Moreover, the results include uncertainty bounds of the cumulative variability distribution $\hat{P}(\lambda) = \int_{x=0}^{\lambda}\hat{p}(x)dx$, in the form of *z*th percentiles $\hat{P}_z(\lambda)$. The percentiles are determined by finding the value $\hat{P}_z(\lambda)$ for which a fraction $\frac{z}{100}$ satisfies $\int_{x=0}^{\lambda}\phi(x|\nu_k,\tau_k)dx <$

$\hat{P}_z(\lambda)$. These bounds provide the analyst with a basis to assess the uncertainty associated with the estimated PVD over λ.

Figure 1 presents a schematic diagram of the BPVA procedure. The dashed line indicates that we used the data available as an initial guess to construct the prior distribution. The solid lines indicate using the mathematical models described in Equations 5.2 and 5.13, aggregating all the available information and delivering more robust results.

Figure 1 - Schematics of the Bayesian Population Variability Analysis procedure

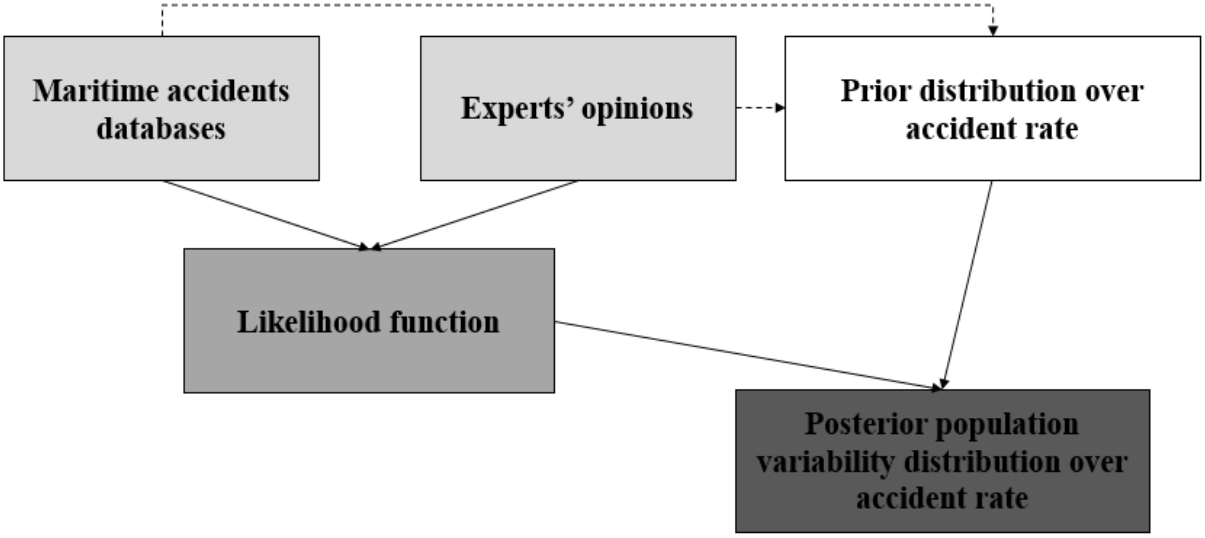

Source: The Author (2021)

5.4 RESULTS AND DISCUSSION

This section applies the BPVA procedure by using real datasets of maritime accidents and expert judgments about events near FNA. Both types of data will be used to construct the likelihood function (3). Then, the BPVA is applied to assess the PVD of the rates of accidents, i.e., collision, fire and explosion, that can occur to oil tankers. We focus on three different types of accidents; hence, we will have one population variability distribution of each accident.

5.4.1 Accident Databases

After collecting the information of accidents from the NTUA-SDL, EMSA and JTSB databases, we have summarized the accident's occurrence in Table 3. We also include the operational feet at risk (OPR) for each database, analogous to the exposure time. This information will be adopted as a type E_1 evidence to build the likelihood function (5.3).

Table 3 - Maritime accident data used in the analysis

		Occurrences			
Database	Period	Collision	Fire	Explosion	OPR $(ship\ years)$
NTUA-SDL	$1980-2007$	606	225	115	38211.2
NTUA-SDL	$1990-2008$	288	78	39	32808
EMSA	$2014-2019$	232	35	35	34009.6
JTSB	$2007-2019$	538	68	5	42591.45

Source: The Author (2021)

5.4.2 Expert opinions

As stated previously, the score of the expert relates to each one's characteristics and knowledge. For instance, the expert E1 accumulated 17 points: 2 from the category (AC), 5 points from the category experience, 5 points from navigation experience in open or restricted water, and 5 points from navigating the November oceanic area. The 17 points were normalized, obtaining a normalized score of 0.8421. We applied the same procedure to the other experts, getting their normalized scores as reported in Table 4.

Table 4 - Expert's scores

Expert	E1	E2	E3	E4	E5	E6	E7	E8	E9
Score	17	16	7	8	12	7	7	5	20
Normalized score	0.8421	0.7895	0.3158	0.3684	0.5789	0.3158	0.3158	0.2105	1

Source: The Author (2021)

Then, we attributed the EF depending on the normalized scores, as follows: (*i*) normalized scores ranging from 0 to 0.333 were labeled as a High EF ($EF_\lambda = 5$); (*ii*) if they range from 0.333 to 0.667, labeled as Moderate EF ($EF_\lambda = 3$); (*iii*) and scores ranging from 0.667 to 1, labeled as Low EF ($EF_\lambda = 1.5$). We illustrate how the error factor impacts a lognormal distribution that models the expert opinions, with the median 10^{-5} (see (14)) in Figure 2. Lower EF implies a distribution centered in the median value, while higher EF increases the dispersion. Thus, the higher the scores, the more confidence we have in that expert and the smaller the error factor.

The questionnaire results showed some divergence among experts. For instance, E3 argues that the frequency of accidents is negligible globally, which justifies the opinion of $0.001/year$ for all the accident rates. The expert reinforces that the actual rates may be even lower than the estimates given. Since accident reports are absent, the expert E4 considers that the navigation around FNA is safe. Expert E5 points out that accidents involving oil tankers in

the open sea are infrequent. As reported by the Brazilian Navy, these accidents are more likely to occur during operation (e.g., loading and unloading) in ports (BRASIL, 2021). Table 5 presents the results obtained from the questionnaires according to experts E1 to E9. The Table 5 also includes our level of confidence in the experts based on their scores. This information will be used as a type E_2 evidence to build the likelihood function (2.29).

Figure 2 - Lognormal distributions for different error factor values

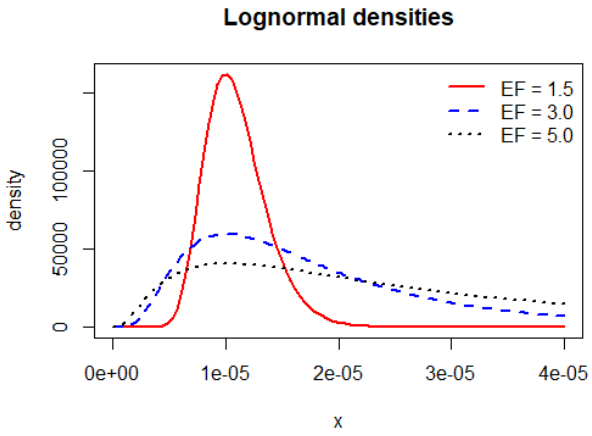

Source: The Author (2021)

Table 5 - Expert's opinions about the frequency of maritime accidents near FNA

	Frequency opinions $(1/year)$			Level of confidence	
Expert	Collision	Fire	Explosion	Level	EF_λ
E1	0.1	0.01	0.001	High	1.5
E2	0.01	0.0001	0.0001	Moderate	3
E3	0.001	0.001	0.001	Low	5
E4	0.01	0.1	0.01	Low	5
E5	0.01	0.01	0.01	Moderate	3
E6	0.1	1	0.01	Low	5
E7	0.1	0.1	0.1	Low	5
E8	0.1	0.1	0.1	Low	5
E9	0.01	0.1	0.01	High	1.5

Source: The Author (2021)

5.4.3 Bayesian Population Variability Analysis

We estimated the prior distributions from statistics extracted from both exposure data and expert opinions. The prior distributions were selected as (5.15), formulated over the

median and the error factor (PVD parameters). We can consider this approach because we have all the data available to construct prior knowledge on the system.

Thus, we can define a, b, c and d as the parameters of the prior distribution defined over the parameters of the accident rates PVD. The parameter a denotes the median estimates, while b is the error factor of the median, c is the central value estimate of the error factor, and d is the error factor of the error factor. We can estimate these parameters as follows (MOURA et al., 2016):

- The parameter a can be estimated as the median of the data set formed by the ratio of the number of events by the OPR and expert opinions. We have then $a = median\left(\left\{\frac{k_i}{t_i}\right\}_{i=1}^{N}, \{\rho_i\}_{i=1}^{M}\right)$ where N denotes the size of the accidents dataset and M is the number of opinions;
- We can compute the error factor as the ratio between the 95th percentile and the median of the distribution; then, $c = \frac{95th\ percentile\left(\left\{\frac{k_i}{t_i}\right\}_{i=1}^{N}, \{\rho_i\}_{i=1}^{M}\right)}{median\left(\left\{\frac{k_i}{t_i}\right\}_{i=1}^{N}, \{\rho_i\}_{i=1}^{M}\right)}$;
- The extent of variability, i.e., the error factor, can be interpreted as the uncertainty measure that characterizes the analyst's confidence in the central value estimates. Then, we fixed the parameters b and d as 5;

We first consider BPVA only uses data from maritime accident databases, a non-expert (NE) scenario. Figure 3 shows the computed cumulative population variability distribution (CPVD) and the 5th and 95th percentile curves, as explained in Section 5.3.3.3. The parameters of the prior distributions were estimated for each accident type and are presented in Table 6.

Table 6 - Parameters for constructing the prior distribution for the NE scenario.

Parameter	Definition	Collision	Fire	Explosion
a	Median estimates	0.013457	0.001861	0.0001484
b	Error factor of the median	5	5	5
c	Estimate of the error factor	1.367431	3.12583	20.03442
d	Error factor of the error factor	5	5	5

Source: The Author (2021)

We can compute the uncertainty bounds as the vertical difference between the 5th and 95th percentile curves for each λ. As shown in Figure 3, the uncertainty bounds are more

significant for the extreme values of the accidents rates for all three CPVDs. These bounds are the widest for the explosion rates because apart from the lack of data in these extremes, the variance of the distribution is the highest (see the parameter c in Table 6). Note that the PVD of fire rates presents a high slope, thus indicating that even with the second-highest error factor (see Figure 3), the estimates deviate little from the central value. This behavior can be explained by the fact that there is no data regarding accidents rates in these extremes, and thus, a reasonable estimate cannot be obtained

Figure 3 - Cumulative population variability for the NE scenario.

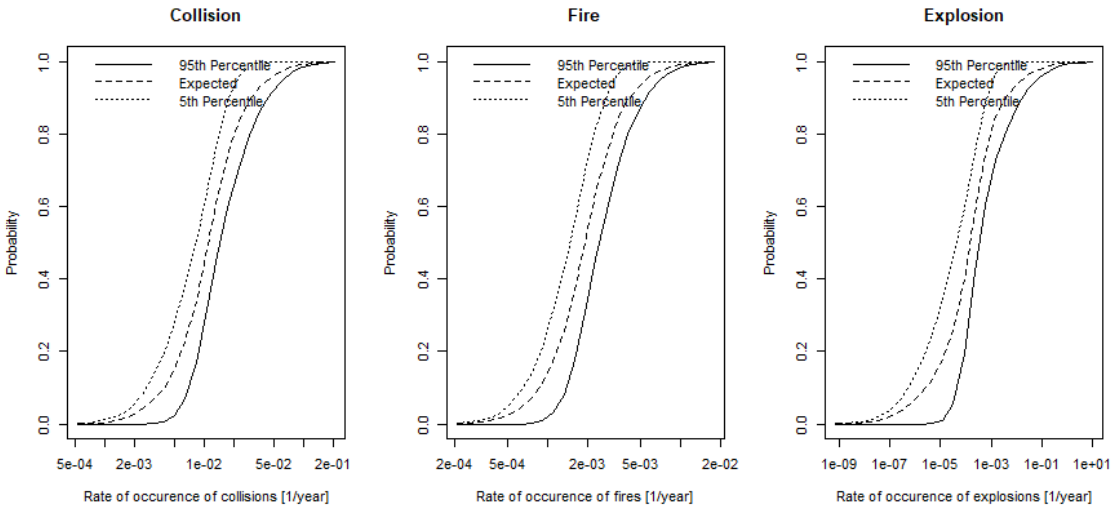

Source: The Author (2021)

We now investigate the experts' opinions on the CPVDs in an expert (E) scenario. We present in Table 7 the parameters of the prior distributions. These opinions are included as the parameter ρ_i to update the median (a) and error factor (c) prior parameters estimates. The likelihood is built with this new data source as detailed in Section 5.3.3.1. Note how the estimates for error factors increased in orders of magnitude even with minor differences in the median estimates compared to the NE scenario. This increase can be justified because some opinions could overestimate the accidents' rates, leading to higher values in the 95th percentile.

Table 7 - Parameters for constructing the prior distribution for the E scenario.

Parameter	Definition	Collision	Fire	Explosion
a	Median estimates	0.012789	0.002063	0.000317

Parameter	Definition	Collision	Fire	Explosion
b	Error factor of the median	5	5	5
c	Estimate of the error factor	7.819487	353.9353	315.36
d	Error factor of the error factor	5	5	5

Source: The Author (2021)

The computed cumulative population variability function, and the 5% and 95% uncertainty bounds, with all the data available, can be seen in Figure 4. We can still note uncertainty bounds are broader in the extremes of the distributions. However, we have reasonable estimates in the central regions of the CPVDs since the uncertainty bounds there are tighter. With the inclusion of the opinions, the CPVDs now cover a wider range of values, resulting from the higher error factors estimates. For instance, in the NE scenario, the CPVD for the fire rates ranges from $2E-4$ to $2E-2$. Once we include this information, the E scenario range increases from $1E-5$ to $1E-1$. In Table 8, we summarize the maximum, minimum, and mean uncertainty bounds for the E and PE scenario and also compute the percentage variation of these bounds. These bounds were calculated by obtaining the difference between the 5^{th} and the 95^{th} percentile cumulative probabilities for each value of λ.

Figure 4 - Cumulative population variability for the E scenario

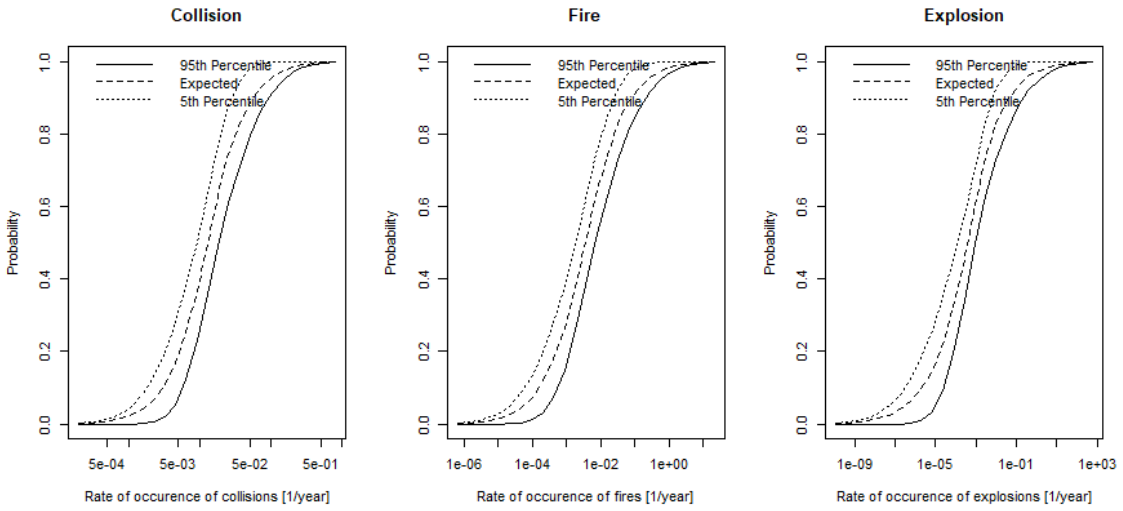

Source: The Author (2021)

Table 8 - Comparison of the uncertainty bounds in the PVDs for the NE and E scenarios. The column ($\Delta\%$) indicates the percentage difference between the bounds.

	Collision			Fire			Explosion		
	NE	E	($\Delta\%$)	NE	E	($\Delta\%$)	NE	E	($\Delta\%$)
Min.	$1.73E-3$	$2.09E-3$	21.03	$1.66E-3$	$2.21E-3$	33.22	$1.08E-3$	$2.13E-3$	97.27
Mean	$1.24E-1$	$1.14E-1$	-8.72	$1.36E-1$	$1.02E-1$	-25.20	$1.25E-1$	$1.02E-2$	-18.31
Max.	$3.34E-1$	$2.81E-1$	-15.85	$3.88E-1$	$2.37E-1$	-38.85	$4.04E-1$	$2.60E-1$	-35.63

Source: The Author (2021)

Note how, in general, the maximum and mean bounds (highlighted in grey) for all three accidents decreased while the minimum bounds increased. Therefore, we can assume we have better estimates for the accidents' rates by including the experts' opinion since the overall mean of the uncertainty bounds reduced.

5.4.4 Sensitivity Analysis

We here varied the original estimates of the experts by one order of magnitude, i.e., one order of magnitude higher and one lower. By doing that, we can assess pessimistic (PE) (higher estimates) and optimistic (OP) (lower estimates) views regarding the occurrence of accidents. The prior parameters that account for the modified opinions are shown in Table 9 and Table 10, respectively.

Estimating the PE scenario's error factors indicates that this view deviates considerably from the estimates obtained from the databases. Thus we have a higher variance for the posterior distribution. Hence, we can see in Figure 5 how the extents of the three accidents' CPVDs are even more significant. Since the variances are higher, the CPVDs cover a wider range of possible values with almost no tendency towards a central value. Note that the explosion CPVD ranges from $1E-14$ to $1E6$.

Table 9 - Parameters for constructing the prior distribution for the PE scenario.

Parameter	Definition	Collision	Fire	Explosion
a	Median estimates	0.014521	0.002214	0.0003192
b	Error factor of the median	5	5	5
c	Estimate of the error factor	68.864	3,297.931	3,132.8
d	Error factor of the error factor	5	5	5

Source: The Author (2021)

Figure 5 - Cumulative population variability for the PE scenario

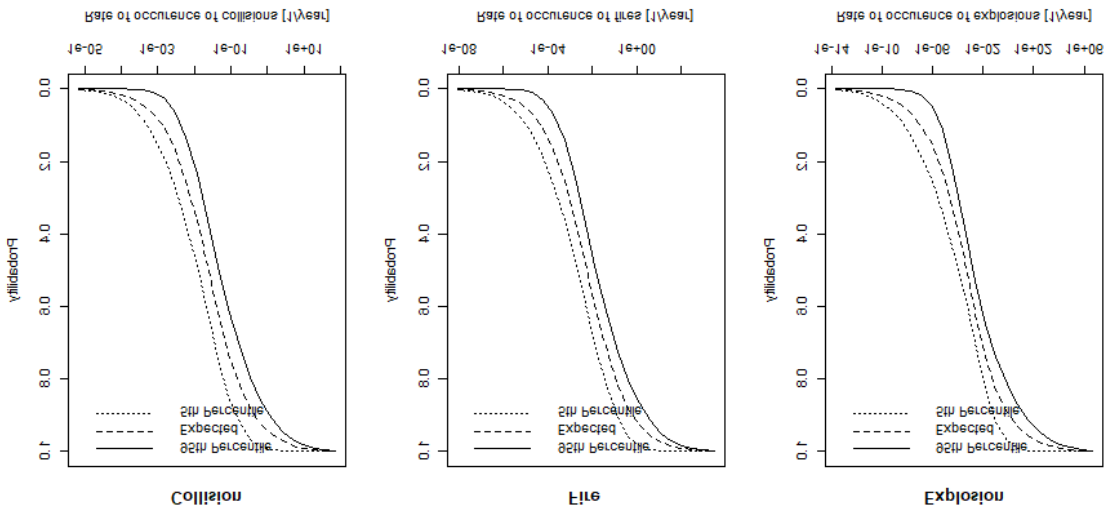

Source: The Author (2021)

The opposite happens for the OP scenario, i.e., the extents of the PVD are shorter due to smaller error factors (see Table 10) since the optimistic opinions are closer to the estimates from the databases. Figure 6 shows these smaller extents and how the uncertainty bounds are still broader in the extremes and narrower in the middle.

Table 10 - Parameters for constructing the prior distribution for the OP scenario.

Parameter	Definition	Collision	Fire	Explosion
a	Median estimates	0.010	0.001967	0.000299
b	Error factor of the median	5	5	5
c	Estimate of the error factor	1.802705	37.10347	33.4456
d	Error factor of the error factor	5	5	5

Source: The Author (2021)

Figure 6 - Cumulative population variability for the OP scenario

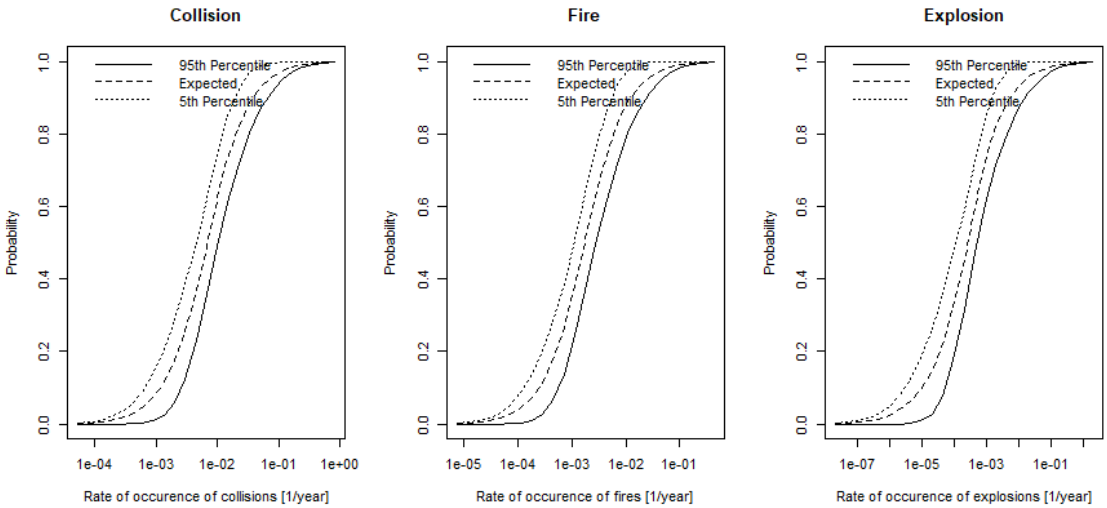

Source: The Author (2021)

Furthermore, Figure 7 presents the expected values (i.e., the mean) of the expected PVDs for each accident rate. At the same time, in Table 11, we computed the percentage variation of the means for each accident in each scenario evaluated. Except in the OP scenario, the accidents' rates increased as we added opinions to the assessment compared to the NE scenario. We have a slight increase for collisions and explosions when we add the views (16.41% and 4.08%, respectively), while for the fire, this increase is more substantial, almost doubling (87.57%). Although the estimates are higher, they are also improved since the uncertainty bounds are narrower in the central regions (see Figure 3 and Figure 4). Note the OP scenario lead to a reduction in the accidents' rates estimates. The highest decrease occurred in collision rates (-38.66%) and explosion (-31.52%) rates, while the fire rate estimated had a minor reduction (-9.00%).

Figure 7 - Means of the accidents' expected PVDs for the NE, E, PE and OP scenarios.

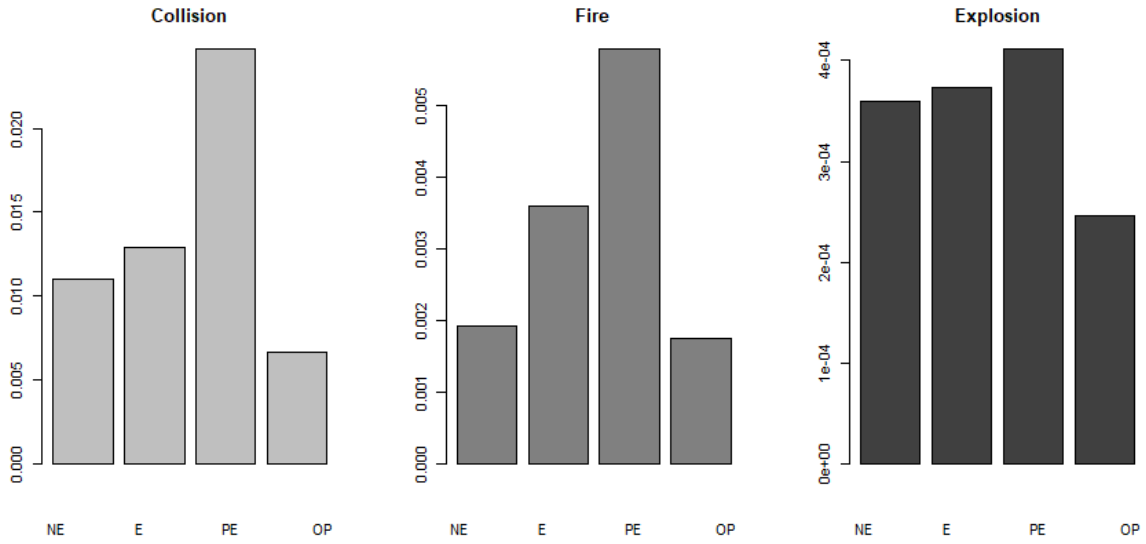

Source: The Author (2021)

Table 11 - Modes percentage variation of the accidents' expected PVDs for the E, PE, and OP scenarios compared to the NE scenario.

	NE	E		PE		OP	
	Mode	Mode	(Δ%)	Mode	(Δ%)	Mode	(Δ%)
Colision	$1.11E-2$	$1.29E-02$	16.41	$2{,}47E-02$	123.61	$6.78E-03$	-38.66
Fire	$1.92E-3$	$3.60E-03$	87.57	$5.79E-03$	201.54	$1.75E-03$	-9.00
Explosion	$3.59E-4$	$3.73E-04$	4.08	$4.11E-04$	14.66	$2.46E-04$	-31.52

Source: The Author (2021)

5.5 CONCLUSION

The model presented in this paper is based on the Bayesian Population Variability Analysis method, which allows evaluating the population variability distributions of maritime accidents (i.e., collision, fire, and explosion) from jointly maritime accident databases and experts' opinions. The PVA permits uncertainty treatment on the measures of interest. The model was fed with available databases of maritime accidents reported. However, some locations, such as the case of FNA we assessed, lack data regarding accidents. Thus, we can use subjective knowledge from experts to complement our information, leading to a better-estimating model. Indeed, the results showed that, in general, the uncertainty bounds of the cumulative posterior variability distribution reduced when we added the judgments. Such a decrease mainly occurred in the central values of the accident rates. Therefore, with narrower bounds, we have more confidence in our estimates.

6 QUANTITATIVE ECOLOGICAL RISK ASSESSMENT FOR OIL SPILLS IN FERNANDO DE NORONHA ARCHIPELAGO

This chapter presents the QERA results according to the general steps proposed by Duarte et al. (2019). The main findings of Chapters 4 and 5 will integrate the exposure assessment and the frequency estimates steps, respectively.

6.1 CHARACTERIZATION OF THE PROBLEM

This methodology step has already been presented in Chapter 1 (Section 1.2).

6.2 IDENTIFICATION OF HAZARDS AND CONSOLIDATION OF SCENARIOS (SCNs)

The primary forces that act on the oil spill are the currents and winds. We chose the months in which the averaged currents and winds are more intense. The central branch of the South Equatorial Current (cSEC) starts to intensify in March, but with a lower wind speed, reaching its highest intensity in July, with even stronger southeast trade winds (LUMPKIN; GARZOLI, 2005; MOLINARI, 1982).

The route that possesses a significant hazard is the REC – CN, which passes from south to east of FNA. Hence, a potential oil spill on this route is likely to be transported to the archipelago coast due to prevailing winds and currents. We defined three initial spill releasing points on this route, and that is also supported by the information of a high traffic intensity registered by the Marine Traffic (MARINETRAFFIC, 2021). The oil simulation results indicate that the only point that leads to a significant amount of oil reaching FNA is the $P2$ $(3°44.3'S;\ 31°51'W)$ (Figure 3 in Section 4.3.2).

Thus, we define the benchmark scenario, the basis for comparing the results of the risk assessment, and three accidental scenarios (SCNs), based on the accidents that could occur in this route and lead to an oil spill:

- SCN-0: Benchmark; a scenario of no impact of oil pollution;
- SCN-1: Collision; striking or being struck by another ship, whether underway, anchored, or moored. This category does not include striking underwater wrecks.
- SCN-2: Fire; incidents where the fire is the initial event.
- SCN-3: Explosion; incidents where the explosion is the initial event.

6.3 ASSESS EXPOSURE TO RISKS

The crude oils present in their composition (around 0.6% to 6% of the weight), the polycyclic aromatic hydrocarbon (PAH) (JOHANSEN et al., 2017). These compounds are toxic to marine life: highly carcinogenic, mutagenic and teratogenic (i.e., can cause congenital disabilities) for the aquatic biota (JOHANSEN et al., 2017). Much effort has been performed to properly document the impacts of oil exposure on marine life, such as a recent study that assessed the consequences on the reef community after the Deepwater Horizon oil spill (LEWIS et al., 2020). One can model the relationship between mortality due to the concentration exposure with a dose-response model.

Studies for the ecotoxicology of the REP due to exposure to oil were not available. Thus, we consider a study performed on other coral reef fishes to estimate the oil impact on the REP (JOHANSEN et al., 2017). The paper results indicate that exposure to more than seven days to oil can cause a 10% mortality regardless of the PAH concentrations they evaluated, i.e., 2.5 mg/L and 5.7 mg/L of PAH. Another study addressed the PAH impacts to the fish reproduction and they found that on polluted locations, only 40% to 60% of the female underwent gonadal development (JOHNSON et al., 2008). This result means that almost half of the females are unable to reproduce.

The oil spill simulation results provided that an oil concentration of 0.5 ton/km^2 reaches FNA. To have the concentration as a mass of oil per volume, we assume a depth of 3m, based on the minimum depth in which fish assessments were performed in the archipelago (BARROS, 2020; SCHMID et al., 2020). Hence, we have an oil concentration of 0.143 kg/m^3 that can be converted to 0.143 mg/L. Assuming that 6% of the oil mass is composed by PAH, we have a PAH concentration in FNA of approximately 0.009 mg/L. This value is above the minimum concentration reported to cause damage to marine life, i.e., 0.0012 mg/L (JOHANSEN et al., 2017). Still, this is a conservative approach since we consider that all the oil will dissolve in the water (DUARTE; DROGUETT, 2016).

The PAH concentration reaching FNA was lower than the concentrations analyzed in the study conducted by (JOHANSEN et al., 2017). Hence, we assume conservative approaches. We consider the prolonged exposure to oil, i.e., more than seven days, supported by the fact that FNA does not have mitigation plans to face oil spills, and the cleaning would take longer (QUEIROZ et al., 2019). Still, since the mortality did not vary significantly with the PAH concentrations, we assume the same mortality of 10% for the bioindicator individuals due to a prolonged exposure to 0.009mg/L of PAH presented in the oil that settle

on FNA. We also assume a 50% reduction in the fecundity rates, based on data analyzed by (JOHNSON et al., 2008). This step of the assessment has conservative assumptions. Despite using data from similar species, the actual ecotoxicology of the REP may be very different. justifying the need for a sensitivity analysis in the mortality and fecundity rates, and how they impact the risks.

6.4 FREQUENCY ESTIMATES

The main findings from the frequency assessment are presented in Chapter 5. After a Bayesian Population Variability Analysis, we could obtain not a single estimate for the accidents rates but a posterior probability distribution on the accidents' rates (Figure 4 in Section 5.4.3). Additionally, we have distributions that account for the expected, 5th, and 95th percentiles after sampling from the model parameters space. Since the results are given with such uncertainty, we can have for each SCN an optimistic (a), expected (b) and pessimistic (c) frequency estimate. For instance, when we refer to SCN-1c, we refer to the scenario in which collisions occur with a pessimistic rate. To be used in the model, the frequency occurrence (F_k) of each scenario k is evaluated as the expected value of the respective distribution accidents' rate, as presented in Table 1.

Table 1 - Frequency of occurrence of each SCN

	Frequency		
Scenario	Optimistic (a)	Expected (b)	Pessimistic (c)
SCN-1	0.002257	0.01286	0.07339
SCN-2	0.00008592	0.00360	0.14980
SCN-2	0.0000008154	0.000373	0.13970

Source: The Author (2021)

As we can see, the pessimistic frequencies for SCN-2 and SCN-3 are very high, even though the expected values are the lowest. The uncertainty in the data leads to an overestimation of the frequencies. Thus, we can expect overestimated risks for these scenarios. On the other hand, the optimistic frequencies approach zero, and we can expect risks close to the benchmark scenario (SCN-0).

6.5 POPULATION MODELING

A fundamental basis for the QERA is stochastic ecological models, i.e., models that simulate the population dynamics of the bioindicator species since the best trade-off between ecological relevance and tractability relies on models at the population level (PASTOROK et al., 2002). Thus, the mathematical expressions describe the population dynamics through endpoints (e.g., population abundance). With this endpoint, one can estimate the risk of harmful effects (e.g., extinction or quasi extinction) caused by events such as industrial accidents. Furthermore, the model is stochastic: the parameters are not deterministic values but random variables that account for natural fluctuations and uncertainty. We could have measurement errors from the data gathering and insufficient information about some parameters regarding the uncertainty. The model can integrate extreme events, such as oil spills, that can significantly impact the population dynamics.

For instance, in the context of oil spills, the ecological risks (hereafter ecorisks) are estimated based on the impact of the concentration of oil that reaches a given ecosystem, such as coral reefs, mangroves, and beaches. To evaluate the effect in the ecosystem, we assess the impact in a defined species representative of that ecosystem, the bioindicator species such as fishes.

Some fish population models have been developed for risk assessment purposes (DUARTE et al., 2013; DUARTE; DROGUETT; CARVALHO, 2015; LI et al., 2020). Notably, such models attempt to describe the population dynamics of the species given various stressful circumstances (e.g., marine pollution and fisheries). The models developed regarding parrotfishes are due to the high fishery pressure on the species, and on the species absence, the coral reefs health is compromised (BAILLE, 2013; PAVLOWICH; KAPUSCINSKI; WEBSTER, 2019; ROOS et al., 2015). However, no one of these models is stochastic nor are tailored for risk assessment.

Therefore, this work aims to develop a stochastic model to evaluate the population dynamics of red-eye parrotfish (REP) (*Sparisoma axillare*) under different oil exposures resulting from potential oil spills. This species was chosen as a bioindicator because it is highly abundant on FNA; it is labeled as vulnerable (VU) by the International Union for the Conservation of Nature (IUCN). Additionally, the species contributes to the health of the coral reefs. The proposed model considers only females, for they are most relevant to avoid extinction since they produce new individuals. Furthermore, the REP is a protogynous hermaphrodite. All individuals are born female, and after reaching a specific size, they change

sex to males. Thus, the extinction of the females is ultimately the extinction of the total population. Hereafter, when not specified, we refer to the female population as population.

With the proposed model, we can describe the female abundance for the next 100 years under varying scenarios: a) a benchmark scenario that simulates the natural population dynamics of the species; b) scenarios with varying exposure to oil, i.e., varying mortality. By varying the mortality, we can assess the added or reduced ecorisks caused by the spill. The quasi-extinction is defined as a lower threshold for population abundance.

RAMAS Metapop v.6.0 software (AKÇAKAYA; ROOT, 2013) was adopted for running the simulations with 10,000 replications. This software is a computational tool for constructing the population model and running probabilistic simulation via the Monte Carlo method (KALOS; WHITLOCK, 2008). We can have the following outputs from the simulations (AKÇAKAYA; ROOT, 2013):

- Cumulative distribution functions (CDFs) for the time to extinction or quasi-extinction within 100 years;
- Time to extinction: the time required by a population to decrease below a given threshold abundance;
- The median time to extinction: the most reasonable time a population needs to reduce to less than a given threshold abundance. It is the median value in the PDF of the time to extinction.

6.5.1 Species description

Parrotfishes (*Scaridae* family) are a dominant group of reef fishes mainly distributed globally in tropical oceans; they usually occupy shallow marine habitats (0 to 50 m), primarily coral reefs. The Scaridae have fused teeth, beak-shaped jaw, scrape the substrate, and remove algae and debris. This characteristic enables the species to have a fundamental role in marine bioerosion.

Healthy coral reefs are composed of topographically complex, three-dimensional structures which buffer shorelines from currents, waves, and storms, replenish sand and provide shelter for many organisms (MALLELA; FOX, 2018). The parrotfishes contribute to the deconstruction of the reef (bioerosion) and construction (sediment production), and thus they play an essential role in achieving a healthy coral reef (MALLELA; FOX, 2018). Furthermore, they also control the algae population, hindering them from growing over alive coral (VÉRAS, 2008). Thus, parrotfishes are a species with significant ecological importance.

Hence, we focus on the red-eye parrotfish (REP), *Sparisoma axillare*, a species restricted to the southwest Atlantic, and that occurs on FNA (Figure 1).

Figure 1 - Sparisoma axillare.

From: (FISHBASE, 2009)

The REP is a protogynous hermaphrodite with two adult color patterns. The initial phase (IP) is predominantly female; they have a grey-brown body white-yellowish flank. In the terminal phase (TP), the body is typically reddish on the back and brownish-white on the belly (MOURA; FIGUEIREDO; SAZIMA, 2001). After a pelagic larval stage, fish settle on the reef about 1cm in length as female juveniles (JU) (GASPAR, 2006). Soon they adopt a color pattern similar to the IP fish. The smallest fish to reach sexual maturity was estimated at $20.2cm$ length fork (LF) (VÉRAS, 2008). Thus, adults can be defined as fish $> 20cm$. The estimated age to reach sexual maturity is 4 years (GASPAR, 2006). Some females may never change sex, regardless of how big they can be; this strategy does not affect the reproductive potential (GASPAR, 2006).

6.5.2 Methodology

6.5.2.1 Materials and data sources

The information used to construct this model comes from the literature available. However, data regarding the REP is very scarce; thus, we relied on data collected for a similar species, the *S. viridae*, in Bonaire, Netherlands Antilles (VAN ROOIJ; VIDELER, 1997). Notably, the main parameters used were the juveniles' and the adults' survival rates and the annual rate of changing sex. More specifically, for the REP, the smallest individual registered to have reached sexual maturity measure $20.2\ cm$ of fork length (FL). The FL is measured

from the tip of the snout to the center of the concave tail (Figure 2). To estimate the age to reach sexual maturity, we use the von Bertalanffy model (VON BERTALANFFY, 1957), which estimates the expected size given the age:

$$L_t = L_\infty(1 - \exp(-k(t - t_0)) \quad (7.1)$$

where L_t is the total length of individuals at age t; L_∞ is the maximum asymptotic length; k is the annual growth rate; and t_0 is the theoretical age in which the individual length equals zero. We use the parameterization made by (GASPAR, 2006), where $L_\infty = 29.78\,cm$, $k = 0.3\,yr^{-1}$ and $t_0 = 0$. Solving for the time in Equation 7.1 we have that the age to reach $20.2cm$ is approximately 3.7 years, and we round to 4 years.

Figure 2 - Fork length measured in a Sparisoma axillare specimen.

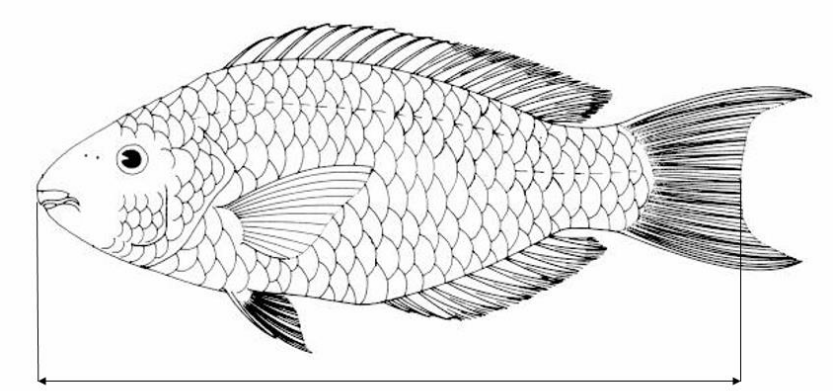

Adapted from: Véras (2008)

The REP has external fecundity, i.e., the female releases oocysts in the water and then fertilizes them by the male sperm. The spawning happens throughout the year (VÉRAS, 2008). After the fertilization, the fish remains in a pelagic larval stage (i.e., an early stage of development in the open ocean) until settling on the reef as juveniles. However, this rate that includes both fecundity and survival rate is a parameter very challenging to estimate (GASPAR, 2006; VAN ROOIJ; VIDELER, 1997). Thus, we calibrated this parameter (a_{12}) as to attempt to maintain the population stable over time.

In matrix ecological models, the dominant eigenvalue (λ_{max}), i.e., the one with the highest absolute values, dictates the population growth (AKÇAKAYA; BURGMAN; GINZBURG, 1999). If $\lambda_{max} < 1$, then the population is decaying, if $\lambda_{max} > 1$, the population is growing and, if $\lambda_{max} = 1$, the population do not vary over time. We chose a_{12} to result in $\lambda_{max} \cong 1.001$, representing a quasi-stationary state. This assumption is supported

by the fact that there is no fishing pressure or human impacts (e.g., tourism) that significantly alter the population dynamics in FNA (DOMINGUEZ et al., 2016; MEDEIROS; MEDEIROS, 2017).

Although a fauna fish assessment performed in FNA revealed a total abundance of 45 REP individuals, there is no precise estimate regarding the total population of REP in the archipelago (SCHMID et al., 2020). Thus, we assume a hypothetical population of 1,000 individuals following a proportion of juveniles and adults from a sample collected by (VÉRAS, 2008), i.e., approximately 60% of the individuals are juvenile, while 40% are adults.

The variables and parameters of the model, with the data source or assumptions, can be seen in Table 2 and Table 3, respectively. The model parameters are also presented as the mean value and the standard deviation (SD).

Table 2 - Description of the model variables.

Variables	**Symbol**	**Description**
Number of juveniles at time t (stage 1)	$N_1(t)$	The abundance of juveniles. Described as the minimum, average and maximum values within a 95% confidence interval
Number of females, initial phase adults at time t (stage 2)	$N_2(t)$	The abundance initial phase adults that remain as female. Described as the minimum, average and maximum values within a 95% confidence interval

Source: The Author (2021)

Table 3 - Description of the model parameters.

Parameter	**Symbol**	**Assumptions**	**Mean (μ)**	**SD (σ)**
Permanence rate as a juvenile (stage 1)	a_{11}	The mean annual survival rate for the S. viridae individuals ranging from 5 to 20cm (1 to 4 years old) is 0.624. The maturity age is assumed to be 4 years (GASPAR, 2006)	0.468	0.020
Transition rate from juvenile (stage 1) to IP (stage 2)	a_{12}	A rate that considers both fecundity of IP and survival of the larvae. Since it is a parameter very challenging to estimate, we calibrated its value until reaching a stable population, i.e., $\lambda_{max} = 1.001$.	0.755	0.002
Transition rate from juvenile (stage 1) to IP (stage 2)	a_{21}	The annual survival rate for juveniles that reach sexual maturity after 4 years	0.156	0.020
The survival rate of adults (male and female)	s_2	The mean annual survival rate for S. viridae individuals that ranges from 20 to 35cm	0.866	0.009
The proportion of IP that changes sex	c	The mean proportion of S. viridae IP individuals that change sex	0.099	0.084
Permanence rate as adult IP (stage 2)	a_{22}	The annual survival rate for S. viridae individuals that ranges from 20 to 35cm and does not change sex. Thus we assume this rate as the product of	0.780	0.029

the natural survival rate (s_2) and the proportion of individuals that remains as female ($1 - c$)

Source: The Author (2021)

6.5.2.2 The model structure

The REP presents two major social categories: territorial fish that live in deeper portions of the reef ($> 3{,}5m$ deep); and group fish that live in the shallow reef scraping the substrate (VAN ROOIJ; VIDELER, 1997; VÉRAS, 2008). The territorial males share their territory with one to three females, while the group males do not mate at all. The females can spawn daily.

There is no significant difference in growth rate, condition on spawning frequency detected between the group and territorial females (VAN ROOIJ; VIDELER, 1997). Hence, they can be treated as one category, the Adult initial phase (IP). We can focus on the female since all the juveniles are females to structure our model in two stages: juveniles and initial phase adults (IP).

For the model simplicity, the juvenile stage includes the larvae that result from the fertilized oocysts, and the fish that reach $5cm$ are recruited to the reef. The juveniles who survive until the age of sexual maturity, approximately 4 years, reach sexual maturity and can become IP, remaining female, or then changing sex. Since our model focuses on females, the survival rate of this stage should consider the mortality and the portion of individuals that remain as female.

We can then project the stage-specific population abundance from a time-step t to a time-step $t + 1$ using the Lefkovitch (or Stage) matrix (LEFKOVITCH, 1965):

$$\begin{bmatrix} N_1(t+1) \\ N_2(t+1) \end{bmatrix} = \begin{bmatrix} a_{11} & a_{12} \\ a_{21} & a_{22} \end{bmatrix} \begin{bmatrix} N_1(t) \\ N_2(t) \end{bmatrix}$$

where $N_i(t)$ denotes the abundance of females in stage i; s_i is the survival rate per year of females in stage i; a_{ij} transition rate per year from stage j (matrix column) to stage i (matrix line); note that when $i = j$ we have the permanence rate in stage i denoted by a_{ii}; c is the annual proportion of IP individuals that change sex.

The proposed model is stochastic; thus, it includes uncertainty in the parameters. The uncertainty in the parameters can be modeled as describing them as probability distribution functions, typically a Normal or Lognormal. One can make good use of a Gaussian approach in the vital rates of biological models because there is a reasonable reason for random values not to be too far away from average, i.e., physical limitations are preventing considerable

deviations and natural forces from equilibrium that bring vital rates back to their average values (TALEB, 2007). RAMAS converts the normal distribution parameters into the corresponding Lognormal counterpart for probabilistic simulation, avoiding bias resulting from truncation because all parameters are greater than zero. A schematic of the model with the stochastic transition rates (represented as lognormal distributions) can be seen in Figure 3.

Figure 3 - Schematic of the female REP life cycle. The values above the arrows are the lognormal distributions that model the annual transition and permanence rates.

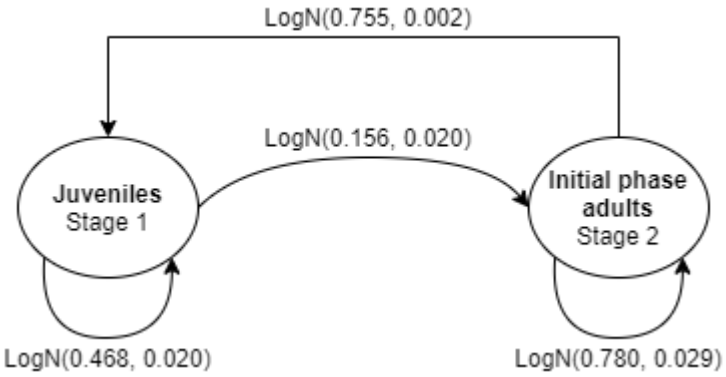

Source: The Author (2021)

6.5.3 Results and Discussion

The initial conditions of the model are based on the rationale presented in Section 6.5.2.1 and are as follows:

- The initial number of juveniles: $N_1(t) = 600$
- The initial number of IPs: $N_2(t) = 400$

Then, we simulate the population dynamics of the REP, concerning the juveniles and IP individuals, i.e., $N_1(t) + N_2(t)$. A projection of the REP abundance over the next 100 years in the FNA can be seen in Figure 4. The solid line is the average value, while the vertical bars are the results within 68% CI ($\pm 1\ SD$).

Since most of the parameters are estimated from a similar species (e.g., a_{11} and a_{22}) or had to be calibrated to result in a steady population over time (a_{12}), we evaluated the model's sensitivity to the parameters in the stage matrix. We considered two different scenarios varying the parameters of the stage matrix by $\pm 1\%$. The expected population abundance of these scenarios and the initial results can be seen in Figure 5.

The results are susceptible to a slight variation in the parameters. Note that with only a 1% increase in the parameters, we have that $\lambda_{max} = 1.011$, and the expected population

reaches 2982, while in the original simulation, the population reached 1104 individuals, a 170.1% increase. Note that since there is no limit for the population size, the population grows unbounded. With a 1% decrease, $\lambda_{max} = 0.991$, and the expected population is 400 individuals, a 63.8% reduction.

Figure 4 - Female REP abundance (juvenile and IP) in FNA over 100 years. The solid lines are the expected values, while the vertical bar, the results within a 68.3% CI ($\pm 1\ SD$).

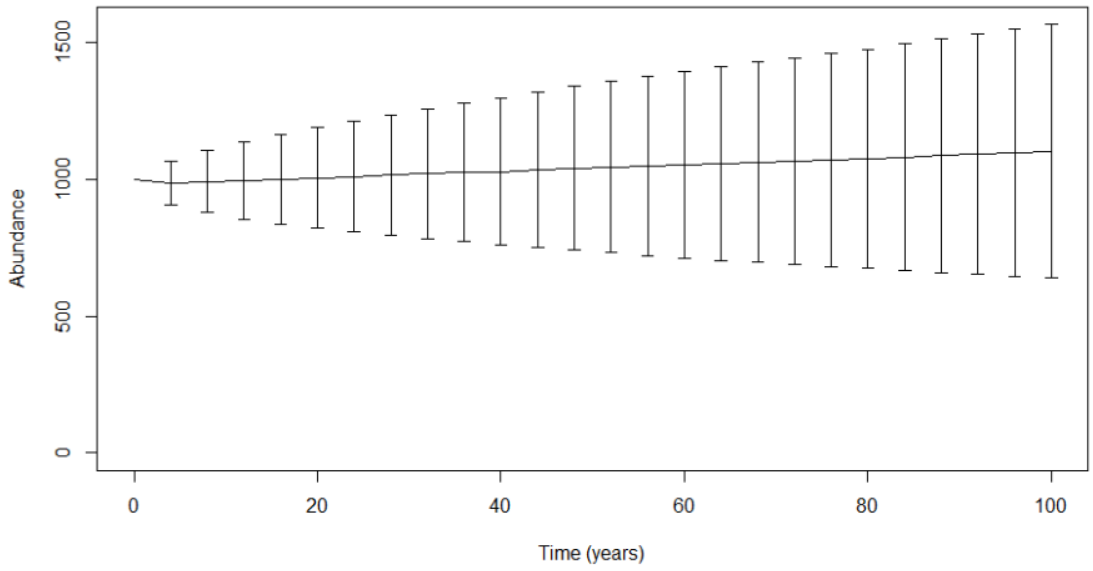

Source: The Author (2021)

Figure 5 - Expected female REP abundance for the original stage matrix parameters (dashed black line), +1% variation on the parameters (dotted red line) and -1% variation (solid blue line).

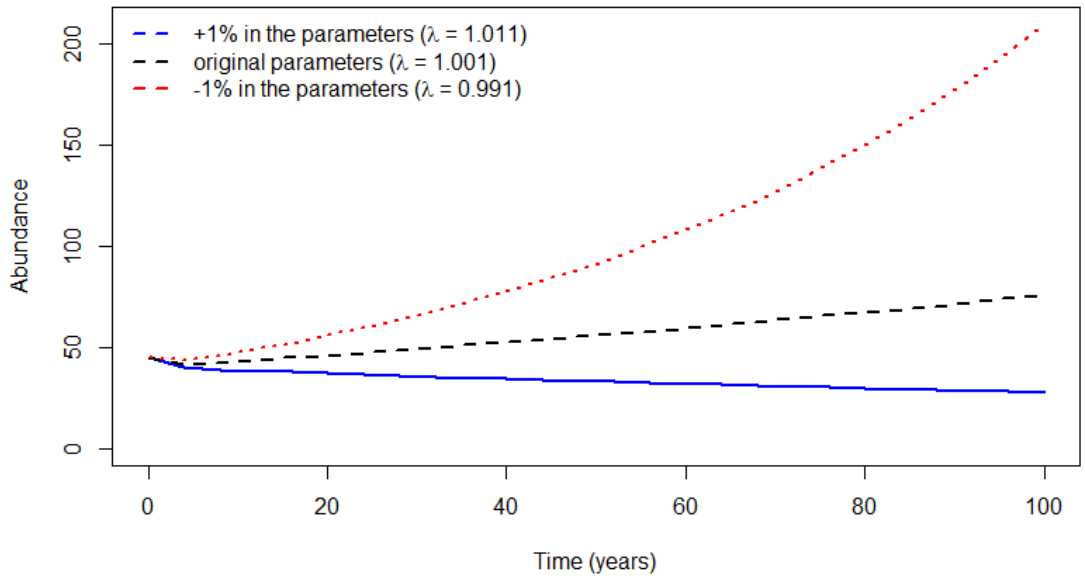

Source: The Author (2021)

Moreover, the most sensible parameters were obtained, computing the respective sensitivities and elasticities. The sensitivities measure the changes in the dominant eigenvalue for small changes in a particular matrix parameter. The elasticities are the proportional sensitivities, i.e., the contribution of each element of the matrix in changing the dominant eigenvalue. The elasticities of the model's parameters are presented in Table 4.

As can be seen, the permanence rate as IP (a_{22}) contributes more to the population dynamics. This result is expected: the more individuals survive in this stage, in which they are sexually mature, the more pups will be generated each time step. Thus, further data gathering for the REP in FNA tailored to construct a population model should estimate this parameter. Then, the most impactful parameter will have reliable estimates with an economy of resources (e.g., time and financial resources), and the model will also be more reliable.

This strategy should cover one of the main limitations of the model: the parameterization was performed using data for a similar species, *S. viridae*, and there is a lack of data regarding REP population dynamics in FNA.

Table 4 - Ecological model parameters elasticities.

Parameter	Description	Elasticity
a_{11}	Permanence rate as a juvenile (stage 1)	0.1372

Parameter	Description	Elasticity
a_{12}	Transition rate from IP (stage 2) to juvenile (stage 1)	0.1561
a_{21}	Transition rate from juvenile (stage 1) to IP (stage 2)	0.1561
a_{22}	Permanence rate as IP (stage 2)	0.5506

Source: The Author (2021)

6.6 Risk Quantification and Categorization

The inputs for the final step are the outputs of the previous steps as follows:

- The oil concentration $C(\boldsymbol{x}, t)$ that reaches the FNA from the numerical simulations of the oil fate and transport, as the third step of the methodology (Chapter 4);
- The dose-response of the REP, i.e., the mortality and fecundity reduction due to the toxic compounds present in the oil. It is also part of the third step of the methodology, that accounts for the consequence assessment (Section 6.3);
- The frequency estimate of each accident, from the Bayesian Population Variability analysis, as the fourth step of the methodology, (Chapter 5);
- The population model for a hypothetical *Sparisoma axillare* population located in the Buraco da Raquel, a important touristic spot in FNA (Figure 6). This location is the most severe spot where the spill would hit. The model was proposed in the fifth step of the methodology (Section 6.5).

All the nine SCNs (SCN-1a, SCN-1b, …, SCN-3c) were incorporated into the metapopulation model, resulting in 10 models with different frequencies of occurrence and consequences. For the simulation of each model, the SCN was randomly selected to occur every time step according to its frequency of occurrence. If it happens, it will increase mortalities by 10% and reduce fecundities by 50%. All the simulations were performed with 10,000 replication. Figure 7 depicts the simulation process for one out of 10,000 replications of a given SCN.

Figure 6 - Location of the fish population representative of the FNA ecosystem health.

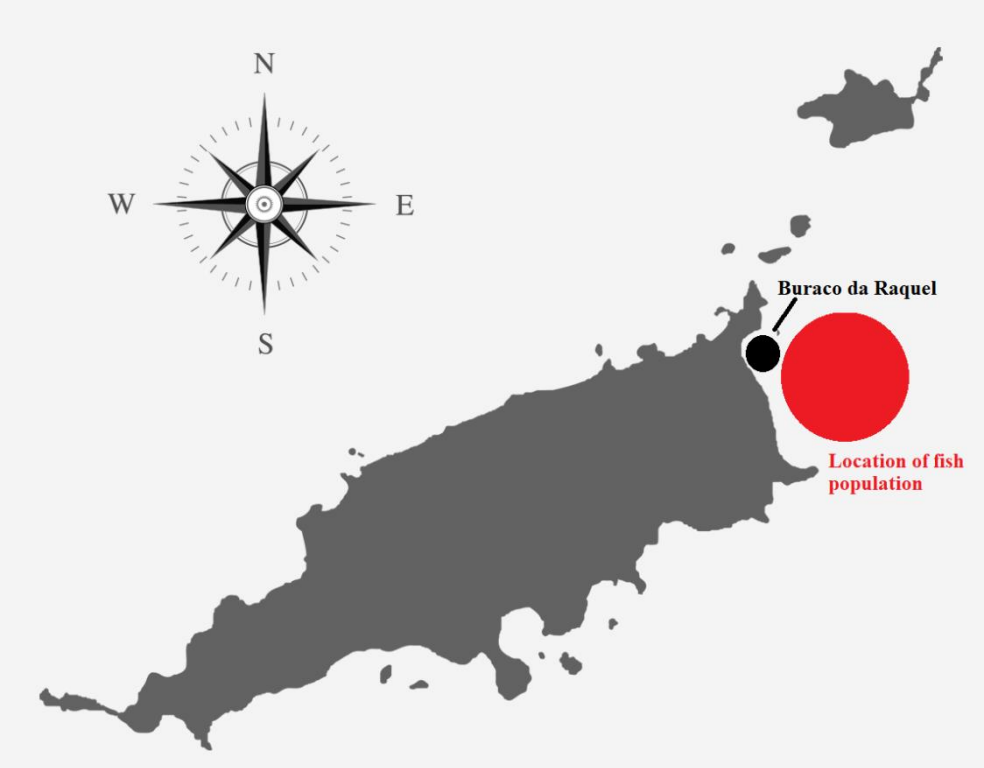

Source: The Author (2021)

The model's results that account for the oil spill were compared to a model without oil impacts, i.e., the benchmark scenario (SCN-0) presented in the fifth step of the methodology. Figure 8 compares the risks of HL of the benchmark scenario with the scenarios in which the oil spills from collision (A), fire (B) and explosion (C). Each point in the curves can be interpreted as "there is a X% probability that the REP abundance will fall below 50% the initial population size (half loss) by time-step T". Based on these results, it is possible to categorize the risks of HL concerning each scenario: Negligible (NE) for SCN-0, SCN-2a, SCN-3a and SCN-3b; Considerable (CO) for SCN-1a, SCN-1b, and SCN-2b; High (HI) for SCN-1c; and Critical (CR) for SCN-2c and SCN-3c.

Figure 7 - Flowchart that represents one of 10,000 replications for the stochastic simulations of the SCN. Dashed boxes indicate specific models.

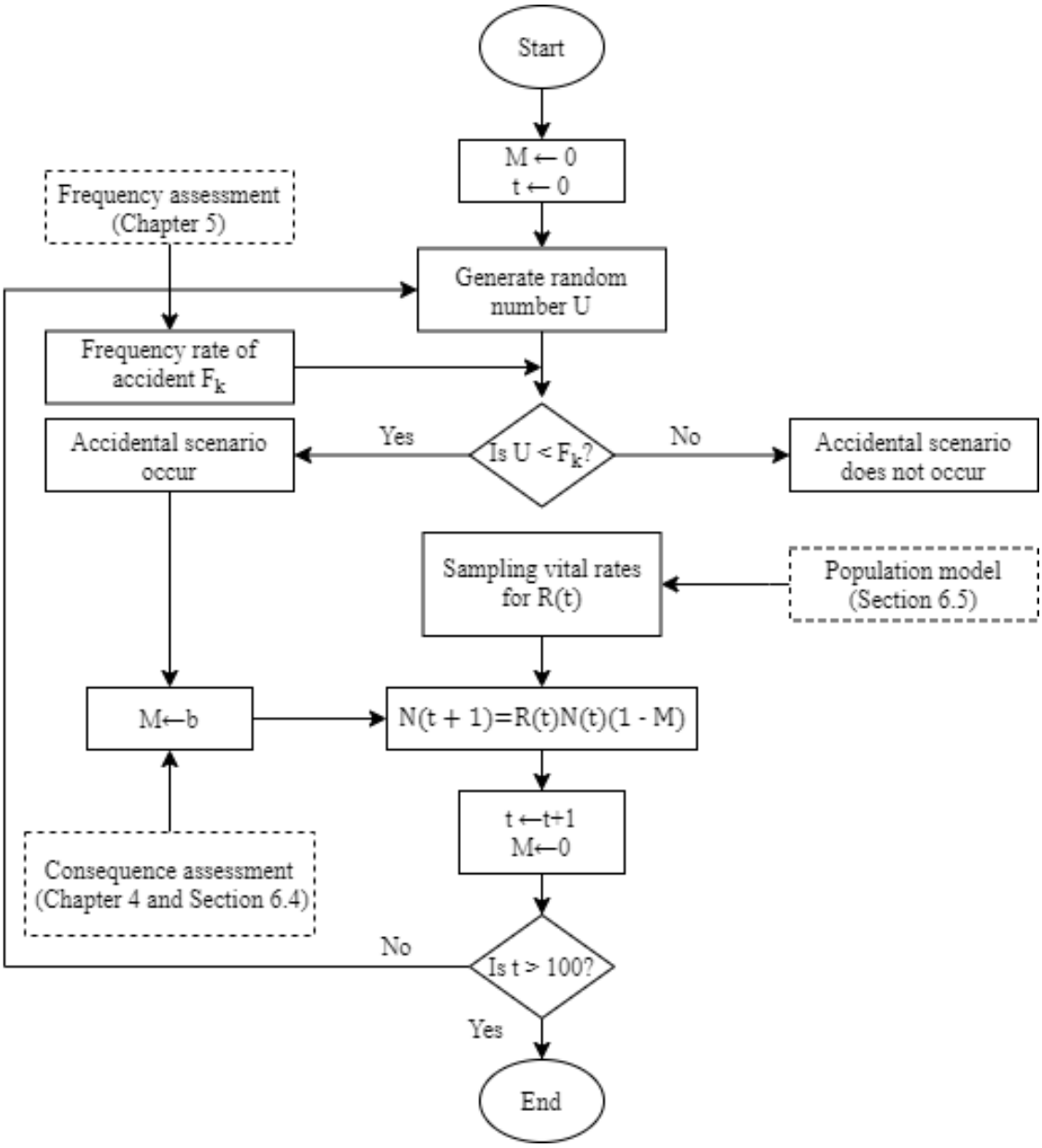

Source: Adapted from Duarte and Droguett (2016).

The models' main outputs are summarized in the Table 5 columns, while each line represents the comparison of each SCN against the benchmark. The + or − symbols can be interpreted as the added or reduced risk, respectively, of each SCN compared to SCN-0. A zero value means there is no difference to the benchmark. We show the risks of HL and the categorization, as proposed by the QERA methodology (DUARTE et al., 2019), and the risks of extinction and the categorization, according to the IUCN criteria (IUCN, 2012), as to compare both risk communication strategies.

Figure 8 - Probability of half loss and risk categorization for the SCNs. (A) Collision, (B) Fire and (C) Explosion.

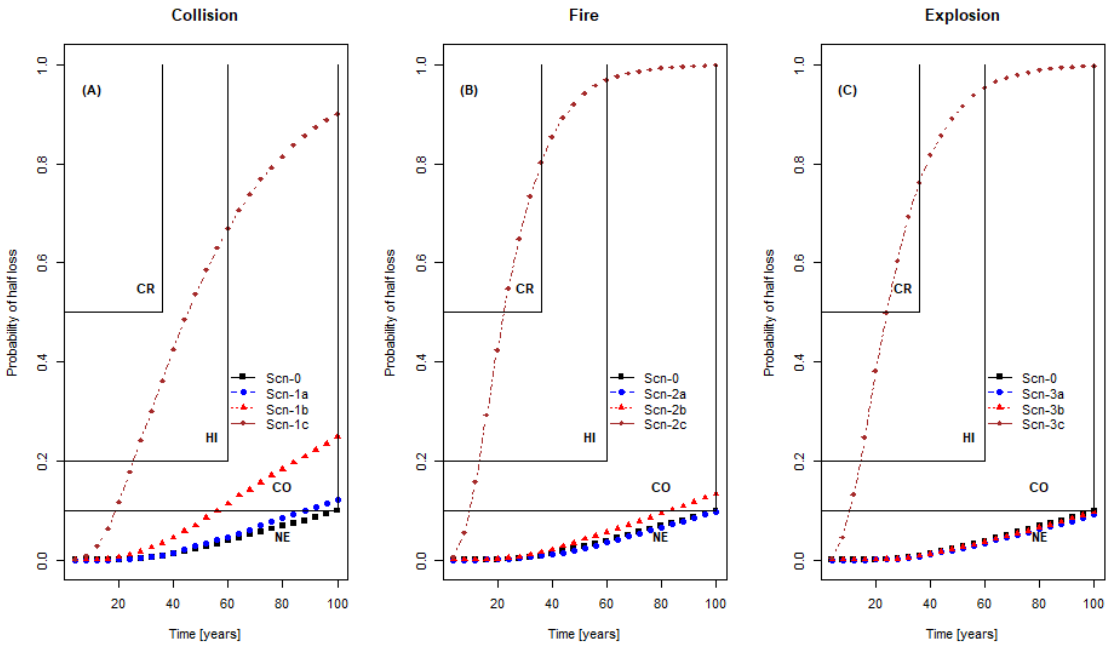

Source: The Author (2021)

Table 5 - Summary of the risk results for each SCN.

Scenario	Risk of HL	Risk of extinction	Expected minimum abundance	IUCN category	HL category
SCN-0	0.0990	0	755.9	NE	NE
SCN-1a	+0.0226	0	−18	NE	CO
SCN-1b	+0.1500	0	−103.3	NE	CO
SCN-1c	+0.8010	+0.0002	−484	NE	HI
SCN-2a	−0.0017	0	−3.9	NE	NE
SCN-2b	+0.0331	0	−29.5	NE	CO
SCN-2c	+0.8995	+0.0210	−680.5	NE	CR
SCN-3a	−0.0080	0	+2.9	NE	NE
SCN-3b	−0.0028	0	−1.7	NE	NE
SCN-3c	+0.8985	+0.0130	−666.4	NE	CR

Note: CR = Critical Risk, HI = High Risk, CO = Considerable Risk, NE = Negligible Risk.

Source: The Author (2021)

We can consider that the accidents are mutually exclusive, i.e., we can not have two or more accidents happening simultaneously. So, we can cumulate the risks caused by potential oil spills according to the optimistic, expected and pessimistic estimates. The cumulated risks are according to HL categories are illustrated in Figure 9. We also assessed the cumulated risks regarding IUCN categorization, as presented in Figure 10. The hatched area describes a simple way to measure uncertainties in the results, i.e., the difference between optimistic and pessimistic scenarios. Note that these are the uncertainties in the model's inputs that are propagated to the outputs. The larger the area, the larger are the uncertainty of the inputs.

Regarding IUCN categories, the optimistic SCNs are labeled as CO, the expected SCNs, as HI, while the pessimistic SCNs, labeled as CR. On the other hand, all the cumulated extinction risks for all scenarios are within the NE category.

Figure 9 - Probability of half loss and risk categorization for cumulated scenarios.

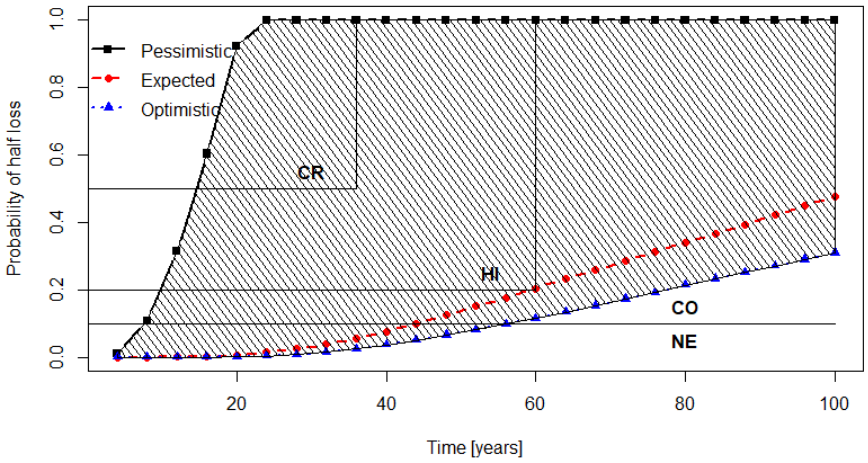

Source: The Author (2021)

Figure 10 - Probability of extinction and risk categorization for cumulated scenarios

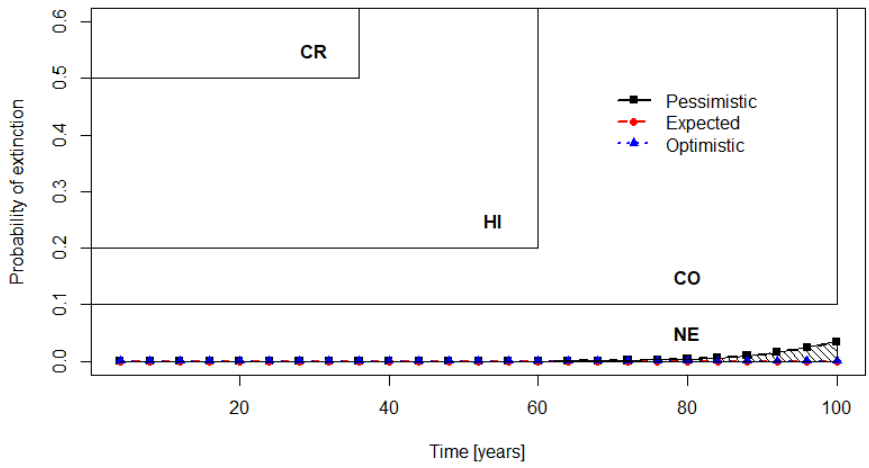

Source: The Author (2021)

6.6.1 Discussion

The benchmark scenario (SCN-0) presents a stable population dynamic, with zero risk of extinction and HL. Thus, any extinction or HL risk estimated with assessing the other scenarios is due to the added risk of potential oil spills.

The considerable uncertainty in the results leads us to categorize risks with two criteria: the IUCN's and the QERA's methodology. Although the former is widely accepted to classify species at risk exposed to several stressors (IUCN, 2012), it can be very optimistic when classifying risks due to one exposure, such as potential oil spills. Thus, the latter is more conservative since the undesirable consequence is less severe than total extinction.

Both optimistic and expected collision scenarios (SCN-1a and SCN-1b) raised the risks to the CO category, with a 0.0226 and 0.15 increase, respectively. The previous SCNs did not impact the extinction risks. Regarding the pessimistic scenario (SCN-1c), the risks reached the HI category, increasing risks by 0.801, and the extinction risks had a slight increase of 0.0001 (Figure 8A and Table 5).

At first, it's intriguing that the low frequency on the fire optimistic scenario (SCN-2a) (Table 1) did not alter the risk category and had a HL risk reduction of 0.0017 instead of increasing it. However, this behavior can be justified because, since the frequency is very low, this SCN resembles SCN-0. With the Monte Carlo simulations, one could expect a slight deviation in the results on each run. In this case, the results deviated negatively. The SCN-2b increased the risks by 0.0331 to the CO category. Due to uncertainty when estimating the fire

rates, as discussed in Chapter 5, the pessimistic scenario (SCN-2c) occurrence frequency is very high compared to the pessimistic and optimistic frequencies. Thus, the risks increased significantly by 0.8995, categorized as CR (Figure 8B and Table 5).

Regarding explosions, SCN-3 was similar to SCN-2. The frequency of the pessimistic and optimistic scenarios (SCN-3a and SCN-3b) were so minor that they resembled SCN-0 (Table 1). Despite the HL risk variation being negative, the risks were almost untouched compared to SCN-0, i.e., a reduction of 0.008 in SCN-3a and 0.0028 in SCN-3b. High uncertainties were also present in the explosion frequencies estimates. Thus the frequency of occurrence of SCN-3c was also high (Table 1), increasing the risks by 0.8985 into the CR category (Figure 8C and Table 5).

We summarized all the results by cumulating the risks of the optimistic, expected, and pessimistic SCNs. Categorizing the risks according to HL categories, the uncertainty bounds are vast, and the actual risks are within Considerable (CO) and Critical (CR) (Figure 9). Even with such uncertainty in the results, one thing is sure: the risks of HL due to potential oil spills in FNA are not to be neglected. On the other hand, the more severe consequence, i.e., the total extinction of the FNA REP population, is within negligible levels for all SCNs (Figure 10).

6.6.2 Comparison of results

The QERA performed in this work was not the first to assess risks of possible oil spills for the FNA. Duarte and Droguett (2016) conducted a first-round QERA focusing on whether the risks of catastrophic oil spills are tolerable or need management (i.e., recovery or control measures that may reduce risks). However, this study was conservative and their main features are as follows:

- The authors did not assess the fate and transport of the oil in the ocean;
- They considered ecosystem's exposure to Dispolen dispersant, rather than to crude oil itself, overestimating the mortality;
- The frequency estimates were obtained in a conservative approach;
- The authors chose as bioindicator an endemic coral species (*Siderastrea stellate),* with different oil tolerability from the REP.

We can compare their results to ours, in order to evaluate if there is consistency between the conservative approach previously applied and our approach that intended to cover the shortcomings of the previous QERA. The comparison can be seen in Figure 11.

Figure 11 - Comparison of risks of half loss with the results reported by Duarte and Droguett (2016)

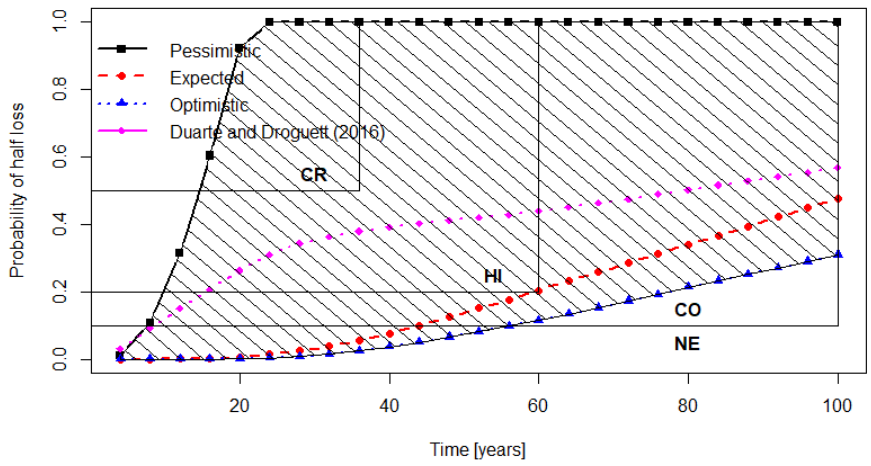

Source: The Author (2021), Duarte and Droguett (2016)

One can note that the cumulated risks of the conservative assessment performed by Duarte and Droguett (2016) falls within our risk region. Most importantly, the risks overestimated by the Duarte and Droguett (2016) are higherthan the cumulated risks of our expected scenario, which is a consistent result, and they are both labeled as HI. Even though their results are consistent with ours, it does not undermine the value of our integrated assessment with more sophisticated models. We properly estimated the frequency of the accidents and simulated the concentration of oil that would reach the FNA, along with the expected mortality and reduction in fecundity of the REP due to oil exposure. With our results, we can determine the risk region where the real risk lies. We can also see how far are their results, mainly in the pessimistic (our most conservative scenario) and expected scenarios.

7 CONCLUSIONS

The main objective of this work was to perform a second-round QERA for oil spills near FNA. This new application features different models that, once integrated via the QERA methodology, can provide better risk results: (i) simulation of the oil spill trajectory and physicochemical transformations in the ocean, (ii) frequency assessment of maritime accidents using BPVA; (iii) a stochastic model for the red-eye parrotfish (*Sparisoma axillare*), a coral reef fish present in FNA responsible for the coral reef health.

First, simulations of the fate and transport of oil spills are critical in a risk assessment for oil spills. This work simulated hypothetical oil spills with oil tankers that navigate near the Fernando de Noronha Archipelago. Six different scenarios were simulated: considering three releasing points defined along the routes of ships passing near the archipelago; the months of March and July, when the sea surface temperature, wind speed, and current intensity are more intense. As a result, we have the oil trajectory and the weathering processes that act on the spill, providing the percentages of oil affected by each of the processes and the portions that remain on the coast and the sea. The advective forces dominate the weathering process, and the oil slick reaches FNA in a short time. Therefore, there would be little time to prepare for mitigation actions, and the simulation reinforces the need for preventive measures when facing potential oil spills. The cases simulated in this work considered the most common Brazilian flag oil tanker that navigates in this region and assumed the volume spilled from only one cargo tank. As a proposal for future works, new simulations could be performed considering foreign oil tankers that navigate nearby FNA and also endangers the archipelago and different volumes of oil spilled.

Second, the frequency assessment was performed using the Bayesian Population Variability Analysis method, which allows evaluating the population variability distributions of maritime accidents (i.e., collision, fire, and explosion) from maritime accident databases and experts' opinions jointly. This method is unprecedented in the context of marine accidents. Some locations, such as the case of FNA we assessed, lack historical records of accidents. Thus, we can use subjective knowledge from experts to complement our information, leading to a better-estimating model. Indeed, the results showed that, in general, the uncertainty bounds of the cumulative posterior variability distribution reduced when we added the judgments. Therefore, with narrower bounds, we have more confidence in our estimates. It is also essential to acknowledge some limitations of the assessment. The model considered some exposure data of more than 20 years ago. Since there is a downward trend in

accidents, the data collected did not reflect the current circumstances. Thus, there should be an effort in collecting data for a new database tailored for risk assessment in different world regions. Then, more data in other locations for the current period would be available, improving the reliability of maritime risk assessments.

Third, the stochastic ecological model proposed can describe the long-term adverse effects of oil pollution in the marine ecosystem. As a bioindicator of the FNA ecosystem health, we chose the red-eye parrotfish (*S. axillare*). This species is responsible for maintaining coral reef health by constructing (sediment production) and deconstruction (bioerosion) of the reef environment. The model was parameterized partially with specific data of FNA species (i.e., initial abundance). However, most of the data came from the same species but in different regions of Brazil (i.e., fertility) and from a similar species with data collected in Bonaire, Netherlands Antilles (i.e., survival rates), which is one limitation of our model. The other limitation concerns the ecotoxicological data. Although we used data from similar species, the real ecotoxicology data for the REP may be different leading to different results. To overcome these shortcomings, a data gathering (e.g., vital rates and ecotoxicology) focused on this species should be carried out, so we could build a more reliable model.

The results of the previous steps were integrated to quantify and categorize the risks of potential oil spills to FNA. The risk results were given within uncertainty bounds, between pessimistic and optimistic SCN frequency of occurrence, to reflect the model's inputs' uncertainty, mainly on the frequency assessment step. According to the IUCN risk categories, the extinction risks of all SCNs are negligible (NE). We also consider a more conservative approach, categorizing the cumulated risks of half loss, i.e., the sum of risks for the pessimistic, expected, and optimistic scenarios. In summary, the actual risks of half loss are within Considerable (CO) and Critical (CRO). Even in such an extended interval, it is clear the risks of half loss due to potential oil spills in FNA are not negligible. Furthermore, we compared our results with a first-round QERA for oil spills performed in the FNA. We can conclude that there is consistency between the results, and our assessment provides more reliable results within an uncertainty region, as a product of the integration of different sophisticated models.

The outputs of this final step provide helpful information on a probabilistic basis since the models used in the previous steps can incorporate uncertainty. The risk results can be categorized to make the risk communication more straightforward and to aid decision-making regarding the best strategies to prevent or cope with an oil spill in FNA.

The assessment performed was an interdisciplinary work involving Production and Marine Engineering, Oceanography, and Biological Sciences. Notably, the work benefits from probabilistic models, and the results can support the decision-making process, subjects of great concern to Production Engineering. At the same time, the risk assessment might provide licensing, risk management, and environmental management information to promote safer and more reliable industrial activities.

Although the work does not aim to perform risk management, we could suggest mitigation measures based on the results. Since the oil simulation showed that a potential spill could reach the archipelago quickly, FNA should propose an emergency plan to account for the communication in advance of the spill. With this fast communication, a trained team could cope with the spill by positioning containment buoys to prevent the oil from reaching FNA. This work results can indicate the most severe spots where such buoys should be placed. In the critical circumstance of the oil going to the beaches, the team has to be prepared and equipped to clean the oil quickly, for longer exposures to oil are even more harmful to marine life.

Finally, we provide future directions that can improve risk assessments for oil spills:

- Although the BPVA could aggregate different information sources to estimate the frequency of the accidents within uncertainty bounds, the model can not contemplate more specific information contributing to the accidents, such as the meteorological conditions. Thus, using Bayesian Networks could tackle this limitation since it could incorporate all the factors that could influence the accidents with information of FNA surroundings.
- Build risk maps in FNA. First, simulate more releasing points to identify the spots in the ocean where the oil would reach FNA should a spill occur. In the ocean around FNA, this first map should help redefine routes or improve monitoring of the passage of ships to avoid accidents. Second, with a broader set of spillage scenarios, construct a risk map for the archipelago to identify the spots that would suffer the most with the oil. This second map would help prioritize the FNA locations to clean the oil if containment measures such as the buoys fail.
- Propose a multi-species stochastic model that can simulate the impacts on the ecosystem more broadly. For instance, beyond the reduction in the vital rates and fecundity of the species, assess the effects in the food chain due to oil pollution.

REFERENCES

AICHE. **Guidelines for Chemical Process Quantitative Risk Analysis**. 2. ed. New York: John Wiley & Sons, 2000.

AIDLEY, D. J. **Animal migration**. Binghamtom, New York: Vail-Ballou Press, 1981.

AKÇAKAYA, H. R. et al. **Species Conservation and Management: case studies.** New York, USA: Oxford University Press, 2004.

AKÇAKAYA, H. R.; BURGMAN, M. A.; GINZBURG, L. R. **Applied Population Ecology**. 2. ed. Sunderland, Massachusetts: Sinauer Associates, 1999.

AKÇAKAYA, H. R.; ROOT, W. T. **RAMAS GIS: Linking Spatial Data with Population Viability Analysis (version 6)**. Setauket, New York: Applied Biomathematics, 2013.

AL-RABEH, A. H.; LARDNER, R. W.; GUNAY, N. Gulfspill Version 2.0: a software package for oil spills in the Arabian Gulf. **Environmental Modelling & Software**, v. 15, n. 4, p. 425–442, jun. 2000.

AMBJORN, C. **Seatrack Web, forecasts of oil spills, a new version**. IEEE US/EU Baltic International Symposium. **Anais**...Institute of Electrical and Electronics Engineers, 2006. Disponível em: <http://ieeexplore.ieee.org/document/7266187>

AMIR-HEIDARI, P. et al. A state-of-the-art model for spatial and stochastic oil spill risk assessment: A case study of oil spill from a shipwreck. **Environment International**, v. 126, p. 309–320, maio 2019.

AMIR-HEIDARI, P.; RAIE, M. Probabilistic risk assessment of oil spill from offshore oil wells in Persian Gulf. **Marine Pollution Bulletin**, v. 136, p. 291–299, nov. 2018.

AMIR-HEIDARI, P.; RAIE, M. A new stochastic oil spill risk assessment model for Persian Gulf: Development, application and evaluation. **Marine Pollution Bulletin**, v. 145, p. 357–369, ago. 2019.

ANNIKA, P. et al. The Poseidon Operational Tool for the Prediction of Floating Pollutant Transport. **Marine Pollution Bulletin**, v. 43, n. 7–12, p. 270–278, jul. 2001.

ANP. **Boletim Mensal da Produção de Petróleo e Gás Natural**. [s.l: s.n.]. Disponível em: <http://www.anp.gov.br/publicacoes/boletins-anp/2395-boletim mensalda-producao-de-petroleo-e-gas-natural>.

ANTÃO, P.; SOARES, C. G. Analysis of the influence of human errors on the occurrence of

coastal ship accidents in different wave conditions using Bayesian Belief Networks. **Accident Analysis and Prevention**, v. 133, n. July, p. 105262, 2019.

ARZAGHI, E. et al. An ecological risk assessment model for Arctic oil spills from a subsea pipeline. **Marine Pollution Bulletin**, v. 135, p. 1117–1127, out. 2018.

ASSUNÇÃO, R. V. et al. Spatial-Temporal Variability of the Thermohaline Properties in the Coastal Region of Fernando de Noronha Archipelago, Brazil. **Journal of Coastal Research**, v. 75, n. sp1, p. 512–516, 3 mar. 2016.

BAILLE, C. **A dynamic model of parrotfish (family: Scaridae) populations for the management of herbivory on Caribbean coral reefs**. [s.l.] Sciences agricoles, 2013.

BARROS, M. J. G. DE. **Análises da Ictiofauna Marinha e Habitats Associados Através de Vídeos Subaquáticos**. Recife: Dissertação (Mestrado em Oceanografia) - Programa de Pós Graduação em Oceanografia, Unviersidade Federal de Pernambuco, 2020.

BARTELL, S. M. et al. An ecosystem model for assessing ecological risks in Québec rivers, lakes, and reservoirs. **Ecol. Modell.**, v. 124, n. 1, p. 43–67, 1999.

BERRISFORD, P. et al. **The ERA-Interim archive Version 2.0**. Shinfield Park: [s.n.]. Disponível em: <https://www.ecmwf.int/en/elibrary/8174-era-interim-archive-version-20>.

BERRY, A.; DABROWSKI, T.; LYONS, K. The oil spill model OILTRANS and its application to the Celtic Sea. **Marine Pollution Bulletin**, v. 64, n. 11, p. 2489–2501, nov. 2012.

BOOIJ, N.; RIS, R. C.; HOLTHUIJSEN, L. H. A third-generation wave model for coastal regions: 1. Model description and validation. **Journal of Geophysical Research: Oceans**, v. 104, n. C4, p. 7649–7666, 15 abr. 1999.

BRASIL. **Decreto n. 92.775 de 05 de junho de 1986: Declara Área de Proteção Ambiental o território federal de Fernando de Noronha, o Atol das Rocas e os Penedos de São Pedro e São Paulo, e dá outras providências**. Brasília - DF, Brasil: Diário Oficial da União, Poder Executivo, 1986.

BRASIL. **Decreto n. 96.693 de 14 de setembro de 1988: Cria o Parque Nacional Marinho de Fernando de Noronha e dá outras providências**. Brasília - DF, Brasil: Diário Oficial da União, Poder Executivo, 1988.

BRASIL. **Atlas de Cartas Piloto: Oceano Atlântico - De Trinidad ao Rio da Prata**.

2ªedição ed. Rio de Janeiro: DHN, 1993.

BRASIL. **Lei Nº9.985, de 18 de Julho de 2000**, 2000.

BRASIL, M. DO. **NORMAM 13: Normas da autoridade marítima para aquaviários.** Brasília, DF: Diretoria de Portos e Costas, 2003.

BRASIL, M. DO. **NORMAM 12: Normas da autoridade marítima para serviços de praticagem**. Brasília, DF: Diretoria de Portos e Costas, 2011.

BRASIL, M. DO. **Relatórios de Investigação de Acidentes Marítimos**. Disponível em: <https://www.marinha.mil.br/dpc/relatorios-de-investigacao-de-acidentes-maritimos>. Acesso em: 5 ago. 2021.

CARRACEDO, P. et al. Improvement of pollutant drift forecast system applied to the Prestige oil spills in Galicia Coast (NW of Spain): Development of an operational system. **Marine Pollution Bulletin**, v. 53, n. 5–7, p. 350–360, jan. 2006.

CETESB. **Avaliação de Risco Ecológico (ARE)**. 1. ed. São Paulo: Companhia Ambiental do Estado de São Paulo, 2020.

CHEN, C. S. Ecological risk assessment for aquatic species exposed to contaminants in Keelung River, Taiwan. **Chemosphere**, v. 61, n. 8, p. 1142–1158, 2005.

CHEN, J. et al. Oil spills from global tankers: Status review and future governance. **Journal of Cleaner Production**, v. 227, p. 20–32, ago. 2019.

CINTRA, M. M. et al. Physical processes that drive the seasonal evolution of the Southwestern Tropical Atlantic Warm Pool. **Dynamics of Atmospheres and Oceans**, v. 72, p. 1–11, dez. 2015.

CMEMS. **Global Ocean 1/12° Physics Analysis and Forecast updated Daily**. Disponível em: <https://resources.marine.copernicus.eu/product-detail/GLOBAL_ANALYSIS_FORECAST_PHY_001_024/INFORMATION>. Acesso em: 25 ago. 2021.

CPR18E. **Guideline for quantitative risk assessment (the "Purple book")**. 3. ed. [s.l.] Publicatiereeks Gevaarlijke Stoffen – PGS, 2005.

DANIEL, J. **Comissão Externa sobre o Derramamento de Óleo no Nordeste**. Brasília: [s.n.]. Disponível em: <https://www.camara.leg.br/proposicoesWeb/prop_mostrarintegra;jsessionid=532824DCF77

0C9B593CD68464F7BB330.proposicoesWebExterno2?codteor=1843890&filename=RRL+1/2019+CEXOLEO>.

DANIEL, P. et al. Improvement of Drift Calculation in Mothy Operational Oil Spill Prediction System. **International Oil Spill Conference Proceedings**, v. 2003, n. 1, p. 1067–1072, 1 abr. 2003.

DE DOMINICIS, M. et al. MEDSLIK-II, a Lagrangian marine surface oil spill model for short-term forecasting – Part 1: Theory. **Geoscientific Model Development**, v. 6, n. 6, p. 1851–1869, 1 nov. 2013a.

DE DOMINICIS, M. et al. MEDSLIK-II, a Lagrangian marine surface oil spill model for short-term forecasting – Part 2: Numerical simulations and validations. **Geoscientific Model Development**, v. 6, n. 6, p. 1871–1888, 1 nov. 2013b.

DOMINGUEZ, P. S. et al. A pesca artesanal no Arquipélago de Fernando de Noronha (PE). **Boletim do Instituto de Pesca**, v. 42, n. 1, p. 241–251, 5 mar. 2016.

DROGUETT, E. L.; GROEN, F.; MOSLEH, A. The combined use of data and expert estimates in population variability analysis. **Reliability Engineering & System Safety**, v. 83, n. 3, p. 311–321, mar. 2004.

DROGUETT, E. L.; MOSLEH, A. Integrated treatment of model and parameter uncertainties through a Bayesian approach. **Proceedings of the Institution of Mechanical Engineers, Part O: Journal of Risk and Reliability**, v. 227, n. 1, p. 41–54, 28 fev. 2013.

DROGUETT, E. L.; MOSLEH, A. Bayesian Treatment of Model Uncertainty for Partially Applicable Models. **Risk Analysis**, v. 34, n. 2, p. 252–270, fev. 2014.

DUARTE, H. DE O. et al. Quantitative Ecological Risk Assessment of Industrial Accidents: The Case of Oil Ship Transportation in the Coastal Tropical Area of Northeastern Brazil. **Human and Ecological Risk Assessment**, v. 19, n. 6, p. 1457–1476, 2013.

DUARTE, H. O. **A methodology for quantitative ecological risk assessment of industrial accidents**. [s.l.] (Dissertação de mestrado) Programa de Pós-graduação em Engenharia de Produção (PPGEP), Universidade Federal de Pernambuco (UFPE), 2011.

DUARTE, H. O. **A novel quantitative ecological and microbial risk assessment methodology: theory and applications**. Recife: Tese (Doutorado) – Universidade Federal de Pernambuco. CTG. Programa de Pós-Graduação Engenharia de Produção, 2016.

DUARTE, H. O. et al. A novel quantitative ecological and microbial risk assessment methodology: theory and practice. **Human and Ecological Risk Assessment**, p. 1–24, 2019.

DUARTE, H. O.; DROGUETT, E. L. Quantitative ecological risk assessment of accidental oil spills on ship routes nearby a marine national park in Brazil. **Human and Ecological Risk Assessment: An International Journal**, v. 22, n. 2, p. 350–368, 17 fev. 2016.

DUARTE, H. O.; DROGUETT, E. L.; CARVALHO, F. Population dynamics of the shortfin mako shark (Isurus oxyrinchus) in the South Atlantic Ocean: a quantitative ecological risk assessment under several harvest regimes. **Hum Ecol Risk Assess (Under Review)**, 2015.

DUARTE, H. O.; DROGUETT, E. L.; MOURA, M. C. Quantitative ecological risk assessment of shortfin mako shark (Isurus oxyrinchus): Proposed model and application example. **Applied Ecology and Environmental Research**, v. 16, n. 3, p. 3691–3709, 2018.

ECMWF. **ERA Interim, Daily**. Disponível em: <https://apps.ecmwf.int/datasets/data/interim-full-daily/levtype=sfc/>. Acesso em: 25 ago. 2021.

ELIOPOULOU, E. et al. Analysis of tanker casualties after the Oil Pollution Act (USA, 1990). **Proceedings of the Institution of Mechanical Engineers, Part M: Journal of Engineering for the Maritime Environment**, v. 226, n. 4, p. 301–312, 8 nov. 2012.

ELIOPOULOU, E.; PAPANIKOLAOU, A. Casualty analysis of large tankers. **Journal of Marine Science and Technology**, v. 12, n. 4, p. 240–250, 28 nov. 2007.

EMSA. **Annual Overview of Marine Casualties and Incidentes 2020**. Lisbon: [s.n.].

EPA. **Guidelines for Ecological Risk Assessment**. Washington, DC: U.S. Environmental Protection Agency, 1998.

EPA. **Glossary, Report on the Environment, US EPA**. [s.l: s.n.]. Disponível em: <www.epa.gov>.

ERICSON, A. C. **Hazard Analysis Techniques for System Safety**. Hoboken, New Jersey: Wiley, 2005.

EURECO. **Review of selected schemes developed for environmental risk assessment of substances hazardous for the aquatic environment**. Luxembourg: Institute for Inland Water Management and Waster Water treatment (RIZA), 1997.

FIRMINO, P. R.; DROGUETT, E. L. **Rede Bayesianas para a parametrização da**

confiabilidade em sistemas complexos. [s.l.] Engenharia de Produção, Universidade Federal de Pernambuco, CTG, 2004.

FISHBASE. **Sparisoma axillare (Steindachner, 1878)**. Disponível em: <https://www.fishbase.se/Summary/SpeciesSummary.php?id=59492&lang=portuguese_po>. Acesso em: 25 jul. 2021.

FOX, R. W. et al. **Introdução à Mecânica dos Fluidos**. Minas Gerais: LTC, 2014.

GASPAR, A. L. B. **Idade, crescimento e padrões de recrutamento do Bobó, Sparisoma axillare, na APA Costa dos Corais**. Recife: Universidade Federal de Pernambuco, 2006.

GEBCO. **Gridded Bathymetry Data**. Disponível em: <https://www.gebco.net/data_and_products/gridded_bathymetry_data/>. Acesso em: 25 ago. 2021.

GILKS, W. R.; RICHARDSON, S.; SPIEGELHALTER, D. **Markov Chain Monte Carlo in Practice**. [s.l.] Chapman and Hall/CRC, 1995.

GILLESPIE, R. G. Oceanid Islands: Models of Diversity. **Enciclopedia of Biodiversity**, p. 1–13, 2001.

GOVE, J. M. et al. Near-island biological hotspots in barren ocean basins. **Nature Communications**, v. 7, n. 1, p. 10581, 2016.

GRECO, S. F.; PODOFILLINI, L.; DANG, V. N. A Bayesian model to treat within-category and crew-to-crew variability in simulator data for Human Reliability Analysis. **Reliability Engineering & System Safety**, v. 206, p. 107309, fev. 2021.

GUO, W. et al. Development and application of an oil spill model with wave–current interactions in coastal areas. **Marine Pollution Bulletin**, v. 84, n. 1–2, p. 213–224, jul. 2014.

GUO, W. Development of a statistical oil spill model for risk assessment. **Environmental Pollution**, v. 230, p. 945–953, nov. 2017.

HACKETT, B.; BREIVIK, Ø.; WETTRE, C. Forecasting the Drift of Objects and Substances in the Ocean. In: **Ocean Weather Forecasting**. Berlin/Heidelberg: Springer-Verlag, 2006. p. 507–523.

HOLLNAGEL, E. **Cognitive Reliability and Error Analysis Method**. Elsevier Science, England: [s.n.].

HONDA, M.; SUZUKI, N. Toxicities of Polycyclic Aromatic Hydrocarbons for Aquatic

Animals. **International Journal of Environmental Research and Public Health**, v. 17, n. 4, p. 1363, 20 fev. 2020.

HOUNSOU-GBO, G. A. et al. Tropical Atlantic Contributions to Strong Rainfall Variability Along the Northeast Brazilian Coast. **Advances in Meteorology**, v. 2015, p. 1–13, 2015.

IBAMA. **Plano de Manejo da APA Fernando de Noronha - Rocas - São Pedro e São Paulo: Resumo Executivo**. [s.l: s.n.]. Disponível em: <http://www.icmbio.gov.br/portal/images/stories/imgs-unidadescoservacao/Resumo Executivo_f.pdf>.

IBAMA. **Manchas de Óleo: Litoral Brasileiro**. Disponível em: <http://www.ibama.gov.br/manchasdeoleo/>. Acesso em: 29 jul. 2021.

ICMBIO. **PARNAMAR - Parque Nacional Marinho de Fernando de Noronha**, 2013. Disponível em: <http://www.parnanoronha.com.br/paginas/91-o-parque.aspx>

ICMBIO. **Operação Emergencial ao Aporte Atípico de Fragmentos de Óleo e Lixo Marinho nas Localidades do Mar de Fora de Fernando de Noronha**. [s.l: s.n.].

IMO. **Formal Safety Assessment - Crude Oil Tankers**. London: International Maritime Organisation, 2008.

ITOPF. **Oil Spill Tanker Statistics 2020**. London, UK: [s.n.].

IUCN. **IUCN Red List Categories: Version 3.1**. 2. ed. Gland, Switzerland and Cambridge, UK: IUCN (International Union for Conservation of Nature), 2012.

IUCN. **Brazilian Atlantic Islands: Fernando de Noronha and Atol das Rocas Reserves - 2020 Conservation Outlook AssessmentWorld Heritage Outlook**. [s.l: s.n.]. Disponível em: <https://worldheritageoutlook.iucn.org/>.

IVAR DO SUL, J. A.; SPENGLER, Â.; COSTA, M. F. Here, there and everywhere. Small plastic fragments and pellets on beaches of Fernando de Noronha (Equatorial Western Atlantic). **Marine Pollution Bulletin**, v. 58, n. 8, p. 1236–1238, ago. 2009.

JIANG, M. et al. Risk analysis of maritime accidents along the main route of the Maritime Silk Road: a Bayesian network approach. **Maritime Policy & Management**, v. 47, n. 6, p. 815–832, 17 ago. 2020.

JIN, M. et al. Oil tanker risks on the marine environment: An empirical study and policy implications. **Marine Policy**, v. 108, p. 103655, out. 2019.

JOHANSEN, J. L. et al. Oil exposure disrupts early life-history stages of coral reef fishes via behavioural impairments. **Nature Ecology & Evolution**, v. 1, n. 8, p. 1146–1152, 17 ago. 2017.

JOHNSON, L. L. et al. The Effects of Polycyclic Aromatic Hydrocarbons in Fish from Puget Sound, Washington. In: GIULIO, R. T. DI; HINTON, D. E. (Eds.). . **The Toxicology of Fishes**. 1. ed. Boca Raton, FL: CRC Press, 2008. p. 1096.

JTSB. **Statistics of Marine Accidents**. Disponível em: <https://www.mlit.go.jp/jtsb/statistics_mar.html>. Acesso em: 5 ago. 2021.

KALOS, M. H.; WHITLOCK, P. A. **Monte Carlo Methods**. Weinheim: Wiley-VCH, 2008.

KAPLAN, S. On A Two-Stage Bayesian Procedure For Determining Failure Rates From Experiential Data. **Power Apparatus and Systems, IEEE Transactions**, v. 102, n. 1, p. 195–202, 1983.

KAREN-KOY, R. E. P. Theoretical and Experimental Ichnology of Mobile Foraging. In: MILLER, W. C. (Ed.). . **Trace fossils: concepts, problems, prospects**. [s.l.] Elsevier B.V., 2007.

KERAMEA, P. et al. Oil Spill Modeling: A Critical Review on Current Trends, Perspectives, and Challenges. **Journal of Marine Science and Engineering**, v. 9, n. 2, p. 181, 10 fev. 2021.

KORB, K. B.; NICHOLSON, A. E. **Bayesian artificial intelligence**. Florida: Chapman & Hall/CRC, 2003.

LARDNER, R. et al. **An operational oil spill model for the Levantine Basin (Eastern Mediterranean Sea)**. International Symposium on Marine Pollution. **Anais**...European Communities, 2006.

LEE, K. et al. **The Behaviour and Environmental Impacts of Crude Oil Released into Aqueous Environments**. Ottawa ed. [s.l.] The Royal Society of Canada, 2015.

LEFKOVITCH, L. P. The study of population growth in organisms grouped by stages. **Biometrics**, v. 21, p. 1–18, 1965.

LEHR, W. et al. Revisions of the ADIOS oil spill model. **Environmental Modelling & Software**, v. 17, n. 2, p. 189–197, jan. 2002.

LESLIE, P. H. On the use of matrices in certain population mathematics. **Biometrika**, v. 33,

p. 183–212, 1945.

LEWIS, J. P. et al. Changes in Reef Fish Community Structure Following the Deepwater Horizon Oil Spill. **Scientific Reports**, v. 10, n. 1, p. 5621, 9 dez. 2020.

LI, Y. et al. Ecological risk assessment of environmental stress and bioactive chemicals to riverine fish populations: An individual-based model of smallmouth bass Micropterus dolomieu☆. **Ecological Modelling**, v. 438, p. 109322, dez. 2020.

LINSTONE, H. A.; TURROF, M. **The Delphi Method: Techniques and Applications**. [s.l.] Addison-Wesley, 2002.

LUMPKIN, R.; GARZOLI, S. L. Near-surface circulation in the Tropical Atlantic Ocean. **Deep Sea Research Part I: Oceanographic Research Papers**, v. 52, n. 3, p. 495–518, mar. 2005.

LUMPKIN, R.; JOHNSON, G. C. Global ocean surface velocities from drifters: Mean, variance, El Niño-Southern Oscillation response, and seasonal cycle. **Journal of Geophysical Research: Oceans**, v. 118, n. 6, p. 2992–3006, jun. 2013.

MACKAY, D. et al. **Oil Spill Processes and ModelsEnvironment Canada**. Ottawa: [s.n.].

MACKAY, D.; PATERSON, S.; TRUDEL, B. **A mathematical model of oil spill behaviour**. Ottawa: [s.n.].

MALLELA, J.; FOX, R. J. The Role of Parrotfishes in the Destruction and Construction of Coral Reefs. In: HOEY, A. S.; BONALDO, R. M. (Eds.). . **Biology of Parrotfishes**. 1. ed. Boca Raton, FL: Taylor & Francis, 2018. p. 161–196.

MARINETRAFFIC. **MarineTraffic: Global Ship Tracking Intelligence | AIS Marine Traffic**. Disponível em: <http://www.marinetraffic.com>.

MARTA-ALMEIDA, M. et al. Efficient tools for marine operational forecast and oil spill tracking. **Marine Pollution Bulletin**, v. 71, n. 1–2, p. 139–151, jun. 2013.

MARTINS, M. R.; MATURANA, M. C. Human Error Contribution in Collision and Grounding of Oil Tankers. **Risk Analysis**, v. 30, n. 4, p. 674–698, abr. 2010.

MARTINS, M. R.; MATURANA, M. C. Application of Bayesian Belief networks to the human reliability analysis of an oil tanker operation focusing on collision accidents. **Reliability Engineering and System Safety**, v. 110, p. 89–109, 2013.

MARTINS, M. R.; PESTANA, M. A.; DROGUETT, E. A. L. A Methodology for Assessing

the Probability of Occurrence of Undesired Events in the Tietê–Paraná Inland Waterway Based on Expert Opinion. **Risk Analysis**, v. 40, n. 6, p. 1279–1301, 17 jun. 2020.

MEDEIROS, P. R.; MEDEIROS, A. M. A. Physical, biological and human-induced effects on the reef fishes of Fernando de Noronha archipelago, Brazil. **Pesquisa e Ensino em Ciências Exatas e da Natureza**, v. 1, n. 1, p. 68, 26 maio 2017.

MEDEIROS, R. C. **O Arquipélago de Fernando de Noronha e a presença militarnaval: uma condicionante Estratégia (I)**Sagres, , 2009. Disponível em: <http://www.sagres.org.br/artigos/marinha_afn.pdf>

MODARRES, M.; KAMINSKIY, M.; KRIVTSOV, V. **Reliability Engineering and Risk Analysis**. New York - Basel: Marcel Dekker, 1999. v. 53

MOLINARI, R. L. Observations of eastward currents in the tropical South Atlantic Ocean: 1978–1980. **Journal of Geophysical Research**, v. 87, n. C12, p. 9707, 1982.

MOSLEH, A. Bayesian modeling of expert-to-expert variability and dependence in estimating rare event frequencies. **Reliability Engineering & System Safety**, v. 38, n. 1–2, p. 47–57, 1992.

MOSLEH, A.; APOSTOLAKIS, G. **Development of a generic data base for failure rate**. International topical meeting on probabilistic safety methods and applications: proceedings. **Anais**...San Francisco, CA: 1985.

MOURA, M. DAS C. et al. Estimation of expected number of accidents and workforce unavailability through Bayesian population variability analysis and Markov-based model. **Reliability Engineering & System Safety**, v. 150, p. 136–146, jun. 2016.

MOURA, R. L.; FIGUEIREDO, J. L.; SAZIMA, I. A new parrotfish (Scaridae) from Brazil, and revalidation of Sparisoma amplum (Ranzani, 1842), Sparisoma frondosum (Agassiz, 1831), Sparisoma axillare (Steindachner, 1878) and Scarus trispinosus (Valenciennes, 1840). **Bulletin of Marine Science**, v. 68, n. 3, p. 505–524, 2001.

NAITO, W. et al. Application of an ecosystem model for aquatic ecological risk assessment of chemicals for a Japanese lake. **Water Res.**, v. 36, n. 1, p. 1–14, 2002.

NITTIS, K. et al. Operational monitoring and forecasting for marine environmental applications in the Aegean Sea. **Environmental Modelling & Software**, v. 21, n. 2, p. 243–257, fev. 2006.

NOAA. **Global Self-consistent Hierarchical High-resolution Geography, GSHHG**. Disponível em: <https://www.ngdc.noaa.gov/mgg/shorelines/data/gshhg/latest/>. Acesso em: 25 ago. 2021.

NRC. **Oil in the Sea III: Inputs, Fates and Effects**. Washing, DC: [s.n.].

O'CONNOR; PATRICK, D. T. **Patrical Reliability Engineering**. 4. ed. New York: John Wiley & Sons, 2002.

ODUM, E. P.; BARRET, G. W. **Fundamentals of ecology**. 5th. ed. Belmont, CA: Thomson Brooks/Cole, 2005.

PAPANIKOLAOU, A. et al. Casualty analysis of Aframax tankers. **Proceedings of the Institution of Mechanical Engineers, Part M: Journal of Engineering for the Maritime Environment**, v. 221, n. 2, p. 47–60, 1 jun. 2007.

PASTOROK, R. A. et al. **Ecological modeling in risk assessment: chemical effects on populations, ecosystems and landscapes**. [s.l.] CRC Press LLC, 2002.

PAUWELS, S. J. Fish Population Modeling: Data Needs and Case Study. In: PASTOROK, R. A. et al. (Eds.). . **Ecological modeling in risk assessment: chemical effects on populations, ecosystems and landscapes**. Boca Raton, FL: CRC Press LLC, 2002. p. 245–266.

PAVLOWICH, T.; KAPUSCINSKI, A. R.; WEBSTER, D. G. Navigating social-ecological trade-offs in small-scale fisheries management: an agent-based population model of stoplight parrotfish (Sparisoma viride) for a Caribbean coral reef fishery. **Ecology and Society**, v. 24, n. 3, p. art1, 2019.

PETROBRAS. **N-2782: Técnicas Aplicáveis à Análise de Riscos Industriais.**Brasil, 2008.

PÖRN, K. The two-stage Bayesian method used for the T-Book application. **Reliability Engineering &. System Safety**, v. 51, n. 2, p. 169–179, 1996.

QUEIROZ, S. et al. Simulation of Oil Spills Near a Tropical Island in the Equatorial Southwest Atlantic. **Tropical Oceanography**, v. 47, n. 1, p. 17–37, 2019.

RAMOS, M. A. **Desenvolvimento de Metodologia Bayesiana de Análise Quantitativa de Risco para Terminais Offshore de GNL: Aplicação para o Porto de Suape**. Recife: Dissertação (Mestrado em Engenharia Química) - Programa de Pós-Graduação em Engenharia Química, Universidade Federal de Pernambuco, 2012.

RAUSAND, M.; HOYLAND, A. **System Reliability Theory; Models, Statistical Methods and Applications**. 2. ed. New York: Wiley, 2004.

REED, M.; AAMO, O. M.; DALING, P. S. Quantitative analysis of alternate oil spill response strategies using OSCAR. **Spill Science & Technology Bulletin**, v. 2, n. 1, p. 67–74, mar. 1995.

REED, M.; GUNDLACH, E.; KANA, T. A coastal zone oil spill model: Development and sensitivity studies. **Oil and Chemical Pollution**, v. 5, n. 6, p. 411–449, jan. 1989.

ROOS, N. C. et al. Modeling sensitive parrotfish (Labridae: Scarini) habitats along the Brazilian coast. **Marine Environmental Research**, v. 110, p. 92–100, set. 2015.

SAFEDOR. **Design, Operation and Regulation for Safety**Hamburg, 2009. Disponível em: <https://cordis.europa.eu/project/id/516278/reporting/es>

SCHMID, K. et al. First fish fauna assessment in the Fernando de Noronha Archipelago with BRUVS: Species catalog with underwater imagery. **Biota Neotropica**, v. 20, n. 4, 2020.

SEBASTIÃO, P.; GUEDES SOARES, C. Modeling the Fate of Oil Spills at Sea. **Spill Science & Technology Bulletin**, v. 2, n. 2/3, p. 121–131, 1995.

SEBASTIAO, P.; SOARES, C. G. Modelling the fate of oil spills at sea. **Spill Sci Technol**, v. 2, p. 121–131, 1995.

SERAFINI, T. Z.; FRANÇA, G. Ilhas oceânicas brasileiras: biodiversidade conhecida e sua relação com o histórico de uso e ocupação humana. **Revista de Gestão Costeira Integrada / Journal of Integrated Coastal Zone Management**, v. 10, n. 3, p. 281–301, 2010.

SHAFIR, A.; VAN-RIJN, J.; RINKEVICH, B. Short and long term toxicity of crude oil and oil dispersants to two representative coral species. **Environ. Sci. Technol.**, v. 41, p. 5571–5574, 2007.

SILVA, M. et al. Circulation and heat budget in a regional climatological simulation of the Southwestern Tropical Atlantic. **Tropical Oceanography**, v. 37, n. 1–2, 20 dez. 2009.

SIMECEK-BEATTY, D.; LEHR, W. J. Extended oil spill spreading with Langmuir circulation. **Marine Pollution Bulletin**, v. 122, n. 1–2, p. 226–235, set. 2017.

SINGPURWALLA, N. D. **Reliability and Risk: a Bayesian perspective**. The George Washington University, Washington DC, USA: John Wiley & Sons Ltd., 2006.

SIQUEIRA, P. G. S. C. et al. Development of a probabilistic model for quantitative risk

assessment of COVID-19 in Brazil. **International Journal of Modern Physics C**, v. 32, n. 05, p. 2150069, 20 maio 2021.

SPAULDING, M. L. et al. Application of three-dimensional oil spill model (WOSM/OILMAP) to Hindcast the Braer spill. **Spill Science & Technology Bulletin**, v. 1, n. 1, p. 23–35, set. 1994.

SPAULDING, M. L. State of the art review and future directions in oil spill modeling. **Marine Pollution Bulletin**, v. 115, n. 1–2, p. 7–19, 2017.

STAMATELATOS et al. **Probabilistic risk assessment procedures guide for NASA managers and practitioners**. Washington, DC: Office of Safety and Mission Assurance, NASA Headquarters, 2002.

STRAMMA, L.; SCHOTT, F. The mean flow field of the tropical Atlantic Ocean. **Deep Sea Research Part II: Topical Studies in Oceanography**, v. 46, n. 1–2, p. 279–303, jan. 1999.

SWAIN, A. D.; GUTTMANN, H. E. **Handbook of Human Reliability Analysis with Emphasis on Nuclear Power Plant Applications**. Washington, DC: US Nucler Regulatory Comission, 1983.

TALEB, N. N. **The Black Swan: The Impact of the Highly Improbable**. Paris: Random House & Penguin, 2007.

TCHAMABI, C. C. et al. A study of the Brazilian Fernando de Noronha island and Rocas atoll wakes in the tropical Atlantic. **Ocean Modelling**, v. 111, p. 9–18, mar. 2017.

TRB; NRC. **Responding to Oil Spills in the U.S. Arctic Marine Environment**. Washington, D.C.: National Academies Press, 2014.

TRUCCO, P. et al. A Bayesian Belief Network modelling of organisational factors in risk analysis: A case study in maritime transportation. **Reliability Engineering & System Safety**, v. 93, n. 6, p. 845–856, jun. 2008.

TRUHAUT, R. Ecotoxicology: objectives, principles and perspectives. **Ecotoxicology and Environmental Safety**, v. 1, p. 151–173, 1977.

UĞURLU, F. et al. Analysis of fishing vessel accidents with Bayesian network and Chi-square methods. **Ocean Engineering**, v. 198, p. 106956, fev. 2020.

UĞURLU, Ö. et al. Marine accident analysis for collision and grounding in oil tanker using FTA method. **Maritime Policy & Management**, v. 42, n. 2, p. 163–185, 17 fev. 2015.

UNG, S.-T. Evaluation of human error contribution to oil tanker collision using fault tree analysis and modified fuzzy Bayesian Network based CREAM. **Ocean Engineering**, v. 179, p. 159–172, maio 2019.

VAN ROOIJ, J. M.; VIDELER, J. J. Mortality estimates from repeated visual censuses of a parrotfish (Sparisoma viride) population: demographic implications. **Marine Biology**, v. 128, n. 3, p. 385–396, 2 jun. 1997.

VÉRAS, D. P. **Biologia reprodutiva dos budiões-batata: Sparisoma axillare e Sparisoma frondosum (Actinopterygii: Scaridae), capturados na costa central do Estado de Pernambuco**. [s.l.] Universidade Federal de Pernambuco, 2008.

VON BERTALANFFY, L. Quantitative Laws in Metabolism and Growth. **The Quaterly Review of Biology**, v. 32, n. 3, p. 15, 1957.

WHITTAKER, R. J.; FERNÁNDEZ-PALACIOS, J. M. **Island Biogeography: Ecology, Evolution and Conservation**. 2nd. ed. Great Britain: Oxford University Press, 2007.

YENDER, R. A. et al. **Oil Spills in Coral Reef: Planning and Response Considerations**. Florida: National Oceanic and Atmospheric Administration - NOAA, 2010.

ZELENKE, B. et al. **General NOAA Operational Modeling Environment (GNOME) technical documentation** (N. O. S. United States Office of Response and Restoration, Ed.): NOAA technical memorandum NOS-OR&R 40.U.S. Dept. of Commerce, National Oceanic and Atmospheric Administration, National Ocean Service, Office of Response & Restoration, 2012. Disponível em: <https://repository.library.noaa.gov/view/noaa/2620>

ZHANG, J. et al. Maritime Transportation Risk Assessment of Tianjin Port with Bayesian Belief Networks. **Risk Analysis**, v. 36, n. 6, p. 1171–1187, jun. 2016.

ZHANG, Y.; BAPTISTA, A. M. SELFE: A semi-implicit Eulerian–Lagrangian finite-element model for cross-scale ocean circulation. **Ocean Modelling**, v. 21, n. 3–4, p. 71–96, jan. 2008.

ZODIATIS, G. et al. **The Mediterranean oil spill and trajectory prediction model in assisting the EU responde agency**. Congreso Nacional de Salvamento en la Mar. **Anais**...Cadiz: 2008.

APÊNCIDE A – OPINIÃO SOBRE OCORRÊNCIA DE ACIDENTES COM PETROLEIROS QUE PASSAM PRÓXIMOS À FERNANDO DE NORONHA

Neste formulário pretende-se avaliar, por meio de opinião de especialistas, a ocorrência de eventos acidentais envolvendo petroleiros que navegam próximos ao arquipélago de Fernando de Noronha (3º 51' 13.71" S, 32º 25' 25.63" W). Os acidentes de interesse são descritos a seguir:

- Abalroamento: Atingir ou ser atingido por outro navio durante navegação em alto mar. Por exemplo, num encontro ou ultrapassagem.
- Fogo: Incidente no qual o fogo é o evento iniciador. Por exemplo, por conta da liberação acidental de substâncias inflamáveis (como gás dos tanques), falha em equipamentos elétricos, etc.
- Explosão: Incidente na qual a explosão é o evento iniciador. Pode ocorrer nos tanques de carga ou de combustível, caldeiras, sala de bombas, acomodações, etc., devido à presença de uma atmosfera explosiva e fonte de ignição.

Alguns dados importantes sobre a região:

- Ventos predominantemente de leste e sudeste durante todo o ano, com intensidades que variam de 3 a 4 na escala Beaufort (7 a 16 nós), podendo ocasionalmente exceder esse valor.
- Correntes predominantemente para direção oeste durante todo o ano, com intensidades que variam de 0,7 a 2 nós, podendo ocasionalmente exceder esse valor.
- Ondas: No verão, predominantemente de leste, com alturas de 1 a 2m. No inverno, predominantemente de sudeste, com alturas de 1 a 3m.
- Visibilidade: durante todo o ano, entre 0 a 10% de nevoeiro, 0 a 10% de ventos fortes e 0 a 10% de visibilidade reduzida (inferior a 2,5 mn).
- Intensidade de tráfego: Segundo dados de 2019 no Marine Traffic, houve uma densidade aproximada de 50 rotas/km² naquele ano.

O questionário consistirá basicamente de perguntas sobre sua ocupação, experiência e opinião sobre a ocorrência dos acidentes. As perguntas sobre nome e informações para

contato serão utilizadas apenas para organizar os resultados e para contatar sobre possíveis dúvidas. Não serão usadas para nenhum fim que não esse.

Referências:
Cartas piloto:
https://www.marinha.mil.br/chm/sites/www.marinha.mil.br.chm/files/u1974/cp.pdf- Carta sinótica: https://www.marinha.mil.br/chm/dados-do-smm-cartas-sinoticas/cartas-sinoticas
Roteiro de navegação:
https://drive.google.com/file/d/1HlrHYxviyKJX1YK6MkLN9s3osbcBCrSN/view?usp=sharing
NORMAM 19:
https://drive.google.com/file/d/1lmoBP3tSLBiKizy0eWkXIfXb3M0xGe3u/view?usp=sharing

Carta Náutica das rotas de navios próximas à Fernando de Noronha

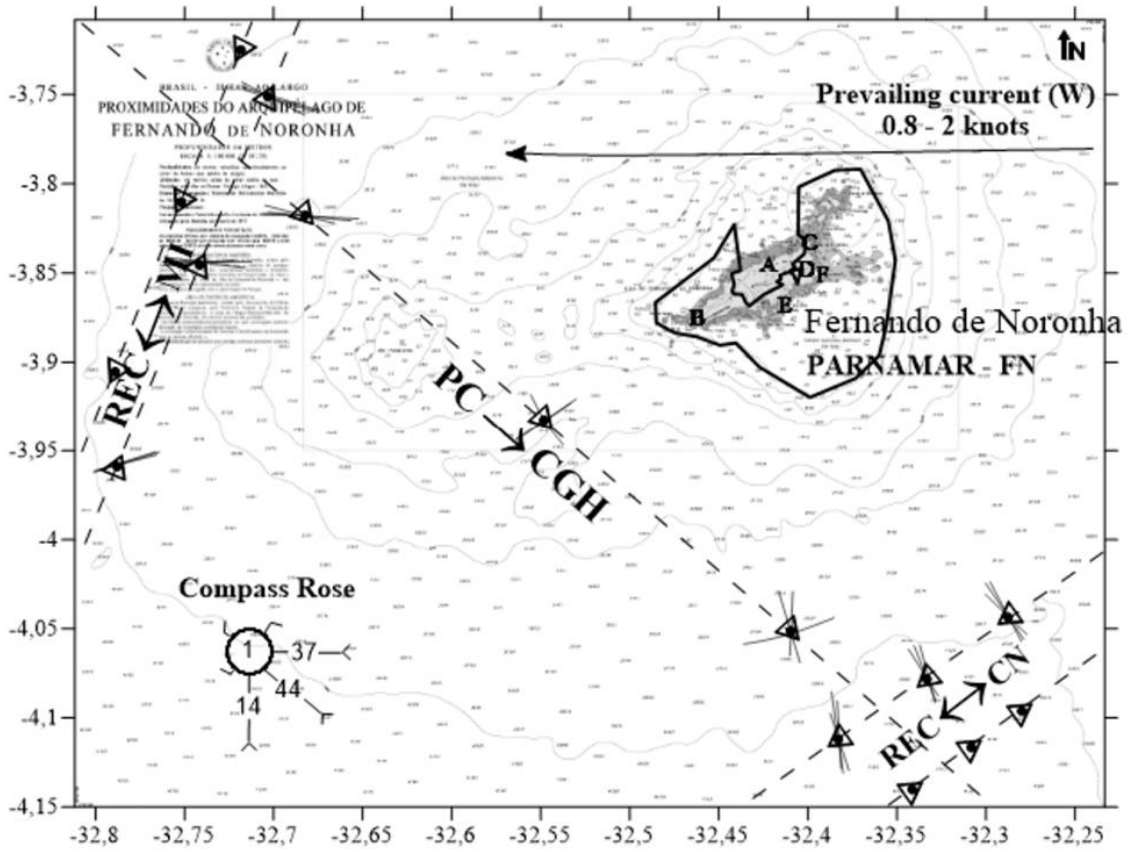

Arranjo geral de um petroleiro

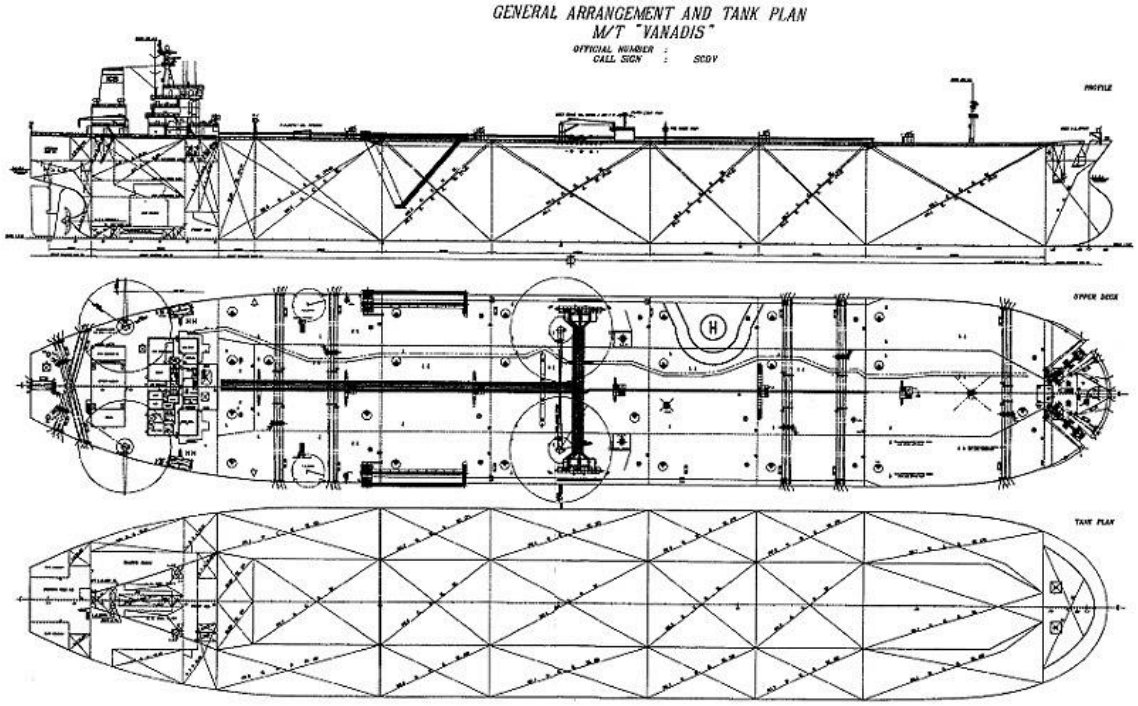

Informações pessoais

Digite seu nome

Sua resposta

E-email para contato

Sua resposta

Qual a sua ocupação? *

- ☐Comandante
- ☐Primeiro oficial
- ☐Prático
- ☐Acadêmico
- ☐Profissional aquaviário (outras funções)

Qual seu tempo de experiência na sua ocupação? *

- ☐0 a 2 anos
- ☐3 a 4 anos
- ☐5 a 6 anos
- ☐7 a 8 anos
- ☐9 a 10 anos
- ☐mais de 10 anos

Qual sua experiência com navegação costeira ou oceânica? *

- ☐0 a 2 anos
- ☐3 a 4 anos
- ☐5 a 6 anos

☐7 a 8 anos
☐9 a 10 anos
☐mais de 10 anos

Você tem experiência navegando na área November (norte oceânica) do Brasil? *
☐Sim
☐Não

Opinião sobre a ocorrência de acidentes

Em sua opinião, qual a frequência de abalroamento envolvendo pelo menos um petroleiro em rotas próximas a Fernando de Noronha?

☐1 a cada ano

☐1 a cada 10 anos

☐1 a cada 100 anos

☐1 a cada 1.000 anos

☐1 a cada 10.000 anos

☐1 a cada 100.000 anos

☐1 a cada 1.000.000 anos ou mais

Em sua opinião, qual a frequência de um evento com fogo em petroleiros em rotas próximas a Fernando de Noronha?

☐1 a cada ano

☐1 a cada 10 anos

☐1 a cada 100 anos

☐1 a cada 1.000 anos

☐1 a cada 10.000 anos

☐1 a cada 100.000 anos

☐1 a cada 1.000.000 anos ou mais

Em sua opinião, qual a frequência de uma explosão em petroleiros em rotas próximas a Fernando de Noronha?

☐1 a cada ano

☐1 a cada 10 anos

☐1 a cada 100 anos

☐1 a cada 1.000 anos

☐1 a cada 10.000 anos

☐1 a cada 100.000 anos

☐1 a cada 1.000.000 anos ou mais

Comentários finais

Se desejar, deixe algum comentário sobre o embasamento de suas opiniões, ou qualquer comentário que achar relevante.

Comentários